THESIS REPORT
Ph.D.

Modeling and Control of Multibody Systems

by N. Screenath
Advisor: P.S. Krishnaprasad

Ph.D. 87-1
Formerly TR 87-163

MODELING and CONTROL OF MULTIBODY SYSTEMS

by

Narasingarao Sreenath

Dissertation submitted to the Faculty of the Graduate School
of the University of Maryland in partial fulfillment
of the requirements for the degree of
Doctor of Philosophy
1987

Advisory Committee:

Professor P.S. Krishnaprasad
Professor Carlos Berenstein
Professor William Levine
Associate Professor Eyad Abed
Associate Professor Prakash Narayan

Abstract

Title of Dissertation: *Modeling and Control of Multibody Systems*

Narasingarao Sreenath, *Doctor of Philosophy, 1987*

Dissertation directed by: *Dr. P. S. Krishnaprasad*

Professor

Electrical Engineering Department

Dynamics of a system of many bodies in space is formulated in a Hamiltonian setting. Typically there are symmetry groups associated to such problems, and one can reduce the phase space by these symmetry groups. Dynamics in the reduced phase space is determined by appropriate Poisson structure. Equilibria for specific cases are obtained and their stability examined using energy-Casimir method. Nonlinear control techniques including exact linearization are applied successfully. A global controllability theorem is proved and feedback stabilization is studied. Applications to robotics and multibody systems in space are discussed. Symbolic computational tools were used extensively in the research. **OOPSS** – an Object Oriented Planar System Simulator package has been developed to automatically generate, analyze, simulate and graphically display the dynamics of planar multibody systems.

to my grandfather Abbayachar

whose philosophy of life is :

कर्मण्येवाधिकारस्ते मा फलेषु कदाचन ।
मा कर्मफलहेतुर्भूर्मा ते सङ्गोऽस्त्वकर्मणि ॥४७॥

Your right is to work only, but never
to the fruit thereof. Let not the fruit of
action be your object, nor let your attach-
ment be to inaction.   .   47

Bhagavad Gita, Chapter II

(ii)

Acknowledgements

I would like to take this opportunity to express my gratitude to my *guru, advisor* and *mentor* Dr. P. S. Krishnaprasad for his superlative guidance, continued encouragement and unrivalled consideration throughout the course of this thesis.

I sincerely appreciate the enlightning discussions with Dr. Jerry Marsden of University of California, Berkeley, which led to a clearer understanding of the geometric aspects of the subject.

My family deserves many thanks for their understanding and moral support, particularly my parents and grandparents who encouraged me to take up graduate studies – without whom this thesis would never have been possible.

I would like to thank my fellow students Tom Posbergh, Wassima Akhrif, Lachen Saydy and Y.G.Oh for helpful discussions and suggestions. I also acknowledge the invaluable assistance provided by the Computer support staff, collectively, since names are numerous to be mentioned individually.

I express my appreciation of the financial support in the form of a research fellowship from the Systems Research Center, University of Maryland (Dr. Baras you are doing an excellent job, keep it up) and from the University Research Initiative Program of the AFOSR.

Last but not the least, I thank my wife Shobha for enduring my random timetable, my nocturnal hours, never complaining in the process but rather encouraging me every step.

Contents

Tables

Figures

ONE

INTRODUCTION

With the advent of large sophisticated spacecraft with multiple missions, the number and size of the attachments on the main satellite body has grown. Control of such multibody spacecraft is difficult since the kinematics and the dynamics in such systems are coupled. A better and deeper understanding of the dynamics is imperative for pragmatic design of such multi-body systems in space. Equipped with this knowledge, we would be able to design control systems to realize the mission objectives.

Spacecraft in general are collections of rigid and elastic bodies, sensors and actuators. Complicating issues such as unmodeled/unmodelable dynamics, nonlinearities, reconfiguration, external disturbances, material properties (including material aging effects) are impossible to treat in a completely rigorous and deterministic way [29]. Inherent inability to model a system perfectly has motivated feedback control. However, a significant degree of modeling is absolutely necessary to develop such control.

Currently large antennae, instrumentation, solar arrays and various manipulator systems are being designed as possible attachments. Examples include SASP (Science and Application Systems Package), LDF (Large Deflector Facility), TWS (Tele-robot Work System) etc.. These attachments are usually connected to the main body by revolute joints. The movement of the one body relative to another induces reaction torques and forces on the main satellite body and also on the connected bodies.

Extensive use of remote manipulators and robots for assembly, construction, repair, and servicing of satellites is being considered seriously [28], [6],[61]. Recent developments in automation and robotics have increased the importance of their applications to future space endeavors. It has already been demonstrated that the RMS (Remote Manipulator System) on the space shuttle could be used to capture and service a satellite [7]. But suitable corrections have to be made on the Space Shuttle to compensate for the arm movements. The MRMS (Mobile RMS) on the proposed Space Station will be used for assembly and construction of Space Station itself [62]. The reaction torques and forces on the Space Station due to the MRMS movement may cause the center of mass of the station to translate and may rotate the station about its center of mass [39]. Tele-operation of manipulator arms is expected to be crucial in replacing a sizable amount of EVA (Extra Vehicular Activity). The ROBIN [6] and the Grumman tele-robot [61] are typical Telerobotic Work System (TWS) configurations. These missions involve complex tasks and call for a higher degree of manipulation and control than is available now. Furthermore, the mission objectives lay down stringent specifications on the attitude and orbit control of such spacecraft.

The above sets of complex tasks and and requirements have generated a number of challenging problems in the area of dynamics and control of multi-body spacecraft. A thorough understanding of the dynamics of such systems is required for good control system design. Knowledge of the relative equilibria and their stability is essential. Movement of these equilibria under feed-back control needs to be examined closely. Thus a need for a complete understanding of such dynamic systems is identified.

With the growing importance of spacecraft configurations with many bodies connected together by revolute joints, problems involving re-orientation of such spacecraft wherein the bodies are comparable in terms of their physical parameters have become important [46]. The spacecraft slewing (large angle) maneuver problem is inherently nonlinear owing to nonlinear kinematics and gyroscopic coupling effects [29]. Time-optimal slewing of spacecraft has been considered in the Lagrangian and Newton-Euler setting and the solutions provided range from using numerical methods [55](like relaxation and continuation methods), to using feedback linearization

[23] and then solving for the control [11].

It is the purpose of this thesis to gain better understanding and insight into the dynamics and control of multi-body systems. We deal with *planar multibody systems* connected in the form of open kinematic chain (no closed loops). Individual bodies are modeled as *rigid bodies*. The thesis is organized as follows : Chapter two gives the basic geometric results which facilitate understanding of the modeling aspects. Chapter three deals with the construction of dynamical models of planar multibody systems in Hamiltonian setting. In Chapter four we give some examples of planar multibody systems, - two-body, three-body and chain-body systems in space , and planar body systems on ground. We examine the equilibria of these dynamical systems and their stability using the energy-Casimir method in Chapter five. Chapter six deals with controllability, feedback linearization and feedback stabilization issues. In Chapter seven we present some symbolic and graphic tools we developed as a part of our research, in particular OOPSS (Object Oriented Planar System Simulator).

Theorems, Lemmas, Corollaries, Definitions and Remarks are numbered individually, with the first number representing the chapter they occur and the second the section. For example, Corollary 3.5.1 is a Corollary in Chapter 3, Section 5 and is the first Corollary in that section. The next Corollary in the same section will be Corollary 3.5.2.

GEOMETRIC PRELIMINARIES

In this chapter we discuss some mathematical definitions and concepts as related to the subject material on hand. We assume that the reader is familiar with the basic concepts such as manifolds, vector fields (see Abraham, Marsden and Ratiu [3] Chapter 3 and 4 for a good exposition of these basic concepts) and symmetries (see Abraham and Marsden [2], Chapter 4, p. 341). As we proceed in this chapter we give necessary ideas and definitions or refer the reader to other sources.

Let M be a smooth manifold. Let $C^{\infty}(U)$ be the set of all real valued smooth functions in a neighborhood U of p, where $U \subset M$. There exists a *tangent vector* at p to every smooth curve in the neighborhood U of p and passing through p. The *tangent space* $T_p M$ to M at p is the set of all tangent vectors to all the smooth curves in the neighborhood U of p and passing through p. The *tangent bundle TM* is defined on M to be

$$TM \;=\; \{T_p M : \forall p \in M\}\,,$$

which is the union of tangent spaces of all points on M. The linear dual of *tangent space* $T_p M$ is the *cotangent space* $T_p^* M$ composed of covectors at p. Similarly the dual of the *tangent bundle TM* is the *cotangent bundle $T^* M$*.

2.1 Lie Groups

The following material has been developed as in Abraham and Marsden [2] Chapter 4.

A *Lie group G* is a smooth manifold with a group structure and the group operations of multiplication and inversion being smooth. The vector space T_eG with the *Lie algebra* structure

$$[\xi, \eta] \;=\; [X_\xi, X_\eta] \qquad \text{for} \xi, \eta \in T_eG$$

is called the *Lie algebra* of G and is denoted by g. Here X_ξ is the vector field obtained by translating ξ to all of G, and e is the identity of G.

Action of a Group : An action of a *Lie Group G* on a smooth manifold M is a smooth mapping $\Phi : G \times M \to M$ such that $\forall x \in M$,

(i) $\Phi(e, x) \;=\; x$,

(ii) for every $g, h \in G$, $\phi(g, \phi(h, x)) = \phi(gh, x)$.

The *action* Φ_g of $g \in G$, is defined as $\Phi_g : M \to M : x \mapsto \Phi(g, x)$. The *orbit* or *flow* of x is given by $G \cdot x \;=\; \{\Phi_g(x) : g \in G\}$.

Infinitesimal Generator : If $\xi \in T_eG$, then $\Phi^\xi : \mathbb{R} \times M \to M : (t, x) \mapsto \Phi(\exp(t\xi), x)$[1] is an $\mathbb{R}$ - action on M i.e., Φ^ξ is a flow on M. The corresponding vector field on M given by

$$\xi_M(x) \;=\; \left. \frac{d}{dt}\Phi(\exp(t\xi), x) \right|_{t=0}$$

is called the *infinitesimal generator* of the action corresponding to ξ.

Pull back & Push forward : Given two manifolds M and N with $\mathcal{F}(N) = \{$set of all real valued C^∞ functions on $N\}$ and $\mathcal{X}(M) = \{$vector fields on M$\}$ and $\phi : M \to N$ is a diffeomorphism, the *pull back* of f by ϕ is

$$\phi^* f \;=\; f \circ \phi \in \mathcal{F}(M).$$

---

[1] see Abraham and Marsden [2] page 256 for the definition of *exponential mapping*.

5

The *push forward* of X by ϕ is defined as

$$\phi_* X = T\phi \circ X \circ \phi^{-1} \in \mathcal{X}(N).$$

2.2 Mechanics on Manifolds

The following material is patterned after Omohundro [43] and Abraham and Marsden [2] Chapter 3 and 4.

2.2.1 Dynamics on Manifolds

The evolution of mechanical systems could be described classically in terms of the generalized coordinates q_i coordinatizing the configuration space Q , and a scalar quantity L called the *Lagrangian* defined on the *tangent space* TQ of Q i.e.,

$$L \; : \; TQ \to \mathbb{R} \; : \; (q_i, \dot{q}_i) \mapsto L(q_i, \dot{q}_i).$$

The *Lagrangian* is the difference between the *kinetic* and the *potential* energies of the system. The dynamics of the system is given by

$$\left[\frac{d}{dt}\left(\frac{\partial L}{\partial \dot{q}_i}\right) - \frac{\partial L}{\partial q_i}\right] = 0.$$

The evolution of classical mechanical systems could also be described in terms of the generalized coordinates q_i, the conjugate momenta p_i and the corresponding *Hamiltonian* H which maps the *cotangent space* into the *real* line i.e.,

$$H \; : \; T^*Q \to \mathbb{R} \; : \; (q_i, p_i) \mapsto H(q_i, p_i)$$

The dynamics of the system could be represented as

$$\dot{q}_i = \frac{\partial H}{\partial p_i},$$

$$\dot{p}_i = -\frac{\partial H}{\partial q_i}.$$

In association with the Hamiltonian description, one has the notion of a *Poisson bracket* $\{\cdot,\cdot\}$. The Poisson bracket

$$\{f,g\} \;=\; \sum_{i=1}^{N}\left[\frac{\partial f}{\partial q_i}\frac{\partial g}{\partial p_i} \;-\; \frac{\partial f}{\partial p_i}\frac{\partial g}{\partial q_i}\right]$$

of two functions of q_i and p_i, defines the *Poisson structure* on the manifold T^*Q. The above bracket is known as the *canonical* bracket.

A Poisson bracket is a bilinear map from pairs of functions to functions which makes the space of smooth functions on T^*Q into a Lie Algebra, and acts on products like a derivative does. The axioms obeyed by the Poisson Brackets are :

Bilinearity : $\qquad\qquad \{af_1 + bf_2,g\} = a\{f_1,g\} \;+\; b\{f_2,g\}\,,$

Anti-symmetry : $\qquad \{f,g\} = -\{g,f\}\,,$

Jacobi's identity : $\qquad \{f,\{g,h\}\} \;+\; \{g,\{h,f\}\} \;+\; \{h,\{f,g\}\} \;=\; 0,$

Derivation property : $\{f,gh\} \;=\; \{f,g\}\,h \;+\; \{f,h\}\,g.$

A manifold P with a Poisson structure is a *Poisson manifold*, on which the Hamiltonian is a function. The dynamics evolve on this *Poisson manifold*. The evolution (dynamical) equations could also be represented in terms of the bracket as

$$\dot{q}_i \;=\; \{q_i,H\}\,,$$
$$\dot{p}_i \;=\; \{p_i,H\}\,.$$

Any function which commutes with every function on the Poisson manifold is automatically a constant of motion and is called a *Casimir* function. Thus ϕ is a Casimir function iff,

$$\{\phi,g\} \;=\; 0 \quad \forall\, g : P \to \mathbb{R}.$$

If there exists a closed nondegenerate two-form [2], ω called a *symplectic structure* then the Poisson manifold P is known as the *symplectic manifold* (P,ω). Here $\omega : \mathrm{Vect}(P) \times \mathrm{Vect}(P) \to F(P)$ is a *bilinear skew-symmetric map*, $F(P)$ is the space of smooth real valued function on P and $\mathrm{Vect}(P)$ is the space of smooth vector fields on P.

---

[2] If $\omega(X,Y) = 0 \ \forall\, Y \in \mathrm{Vect}(P)$ implies $X = 0$, then ω is nondegenerate.

Let $f, g \in F(P)$ and let X_f be a vector field of F such that

$$\omega(X_f, Y) \;=\; df(Y) \quad \forall Y \in \text{Vect}(P)$$

Now the Poisson bracket could be defined as

$$\{\cdot, \cdot\} : F(P) \times F(P) \;\to\; F(P) : (f, g) \mapsto \{f, g\} = \omega(X_f, X_g)$$

From the properties of ω it follows that $(F(P), \{\cdot, \cdot\})$ is a Lie algebra. Since ω is a nondegenerate form, the associated Poisson structure is said to be nonsingular. So the concept of Poisson manifold generalizes the notion of symplectic manifold.

A natural symplectic structure arises from Lagrangian mechanical systems on the configuration space Q. The Lagrangian description is based on the tangent bundle TQ. The Hamiltonian lives on the cotangent bundle T^*Q (momenta being derivatives of L with respect to velocity are naturally dual to velocities and thus are covectors). The *fiber derivative* FL relates points on the tangent bundle to points on the cotangent bundle. The following diagram helps keep the relations in mind.

$$T^*Q \xleftarrow{\ FL\ } TQ \xrightarrow{\ L\ } \mathbb{R}$$

with H from T^*Q and E from TQ both mapping to $\mathbb{R}$.
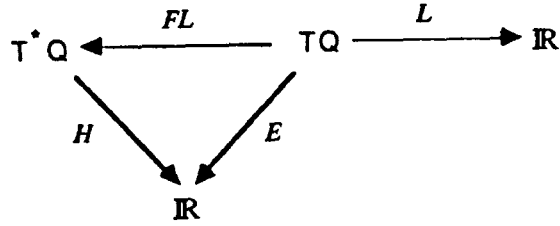
Here E is called the *energy* of the Lagrangian. T^*Q has a *canonical* symplectic structure $\omega = -d\theta$ where θ is an intrinsically defined one-form, i.e., in the coordinate notation $\theta = \sum_i p_i \, dq_i$.

2.2.2 Momentum Mapping

Consider two symplectic manifolds (M, ω) and (N, ρ). A map $f : (M, \omega) \to (N, \rho)$ is *symplectic* if $f^* \cdot \rho = \omega$. Let (P, ω) be a connected symplectic manifold. An action $\Phi : G \times P \to P$ of a group G is a *symplectic action* if for each $g \in G$ the map $\Phi_g : P \to P : x \mapsto \Phi(g, x)$ is *symplectic*. Let $\mathbf{g}$ and $\mathbf{g}^*$ be the Lie algebra of G and its dual respectively. A mapping $J : P \to \mathbf{g}^*$ is a *momentum mapping* of the action

Φ_g if for every $\xi \in \mathbf{g}$

$$d(\hat{J}(\xi))(x) \;=\; \mathbf{i}_{\xi_P}\omega$$

where $\hat{J}(\xi)(x) = J(x) \cdot \xi$ and $\mathbf{i}_X$ is and inner product [3].

Let Φ be an action on Q and let $\Phi^{T^*} = T^*\Phi_{g^{-1}}$ be the *lifted action* on $P = T^*Q$. Then this action is symplectic with respect to the canonical symplectic structure and has an Ad^* *equivariant momentum mapping* given by

$$J \;:\; P \to g^* \;:\; \hat{J}(p) \;=\; J(p).\xi \;=\; p \cdot \xi_Q(q)$$

where $\xi \in g$ and ξ_Q is the infinitesimal generator of the action corresponding to ξ. The *momentum* for a vector field X on Q is

$$P(X) \;:\; T^*Q \to \mathbb{R} \;:\; p \mapsto p \cdot X(q)$$

The following diagram commutes.

If L is the Lagrangian on TQ with $\theta_L = (FL)^*\theta$ and L is invariant under the action $\Phi_g^T = T\Phi_q$, then the momentum mapping

$$\hat{J}(\xi)(v_q) \;=\; FL(v_q) \cdot \xi_Q(q)$$

is Ad^* equivariant and J is an integral of the Lagrangian equations.

EXAMPLE : Consider $Q = \mathbb{R}^3$ and $G = SO(3)$; one can identify $so(3) = T_eSO(3)$, the Lie Algebra of $SO(3)$, with $\mathbb{R}^3$ as follows. Define

$$\mathbb{R}^3 \to T_eSO(3) \;:\; \underline{x} = [x_1, x_2, x_3]^T \mapsto \hat{\underline{x}} = \begin{bmatrix} 0 & -x_3 & x_2 \\ x_3 & 0 & -x_1 \\ -x_2 & x_1 & 0 \end{bmatrix}$$

_____

[3]see Abraham and Marsden [2] page 115 for definition of the inner product

An easy computation shows that for $\underline{x}, \underline{y} \in \mathbb{R}^3$

$$(\underline{x} \times \underline{y}) = [\hat{x}, \hat{y}] = \hat{\underline{x}} \cdot \hat{\underline{y}} - \hat{\underline{y}} \cdot \hat{\underline{x}}.$$

Thus $T_e SO(3) = so(3)$ the Lie algebra of $SO(3)$ can be viewed as $\mathbb{R}^3$ with the cross product being identified with the Lie bracket.

Consider the group action $\Phi : SO(3) \times Q \to Q : (A, q) \mapsto Aq$. If $\xi \in \mathbb{R}^3$ then $\hat{\xi} \in so(3)$. Now the infinitesimal generator ξ_Q can be seen to be

$$
\begin{aligned}
\xi_Q &= \frac{d}{dt}\left(\Phi(\exp(t\hat{\xi}), q)\right)\Big|_{t=0} \\
&= \frac{d}{dt}\left(\exp(t\hat{\xi}) \cdot q\right)\Big|_{t=0} \\
&= \hat{\xi} \cdot q \\
&= \xi \times q
\end{aligned}
$$

The momentum mapping $J(p)$ where $p \in T^*Q$ is given by

$$J(p) \cdot \xi = p \cdot \hat{\xi} q$$

Working on TQ we have

$$
\begin{aligned}
\hat{J}(\hat{\xi})(q, v) &= < v, \hat{\xi} q > \\
&= < q \times v, \xi >
\end{aligned}
$$

or

$$J(q, v) = q \times v$$

which is just the angular momentum of the system.

PLANAR MULTIBODY SYSTEMS

The problem of dynamics and control of multibody systems has long been of special interest to the aerospace community [12] [22] [47] [57]. The methods used for the generation of equations of motion, in general, could be grouped broadly under vectorial mechanics (Newton-Euler formulation) and analytical mechanics (Lagrangian-Hamiltonian formulation) [38].

The Newton-Euler method involves the application of Newton's laws of motion and Euler's equations to generate the necessary dynamical equations. Since the method utilizes physically observable quantities, for relatively small systems, it is intuitively appealing. However, for more complex systems the computations can become tedious. Efforts have been made to take advantage of ways to mechanize the formulations [22], [13], [59]. Symbolic processing capabilities have been exploited to generate automatically the dynamical equations [14], [49], [60] . More on this in Chapter 7.

The Lagrangian method requires the formulation of a scalar quantity called the Lagrangian. This quantity is the difference between the kinetic and potential energies of the system. A systematic procedure of partial differentiation involving the Lagrangian would result in a set of second-order ordinary differential equations which represent the dynamics of the system [38].

Hamiltonian methods involve the formulation of a single variational equation using

Hamilton's principle [1]. Much of Newtonian mechanics is inherent in this single equation. The representation of the dynamical system is by a set of canonical, first order, ordinary differential equations with a simple structure. An underlying Poisson structure provides an elegant representation of the first order dynamical equations in terms of the bracket. The Poisson structure can also help us identify the kinematically conserved quantities, the Casimirs. Casimirs could be effectively employed to study the stability of equilibria. The chaotic solutions produced by the splitting of the *homoclinic orbits* when the system is perturbed, could be studied using Melnikov's method (see Guckenheimer and Holmes [17]). Hamiltonian methods have been applied to dynamical systems in space in the past by Pringle [44], [45] and more recently by Krishnaprasad [32], Krishnaprasad and Berenstein [33], and Krishnaprasad and Marsden [34].

Satellite Dynamicists are interested in both rigid and flexible body formulations [38]. In this research we will focus on satellites modeled as rigid bodies.

Here we formulate the dynamics of a planar system of *arbitrary* number of rigid bodies connected in the form of a tree structure using Lagrangian and Hamiltonian formulations. We start by giving the notation used, followed by the Lagrangian dynamics. The Legendre transformation which maps the Lagrangian equations to the Hamiltonian equations is given next. We discuss the underlying symmetries and the procedure of reduction and effectively use it to get the reduced dynamics in the Hamiltonian setting.

3.1 Notation

Consider a system of arbitrary number of planar rigid bodies connected in the form of a topological tree[1] (no closed paths). To define the system mathematically, each individual body should be assigned a unique label. A set of consecutive integers is used as labels. Let,

N - total number of bodies in the system.

---

[1]i.e., there exists a unique path from one body to another – also referred as an open kinematic chain

12

Body 1 could be chosen arbitrarily. Let body 1 be the *principal* or the *main* body of the system. All other bodies are given distinct integer labels varying from 2 to N inclusive. For simplicity of computation, it is convenient to label the bodies such that the body labels are of increasing magnitude along any topological path starting at body 1.

A body is considered *inboard* of body i if it is contained in the topological path connecting body 1 and body i. A body is considered *outboard* of body i if it is not *inboard* of body i, and if body i is contained in the topological path connecting body 1 and the body under consideration.

Similarly it is necessary to assign unique labels to all joints. An efficient way of doing it is the following. The joint connecting body i and the body which is contiguous to and inboard to body i is labeled i-1. Hinge 0 is assumed to be the center of mass of body 1.

Let,

i - body label of body i ,

$J(i)$ - body label of the body contiguous to and inboard of body i ,

$O_{J(i),\,i}$ - joint label of joint connecting body i and body $J(i)$; also referred to as joint $(i-1)$,

$S_{k-1,i}$ - set of all body labels associated with those bodies lying on the topological path from joint $k-1$ to the center of mass of body i ,

Figure 3.1 shows one way of labeling a system of 12 bodies connected in the form of a tree. The topological path connecting joint 0 (body 1) and body 6 , i.e., the set of body labels in the path connecting body 1 (joint 0) and body 6, $S_{0,6}$, is given by

$$S_{0,6} = [1,2,5,6]. \tag{1.1}$$

Here, body 5 is considered inboard of body 6. Body 6 is considered *outboard* of bodies 1, 2 and 5. Body 9 is neither *inboard* nor *outboard* of body 5. The body contiguous
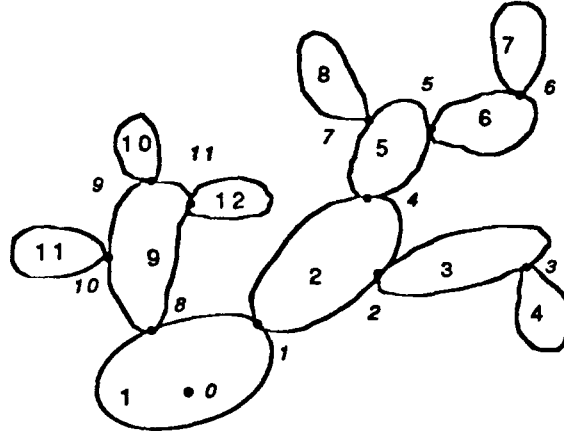
Figure 3.1: Planar 12-body system connected in the form of a tree
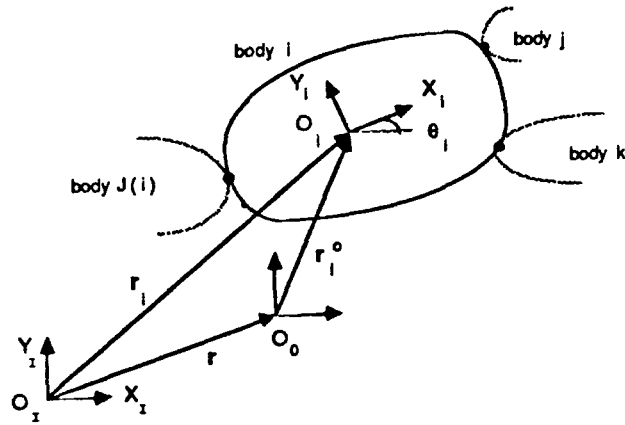
Figure 3.2: Origins and body angles

to and *inboard* of body 5, i.e., $J(5)$ is body 2. The joint connecting body 5 and $J(5)$, (body 2) is labeled joint 4 (i.e., joint (5-1)).

To formulate the equations of motion of the system under consideration, define the origin of the inertial coordinate system to be fixed at the point of reference with its Z axis being perpendicular to the plane of the paper. Define a local frame of reference for each body, *the origin of which is fixed to the body center of mass*. The Z axes of the local frames of reference are also perpendicular to the plane of paper. Refer to Figure 3.2.

O_i - origin of the local frame of reference of body i located at the center of

mass of body i ,

O_o - center of mass of the system of N rigid bodies,

O_I - reference point and origin of inertial coordinate system,

θ_i - angle made by the local frame of reference to the inertial frame of reference,

$\theta_{i,j}$ - angle made by the local frame of reference of body i with respect to the local frame of reference of body j; equal to $(\theta_i - \theta_j)$,

ω_i - inertial angular velocity of body i along the Z axis (perpendicular to the plane of the paper); equal to $\frac{d\theta_i}{dt}$,

$R(\theta_i)$ - (2×2) rotation matrix associated with body i ,

$$R(\theta_i) = \begin{bmatrix} \cos(\theta_i) & -\sin(\theta_i) \\ \sin(\theta_i) & \cos(\theta_i) \end{bmatrix}, \quad i = 1,\ldots,N. \qquad (1.2)$$

To complete the description of the multibody system, define a set of position vectors (see Figure 3.3) and associated physical parameters of the system : let,

α_i - inertial vector from joint $(i-1)$ to the center of mass of body i ,

β_i - inertial vector from joint $(J(i)-1)$ to joint $(i-1)$,

$\tilde{\alpha}_i$ - vector from joint $(i-1)$ to the center of mass of body i in the local frame of reference of body i ,

$\tilde{\beta}_i$ - vector from joint $(J(i)-1)$ to joint $(i-1)$ in the local frame of reference of body $J(i)$,

r - vector from the reference point to the system center of mass,

r_i^o - vector from the center of mass of the system of N bodies to the center of mass of body i ,
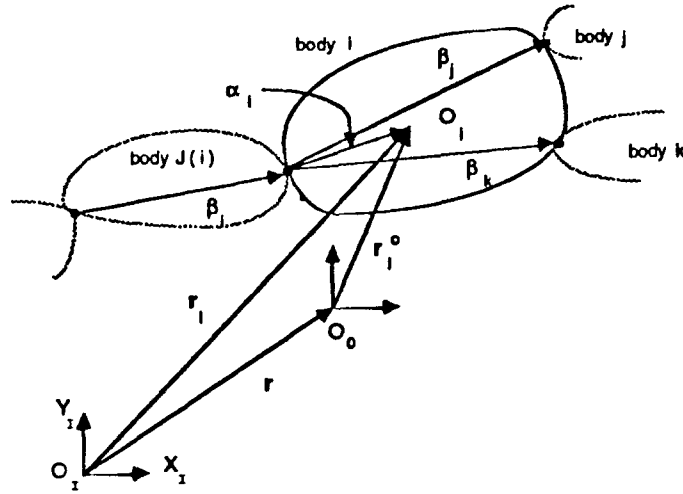
Figure 3.3: Body and inertial vectors

$\mathbf{r}_i$ - vector from the reference point to the center of mass of body i .

See Figure 3.2 for a description of some of these vectors.

Note that for all $i = 2, \ldots, N$,

$$
\begin{aligned}
\mathbf{r}_i &= \mathbf{r} + \mathbf{r}_i^o \\
&= \mathbf{r} + \mathbf{r}_1^o + \sum_{j \in S_{0,i}, \; j \neq 1} \beta_j + \alpha_i \\
&= \mathbf{r}_1 + \sum_{j \in S_{0,i}, \; j \neq 1} \beta_j + \alpha_i,
\end{aligned}
\tag{1.3}
$$

m_i - mass of body i ,

$$
m = \sum_{i=1}^{N} m_i,
\tag{1.4}
$$

I_i - moment of inertia of body i at its center of mass and along an axis perpendicular to the plane of the paper,

K_i - kinetic energy of body i

16

3.2 Basic Kinematics

The configuration space Q for the planar N-body system is the subset of $SE(2) \times \cdots \times SE(2)$ (N copies of the special Euclidean group of the plane) consisting of pairs $((R(\theta_1), \mathbf{r}_1), \ldots, (R(\theta_N), \mathbf{r}_N))$ and satisfying the *joint constraints* :

$$
\begin{aligned}
\mathbf{r}_k &= \mathbf{r}_1 + \sum_{j \in S_{0,k}, \ j \neq 1} \beta_j + \alpha_k \\
&= \mathbf{r}_1 + \sum_{j \in S_{0,k}, \ j \neq 1} R(\theta_{J(j)}) \tilde{\beta}_j + R(\theta_k) \tilde{\alpha}_k, \quad k = 2, \ldots, N.
\end{aligned} \tag{2.1}
$$

Notice that Q is of dimension $N + 2$ and is parametrized by $\theta_1, \ldots, \theta_N$ and, say $\mathbf{r}_1$; i.e. $Q \approx \underbrace{S^1 \times \cdots S^1}_{N \text{ times}} \times \mathbb{R}^2$. We form the velocity phase space TQ and momentum phase space T^*Q.

The Lagrangian on TQ is the map $L : TQ \to \mathbb{R}$, obtained by summing the kinetic energies of the individual bodies, i.e.,

$$
L = \sum_{k=1}^{N} K_k, \tag{2.2}
$$

where K_k is the kinetic energy of body k. The equations of motion then are the Euler-Lagrange equations for this L on TQ :

$$
\left[\frac{d}{dt} \left(\frac{\partial L}{\partial \dot{\underline{q}}} \right) - \frac{\partial L}{\partial \underline{q}} \right] = 0. \tag{2.3}
$$

where, $\underline{q} = [\theta_1, \ldots, \theta_N]^T$. Equivalently, they are Hamilton's equations for the corresponding Hamiltonian.

To formulate L in terms of the kinematic parameters we proceed as follows : let $\mathbf{X}_k$ denote a position vector in body k relative to the center of mass of body k, and let $\rho_k(\mathbf{X}_k)$ denote the mass density of body k (see Figure 3.4). Then the inertial position of the point with material label $\mathbf{X}_k$ is

$$
\mathbf{x}_k = R(\theta_k) \mathbf{X}_k + \mathbf{r}_k.
$$

Thus

$$
\dot{\mathbf{x}}_k = \dot{R}(\theta_k) \mathbf{X}_k + \dot{\mathbf{r}}_k,
$$
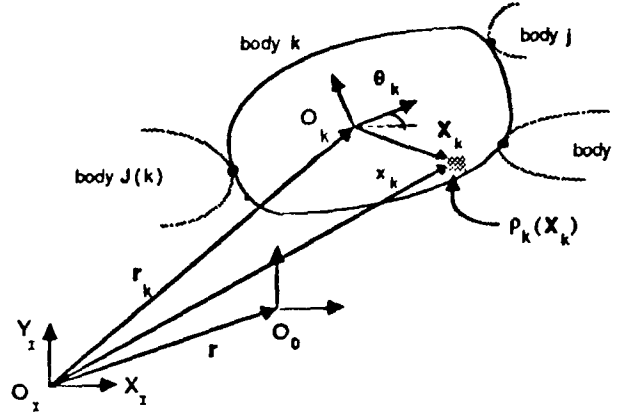
Figure 3.4: Position vectors in body i

and so the kinetic energy of body k is

$$
\begin{aligned}
K_k &= \frac{1}{2}\int_{B_k} \rho_k(\mathbf{X}_k)\parallel \dot{\mathbf{x}}_k \parallel^2 d^2\mathbf{X}_k \\
&= \frac{1}{2}\int_{B_k} \rho_k(\mathbf{X}_k) < \dot{R}(\theta_k)\mathbf{X}_k + \dot{r}_k, \dot{R}(\theta_k)\mathbf{X}_k + \dot{r}_k > d^2\mathbf{X}_k \\
&= \frac{1}{2}\int_{B_k} \rho_k(\mathbf{X}_k)[< \dot{R}(\theta_k)\mathbf{X}_k, \dot{R}(\theta_k)\mathbf{X}_k > + 2 < \dot{R}(\theta_k)\mathbf{X}_k, \dot{r}_k > \\
&\quad + \parallel \dot{r}_k \parallel^2]d^2\mathbf{X}_k.
\end{aligned}
\tag{2.4}
$$

Here B_k denotes the extent of body k and $\rho_k d^2\mathbf{X}_k$ denotes its mass measure. But

$$
\begin{aligned}
< \dot{R}(\theta_k)\mathbf{X}_k, \dot{R}(\theta_k)\mathbf{X}_k > &= tr(\dot{R}(\theta_k)\mathbf{X}_k(\dot{R}(\theta_k)\mathbf{X}_k)^T) \\
&= tr(\dot{R}(\theta_k)\mathbf{X}_k\mathbf{X}_k^T\dot{R}(\theta_k)^T),
\end{aligned}
\tag{2.5}
$$

and

$$
\int_{B_k} \rho_k(\mathbf{X}_k) < \dot{R}(\theta_k)\mathbf{X}_k, \dot{r}_k > d^2\mathbf{X}_k = < \dot{R}(\theta_k)\int_{B_k} \rho_k(\mathbf{X}_k)\mathbf{X}_k d^2X_k, \dot{r}_k > = 0,
\tag{2.6}
$$

since $\mathbf{X}_k$ is the vector relative to the center of mass of body k. Substituting (2.5) and (2.6) into (2.4) and defining the matrix

$$
\mathbf{I}^k = \int_{B_k} \rho(\mathbf{X}_k)\mathbf{X}_k\mathbf{X}_k^T d^2\mathbf{X}_k,
\tag{2.7}
$$

18

we get

$$
\begin{aligned}
K_k &= \frac{1}{2}tr(\dot{R}(\theta_k)\mathbf{I}^k\dot{R}(\theta_k)^T) + \frac{1}{2}m_k \parallel \dot{\mathbf{r}}_k \parallel^2 \\
&= \frac{1}{2}tr(\dot{R}(\theta_k)\mathbf{I}^k\dot{R}(\theta_k)^T) + \frac{1}{2}m_k \parallel \dot{\mathbf{r}}_k^o + \dot{\mathbf{r}} \parallel^2 \\
&= \frac{1}{2}tr(\dot{R}(\theta_k)\mathbf{I}^k\dot{R}(\theta_k)^T) + \frac{1}{2}m_k \left[\parallel \dot{\mathbf{r}}_k^o \parallel^2 + 2 < \dot{\mathbf{r}}_k^o, \dot{\mathbf{r}} > + \parallel \dot{\mathbf{r}} \parallel^2 \right]. \quad (2.8)
\end{aligned}
$$

For later convenience, we shall rewrite the energy (2.2) in terms of $\omega_k = \dot{\theta}_k$, and $\mathbf{r}_k^0$'s. To do this, note by definition the vector from the reference point to the center of mass of the system in the inertial coordinate system is given by

$$
\mathbf{r} = \frac{1}{m} \sum_{k=1}^{N} m_k \mathbf{r}_k. \quad (2.9)
$$

Substituting for $\mathbf{r}_i$ from (1.3) and simplifying we have,

$$
\mathbf{r} = \mathbf{r}_1 + \frac{1}{m} \sum_{l=2}^{N} m_l \left[\sum_{j \in S_{0,l}, \, j \neq 1} \beta_j + \alpha_l \right]. \quad (2.10)
$$

Keeping in mind that $\mathbf{r}_1 = \mathbf{r} + \mathbf{r}_1^o$, we rewrite the above equation as,

$$
\begin{aligned}
\mathbf{r}_1^o &= -\frac{1}{m} \sum_{l=2}^{N} m_l \left[\sum_{j \in S_{0,l}, \, j \neq 1} \beta_j + \alpha_l \right] \\
&= -\sum_{l=2}^{N} \epsilon_l \left[\sum_{j \in S_{0,l}, \, j \neq 1} \beta_j + \alpha_l \right], \quad (2.11)
\end{aligned}
$$

$$
\text{where} \quad \epsilon_l = \frac{m_l}{m}. \quad (2.12)
$$

We know that,

$$
\mathbf{r}_k^o = \mathbf{r}_1^o + \sum_{j \in S_{0,k}, \, j \neq 1} \beta_j + \alpha_k. \quad (2.13)
$$

From (2.11) and (2.13) we get,

$$
\begin{aligned}
\mathbf{r}_k^o &= -\sum_{l=2}^{N} \epsilon_l \left[\sum_{i \in S_{0,l}, \, i \neq 1} \beta_i + \alpha_l \right] + \sum_{j \in S_{0,k}, \, j \neq 1} \beta_j + \alpha_k \\
&= \sum_{l=1}^{N} [a_{k,l}\beta_l + b_{k,l}\alpha_l] \quad, \quad (2.14)
\end{aligned}
$$

where,

$$a_{k,l} = \begin{cases} 1 - \sum_{j=2}^{N} I_{l,j}\epsilon_l & \text{if } l \in S_{0,k} \text{ and } k \neq 1, \\ -\sum_{j=2}^{N} I_{l,j}\epsilon_l & \text{otherwise}, \end{cases}$$

$$I_{l,j} = \begin{cases} 1 & \text{if } l \in S_{0,j}, \\ 0 & \text{otherwise}, \end{cases}$$

$$b_{k,l} = \begin{cases} 1 - \epsilon_l & \text{if } l = k, \\ -\epsilon_l & \text{if } l \neq k. \end{cases}$$

Differentiating (2.14) w.r.t. time we get

$$\dot{\mathbf{r}}_k^o = \sum_{l=1}^{N} \left[a_{k,l}\dot{\beta}_l + b_{k,l}\dot{\alpha}_k \right]. \tag{2.15}$$

Now we substitute

$$\beta_l = R(\theta_{J(l)})\tilde{\beta}_l \quad \text{so} \quad \dot{\beta}_l = \dot{R}(\theta_{J(l)})\tilde{\beta}_l,$$

$$\alpha_l = R(\theta_l)\tilde{\alpha}_l \quad \text{so} \quad \dot{\alpha}_l = \dot{R}(\theta_l)\tilde{\alpha}_l,$$

into (2.14) to get

$$\begin{aligned}
\mathbf{r}_k^o &= \sum_{l=1}^{N} \left[a_{k,l}R(\theta_{J(l)})\tilde{\beta}_l + b_{k,l}R(\theta_l)\tilde{\alpha}_l \right] \\
&= \sum_{l=1}^{N} R(\theta_l)\tilde{\delta}_{k,l},
\end{aligned} \tag{2.16}$$

and into (2.15) to get

$$\begin{aligned}
\dot{\mathbf{r}}_k^o &= \sum_{l=1}^{N} \left[a_{k,l}\dot{R}(\theta_{J(l)})\tilde{\beta}_l + b_{k,l}\dot{R}(\theta_l)\tilde{\alpha}_l \right] \\
&= \sum_{l=1}^{N} \dot{R}(\theta_l)\tilde{\delta}_{k,l},
\end{aligned} \tag{2.17}$$

where $\tilde{\delta}_{k,l}$ is given by

$$\begin{aligned}
\tilde{\delta}_{k,l} &= \sum_{\forall i,\ s.t.\ J(i) = l} \left[a_{k,i}\tilde{\beta}_i \right] + b_{k,l}\tilde{\alpha}_l \\
&= \begin{bmatrix} \tilde{\delta}_{k,l}^1 \\ \tilde{\delta}_{k,l}^2 \end{bmatrix}.
\end{aligned} \tag{2.18}$$

20

Also from (1.2)

$$
\begin{aligned}
\dot{R}(\theta_l) &= \frac{d}{dt}\begin{bmatrix} \cos(\theta_l) & -\sin(\theta_l) \\ \sin(\theta_l) & \cos(\theta_l) \end{bmatrix} \\
&= \begin{bmatrix} -\sin(\theta_l) & -\cos(\theta_l) \\ \cos(\theta_l) & -\sin(\theta_l) \end{bmatrix}\omega_l := R(\theta_l)\begin{bmatrix} 0 & -\omega_l \\ \omega_l & 0 \end{bmatrix} \\
&:= R(\theta_l)\hat{\omega}_l.
\end{aligned}
\tag{2.19}
$$

From (2.17) and (2.19) we find

$$
\begin{aligned}
\parallel \dot{\mathbf{r}}_k^o \parallel^2 &= \langle \sum_{j=1}^{N}[\dot{R}(\theta_j)\tilde{\delta}_{k,j}],\ \sum_{l=1}^{N}[\dot{R}(\theta_l)\tilde{\delta}_{k,l}]\rangle \\
&= \sum_{j=1}^{N}\sum_{l=1}^{N}\tilde{\delta}_{k,j}^{T}.\dot{R}(\theta_j)^{T}.\dot{R}(\theta_l).\tilde{\delta}_{k,l} \\
&= \sum_{j=1}^{N}\parallel \tilde{\delta}_{k,j}^{T}\parallel^2 \omega_j^2 \\
&\quad + 2\sum_{j=1}^{N-1}\sum_{l=j+1}^{N}\tilde{\delta}_{k,j}^{T}.\begin{bmatrix} \cos(\theta_j-\theta_l) & \sin(\theta_j-\theta_l) \\ -\sin(\theta_j-\theta_l) & \cos(\theta_j-\theta_l) \end{bmatrix}.\tilde{\delta}_{k,l}\omega_l\omega_j
\end{aligned}
\tag{2.20}
$$

Substituting from (2.18) for $\tilde{\delta}_{k,l}$ in the above equation we get,

$$
\begin{aligned}
\parallel \dot{\mathbf{r}}_k^o \parallel^2 &= \sum_{j=1}^{N}\parallel \tilde{\delta}_{k,j}\parallel^2 \omega_j^2 + 2\sum_{j=1}^{N-1}\sum_{l=j+1}^{N}\left\{\left[\tilde{\delta}_{k,j}^1\tilde{\delta}_{k,l}^1 + \tilde{\delta}_{k,j}^2\tilde{\delta}_{k,l}^2\right]\cos(\theta_j-\theta_l)\right. \\
&\quad \left. + \left[\tilde{\delta}_{k,j}^1\tilde{\delta}_{k,l}^2 - \tilde{\delta}_{k,j}^2\tilde{\delta}_{k,l}^1\right]\sin(\theta_j-\theta_l)\right\}\omega_l\omega_j \\
&= \sum_{j=1}^{N}\parallel \tilde{\delta}_{k,j}\parallel^2 \omega_j^2 + 2\sum_{j=1}^{N-1}\sum_{l=j+1}^{N}\left\{\left[\tilde{\delta}_{k,j}.\tilde{\delta}_{k,l}\right]\cos(\theta_{j,l})\right. \\
&\quad \left. + \left[|\tilde{\delta}_{k,j}\times\tilde{\delta}_{k,l}|\right]\sin(\theta_{j,l})\right\}\omega_l\omega_j,
\end{aligned}
\tag{2.21}
$$

where $\theta_{j,l} = (\theta_j - \theta_l)$ and

$$
|\tilde{\delta}_{k,j}\times\tilde{\delta}_{k,l}| := \left[\tilde{\delta}_{k,j}^1\tilde{\delta}_{k,l}^2 - \tilde{\delta}_{k,j}^2\tilde{\delta}_{k,l}^1\right].
\tag{2.22}
$$

Recall that the Lagrangian for the system which is also the total kinetic energy of the

system is then given by,

$$L = \frac{1}{2}\sum_{k=1}^{N} tr(\dot{R}(\theta_k)\mathbf{I}^k\dot{R}(\theta_k)^T) + \frac{1}{2}\sum_{k=1}^{N} m_k \left[\| \dot{\mathbf{r}}_k^o \|^2 + 2 < \dot{\mathbf{r}}_k^o, \dot{\mathbf{r}} > + \| \dot{\mathbf{r}} \|^2\right]. \quad (2.23)$$

But

$$\sum_{k=1}^{N} m_k \mathbf{r}_k^o = 0 \quad \text{so} \quad \sum_{k=1}^{N} m_k \dot{\mathbf{r}}_k^o = 0, \quad (2.24)$$

and from (2.19) we can see that

$$\begin{aligned}
tr(\dot{R}(\theta_k).\mathbf{I}^k.\dot{R}(\theta_k)^T) &= tr(R(\theta_k)^T.\hat{\omega}_k^T.\mathbf{I}^k.\hat{\omega}_k.R(\theta_k)) = tr(\hat{\omega}_k^T\mathbf{I}^k\hat{\omega}_k) \\
&= tr(\hat{\omega}_k^T\hat{\omega}_k\mathbf{I}^k) = tr(\begin{bmatrix} \omega_k^2 & 0 \\ 0 & \omega_k^2 \end{bmatrix}\mathbf{I}^k) = \omega_k^2 tr(\mathbf{I}^k) \\
&:= \omega_k^2 I_k, \quad (2.25)
\end{aligned}$$

where,

$$I_k = \int_{B_k} \rho(X_k, Y_k)(X_k^2 + Y_k^2)dX_kdY_k,$$

is the moment of inertia of the body k about the Z axis of the local frame of reference. Substituting (2.24) and (2.25) into (2.23) gives

$$L = \frac{1}{2}\sum_{k=1}^{N} \left\{I_k\omega_k^2 + m_k \| \dot{\mathbf{r}}_k^o \|^2 + m_k \| \dot{\mathbf{r}} \|^2\right\}.$$

Finally simplifying using (2.21) we get

$$\begin{aligned}
L &= \frac{1}{2}\left\{\sum_{k=1}^{N} \tilde{I}_k\omega_k^2 + 2\sum_{j=1}^{N-1}\sum_{l=j+1}^{N} \tilde{\lambda}_{jl}(\theta_{l,j})\omega_j\omega_l\right\} + \frac{1}{2}m \| \dot{\mathbf{r}} \|^2 \\
&= \frac{1}{2}\underline{\omega}^T\mathbf{J}\underline{\omega} + \frac{\| \mathbf{p} \|^2}{2m}, \quad (2.26)
\end{aligned}$$

where, $\mathbf{p} = m\dot{\mathbf{r}}$ is the system *linear momentum*, m is as given by (1.4),

$$\underline{\omega} = [\omega_1, \cdots, \omega_N]^T, \quad (2.27)$$

$$\mathbf{J} = \begin{bmatrix} \tilde{I}_1 & \tilde{\lambda}_{12} & \cdots & \tilde{\lambda}_{1N} \\ \tilde{\lambda}_{12} & \tilde{I}_2 & \cdots & \tilde{\lambda}_{2N} \\ \vdots & \vdots & \ddots & \vdots \\ \tilde{\lambda}_{1N} & \tilde{\lambda}_{2N} & \cdots & \tilde{I}_N \end{bmatrix} \quad (2.28)$$

is a symmetric nonsingular matrix; for the sake of clarity the arguments of $\tilde{\lambda}_{jl}$ have been dropped,

$$\tilde{\lambda}_{jl}(\theta_{l,j}) = \left[\sum_{k=1}^{N} m_k (\tilde{\delta}_{kj}.\tilde{\delta}_{kl})\right] \cos(\theta_{l,j}) + \left[\sum_{k=1}^{N} m_k (|\tilde{\delta}_{kj} \times \tilde{\delta}_{kl}|)\right] \sin(\theta_{l,j}), (2.29)$$

note that $\tilde{\lambda}_{jl} = \tilde{\lambda}_{lj}$;

$$\tilde{I}_k = I_k + \sum_{j=1}^{N} m_j \parallel \tilde{\delta}_{jk} \parallel^2 . \qquad (2.30)$$

Remark 3.2.1 : The $\tilde{I}_k$ of a body k is the moment of inertia of an "augmented" body k with *lumped reduced masses* at the joints through which it is connected to other bodies. It is to be noted here that the concept of "augmented" bodies arises naturally in the context of multibody problems in our formulation.

Remark 3.2.2 : The term "augmented body" was first used by Hooker and Margulies [22] in the context of tree connected multibody dynamics. They define "augmented body" k as follows. Consider a body k in the multibody system. For each joint $(l - 1)$ on the body k the mass distribution of body k is augmented by the mass equal to

$$m_k^l = \sum_{j \in S_{k-1,l}, \, j \neq k} m_j.$$

Obviously the *mass* of the "augmented body" is defined as equal to

$$\widehat{m}_k = m_k + \sum_{\forall j, \, s.t. \, J(l)=k} m_k^l.$$

The center of mass of the "augmented body" (also known as the *connection barycenter* or simply *barycenter*) could be obtained easily. The inertia dyadic for this "augmented body" about its *barycenter* figures prominently in the formulation of the system dynamics. Also see Wittenburg [59]. In contrast a quick look at (2.30) and (2.18) indicates that in our formulation we use *lumped reduced masses* at the joints instead of lumped masses.

3.3 Legendre Transformation

The *Legendre Transformation* maps the Lagrangian equations into the corresponding Hamiltonian equations. Classically, the name *Legendre transformation* (see Courant and Hilbert [8]) is reserved for a map from

$$L(\underline{q},\underline{\dot{q}}) \mapsto H(\underline{q},\underline{p}) = \underline{\dot{q}}^T \underline{p} - L(\underline{q},\underline{\dot{q}}), \tag{3.1}$$

where $L : TQ \to \mathbb{R}$ is the Lagrangian, $H : T^*Q \to \mathbb{R}$ is the Hamiltonian, and

$$\underline{q} = [q_1, \ldots, q_N]^T, \tag{3.2}$$

$$\underline{p} = [p_1, \ldots, p_N]^T = \frac{\partial L}{\partial \underline{\dot{q}}}. \tag{3.3}$$

Here, we state a theorem which gives the Legendre transformation explicitly with the proof given in coordinate notation. Using this transformation we construct the Hamiltonian for the system of N planar rigid bodies connected in the form of tree structure. Some definitions are in order before we give the theorem.

Definition 3.3.1 : Let (E, π, M) and (F, ρ, M) be *fiber bundles* with the same base space M. Let $\pi : E \to M : e \mapsto m$ and $\rho : F \to M$. If $e_0 = \pi^{-1}m \subset E$, then e_0 is a *fiber* of E. The concept of *fiber bundle* generalizes the notion of a product space.

Let $f : E \to F$ be a smooth map which is fiber preserving, then $\pi(e) = \rho \circ f(e)$, i.e., the following diagram commutes.

$$
\begin{array}{ccc}
E & \xrightarrow{\;\;f\;\;} & F \\
 & \pi \searrow \quad \swarrow \rho & \\
 & M &
\end{array}
$$

Let $\pi(e_m) = m \in M$ and $f_m = f|E_m = f|\pi^{-1}(m)$. Then the *fiber derivative*

of f_m (Frechet derivative of f_m) evaluated at e_m is the map

$$Ff : E \rightarrow \bigcup_{m \in M} L(E_m, F_m),$$
$$e_m \mapsto Df_m(e_m) \in L(E_m, F_m).$$

For our purposes we specialize M to be the configuration space Q, E to be TQ the tangent bundle of Q, and F to be $Q \times \mathbb{R}$. We consider the Lagrangian L on the *velocity phase space* TQ as the map $L : TQ \rightarrow \mathbb{R}$. Let $\tilde{L} : TQ \rightarrow Q \times \mathbb{R} : v_q \mapsto q \times \mathbb{R}$. Then the *fiber derivative* $F\tilde{L}$ is

$$F\tilde{L}(v_q) \approx FL(v_q) = DL_q \in L(TQ_q, \mathbb{R}) = T^*Q$$

The Hamiltonian on the *momentum phase space* T^*Q is a map $H : T^*Q \rightarrow \mathbb{R}$ that can be expressed in terms of FL.

Definition 3.3.2 : The *action A* is defined as $A : TQ \rightarrow \mathbb{R}$, by $A(v_x) = FL(v_x).v_x$; in coordinate notation $A(\underline{q}, \underline{\dot{q}}) = \underline{\dot{q}}^T \frac{\partial L}{\partial \underline{\dot{q}}}$. The *energy* function E, defined by $E = A - L$ is determined on TQ by L.

When E is translated to T^*Q by means of the *fiber derivative* of L, $FL : TQ \rightarrow T^*Q$, we get a suitable Hamiltonian. Then solution curves in both T^*Q and TQ will coincide when projected to Q, i.e., the solution curves of the Hamiltonian and the Lagrangian equations coincide on Q. τ_Q and τ_Q^* are maps from TQ and T^*Q to Q respectively. The following diagram helps keep the relations straight.
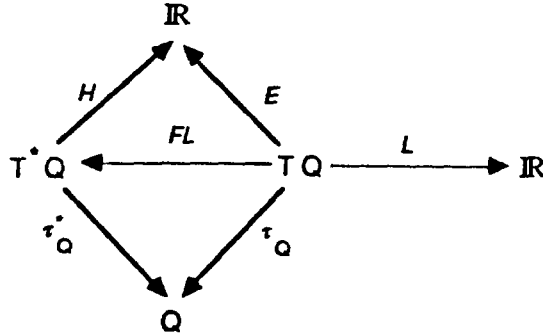
Definition 3.3.3 : Let M be a manifold. Define $\tau_M : TM \rightarrow M$ and $c(t) : I \rightarrow$

25

TM. Then $\tau_M \circ c : I \to M$ is a *base integral curve.*

Theorem 3.3.1 : Let L be the Lagrangian on Q with a diffeomorphic *fiber derivative* $FL : TQ \to T^*Q$, and let $H = E \circ (FL)^{-1} : T^*Q \to \mathbb{R}$, where E is the *energy* of L. Then the vector fields X_E and X_H are related by $(FL)_* X_E = X_H$. Furthermore X_E and X_H have the same base integral curves.

Proof : The proof of this theorem is given here in coordinate notation (for more details and a 'coordinate free' proof see Theorem 3.6.2 and Example 3.6.10, Abraham and Marsden [2]).

Let $\underline{q} = [q_1, \ldots, q_N]^T$ and $\underline{p} = [p_1, \ldots, p_N]^T$. By the definition of *fiber derivative* FL we have

$$FL : TQ \quad \to \quad T^*Q : (\underline{q}, \dot{\underline{q}}) \mapsto (\underline{q}, \underline{p}) = \left(\underline{q}, \frac{\partial L}{\partial \dot{\underline{q}}} \right).$$

Recall from the definition of the *action* we have $A(\underline{q}, \dot{\underline{q}}) = \dot{\underline{q}}^T \frac{\partial L}{\partial \dot{\underline{q}}}$ and $\underline{p} = \frac{\partial L}{\partial \dot{\underline{q}}}$ from (3.3), so,

$$
\begin{aligned}
H(\underline{q}, \underline{p}) &= E \circ (FL)^{-1}(\underline{q}, \underline{p}) \\
&= A(\underline{q}, \dot{\underline{q}}) - L(\underline{q}, \dot{\underline{q}}) \\
&= \dot{\underline{q}} \frac{\partial L}{\partial \dot{\underline{q}}} - L(\underline{q}, \dot{\underline{q}}) \\
&= \dot{\underline{q}}^T \underline{p} - L(\underline{q}, \dot{\underline{q}}),
\end{aligned}
\tag{3.4}
$$

which is the Hamiltonian.

Taking partials on (3.4) yields

$$
\begin{aligned}
\frac{\partial H}{\partial p_i} &= \dot{q}_i + \sum_j \frac{\partial \dot{q}_j}{\partial p_j} p_j - \sum_j \frac{\partial L}{\partial \dot{q}_j} \frac{\partial \dot{q}_j}{\partial p_j} \\
&= \dot{q}_i.
\end{aligned}
\tag{3.5}
$$

Keeping in mind the Lagrangian dynamical equations $\frac{d}{dt} \left(\frac{\partial L}{\partial \dot{q}_i} \right) - \frac{\partial L}{\partial \underline{q}} = 0$, and (3.3) we find that

$$\dot{\underline{p}}_i = \frac{\partial L}{\partial q_i},$$

or from (3.4) we have,

$$\frac{\partial H}{\partial q_i} = -\frac{\partial L}{\partial q_i}$$
$$= -\dot{p}_i. \tag{3.6}$$

So from (3.5) and (3.6) we find that

$$\left.\begin{array}{rcl}\underline{\dot{q}} & = & \frac{\partial H}{\partial \underline{p}} \\[2mm] \underline{\dot{p}} & = & -\frac{\partial H}{\partial \underline{q}}\end{array}\right\}, \tag{3.7}$$

which are the Hamiltonian dynamical equations with the Hamiltonian given by (3.4).
Q.E.D.

3.3.1 Hamiltonian for the Multibody Problem

In the planar multibody problem, the configuration space Q can be coordinatized by $(\theta_1, \ldots, \theta_N, \mathbf{r}_1)$ and the tangent space TQ by $(\theta_1, \ldots, \theta_N, \omega_1, \ldots, \omega_N)$, i.e., $\underline{\dot{q}} = [\omega_1, \ldots, \omega_N]^T$. The Lagrangian, from (2.26), is given by

$$L = \frac{1}{2}\underline{\omega}^T \mathbf{J}\underline{\omega} + \frac{\| \mathbf{p} \|^2}{2m}. \tag{3.8}$$

With $\underline{p} = \underline{\mu} = [\mu_1, \ldots, \mu_N]^T$, a simple calculation from (3.3) indicates that

$$\underline{\mu} = \frac{\partial L}{\partial \underline{\omega}}$$
$$= \mathbf{J}\underline{\omega}. \tag{3.9}$$

Constructing the Hamiltonian analogous to (3.1) using (3.9) leads to

$$H = \frac{1}{2}\underline{\mu}^T \mathbf{J}^{-1}\underline{\mu} + \frac{\| \mathbf{p} \|^2}{2m}, \tag{3.10}$$

where $\mu = [\mu_1, \ldots, \mu_N]^T$ and μ_k's, $k = 1, \cdots, N$, are the *conjugate momenta*.

Remark 3.3.1: By making use of the reduction technique due to Arnold [1] and Marsden and Weinstein [41] we can prove that in the general case of a system of N planar rigid bodies connected in the form of a tree, the Hamiltonian is indeed given by (3.10), with the linear momentum equal to zero. This we do in the next section.

3.4 Symmetries

In this section we recognize the basic symmetries involved in the planar N rigid body problem and reduce the dynamics accordingly. The reduction technique used here goes back to Arnold [1] and Marsden and Weinstein [41]. One starts with a Poisson manifold P and a Lie group G acting on P by canonical transformations. The reduced phase space P/G (assume it has no singularities) has a natural Poisson structure whose symplectic leaves are the Marsden-Weinstein-Meyer spaces $J^{-1}(\mu)/G_\mu \approx J^{-1}(\mathcal{O})/G$ where $\mu \in \mathbf{g}^*$, the dual of the Lie algebra of G, $J : P \to \mathbf{g}^*$ is an equivariant momentum map for the action of G on P, G_μ is the isotropy group of μ (relative to the coadjoint action) i.e., $G_\mu = \left\{ g \in G \ : \ Ad^*_{g^{-1}}\mu = \mu \right\}$, and $\mathcal{O}$ is the coadjoint orbit through μ. The coadjoint orbit $\mathcal{O}$, is even dimensional and possess a natural symplectic structure known as Kirillov 2-form (see Kirillov [35]). For details, we refer the reader to Chapter 2 for a brief exposition on *momentum map* (also see Abraham and Marsden [2] Chapter 4, Section 4.3) and Marsden and Weinstein [41] for the Marsden-Weinstein reduction theorem.

3.4.1 Reduction to the Center of Mass Frame

We reduce the dynamics by the action of the translation group $\mathbb{R}^2$. This group acts on the original configuration space Q by

$$\mathbf{v} \cdot ((R(\theta_1), \mathbf{r}_1), \ldots, (R(\theta_N), \mathbf{r}_N)) = ((R(\theta_1), \mathbf{r}_1 + \mathbf{v}), \ldots, (R(\theta_N), \mathbf{r}_N + \mathbf{v})) \quad (4.1)$$

This is well-defined since the joint constraints (2.1) are preserved by this action. The induced momentum map on TQ is calculated by the standard formula

$$J_\xi = \frac{\partial L}{\partial \dot{q}_i} \xi^i_Q(q), \quad (4.2)$$

or on T^*Q by

$$J_\xi = p_i \xi^i_Q(q), \quad (4.3)$$

where ξ^i is the infinitesimal generator of the action on Q. (see Abraham and Marsden [2]). To compute (4.2) and (4.3) we parametrize Q by $\theta_1, \ldots, \theta_N$ and $\mathbf{r}$ with $\mathbf{r}_k$, $k =$

$1, \ldots, N$ determined by (2.14). From (2.26) we see that the momentum conjugate to $\mathbf{r}$ is

$$\mathbf{p} = \frac{\partial L}{\partial \dot{\mathbf{r}}} = m\dot{\mathbf{r}},$$

and so (4.2) and (4.3) gives

$$J_\xi = \langle \mathbf{p}, \xi \rangle, \quad \xi \in \mathbb{R}^2. \tag{4.4}$$

Thus $J = \mathbf{p}$ is conserved since $\mathbf{H}$ is cyclic in $\mathbf{r}$ and so is translation invariant. The corresponding reduced space is obtained by fixing $\mathbf{p} = \mathbf{p}_0$ and letting

$$P_{\mathbf{p}_0} = J^{-1}(\mathbf{p}_0)/\mathbb{R}^2, \tag{4.5}$$

(see Chapter 4, Abraham and Marsden, [2],). But $P_{\mathbf{p}_0}$ is clearly isomorphic to $T^*(\underbrace{S^1 \times \cdots \times S^1}_{N \ times})$ i.e. to the space of $\theta_1, \ldots,\ \theta_N$ and their conjugate momenta $(\mu_1, \ldots, \mu_N)$. The reduced Hamiltonian is simply the Hamiltonian corresponding to (2.26) with $\mathbf{p}$ regarded as a constant.

Note that in this case the reduced symplectic manifold is a cotangent bundle, in agreement with the cotangent bundle reduction theorem (Abraham and Marsden [2], Kummer [36]). The reduced phase space has the *canonical* symplectic form; one can also check this directly here.

In (2.26) we can adjust L by a constant and thus assume $\mathbf{p} = 0$; this obviously does not affect the equations of motion.

Reduced Hamiltonian

The Lagrangian from (2.26) is given by

$$L = \frac{1}{2}\underline{\omega}^T \mathbf{J}\underline{\omega} + \frac{\|\mathbf{p}\|^2}{2m}. \tag{4.6}$$

Assuming $\mathbf{p} = 0$, and using the *Legendre transform* and the corresponding conjugate momentum vector (see section 3.3.1) $\underline{\mu} = \mathbf{J}\underline{\omega}$, we get the Hamiltonian as,

$$H = \frac{1}{2}\underline{\mu}^T \mathbf{J}^{-1}\underline{\mu}. \tag{4.7}$$

It is to be noted here that $\mathbf{J} = \mathbf{J}(\underline{q})$ where $\underline{q} = [\theta_1, \cdots, \theta_N]$.

Let us observe that the reduced system is given by geodesic flow on $\underbrace{S^1 \times \cdots \times S^1}_{N \ times}$ since (2.26) is quadratic in the velocities. Indeed the metric tensor is just the matrix $\mathbf{J}$ given by (2.28).

Remark 3.4.1 : The reduction to center of mass coordinates here is somewhat simpler and more symmetric than the Jacobi-Haretu reduction to center of mass coordinates for n point masses. (Just taking the positions relative to the center of mass does not achieve this since this does not reduce the dimension at all!) What is different here is that the bodies are connected by revolute joints, and so by (2.13), $\mathbf{r_k}^0$'s for $j = 1, \ldots, N$, are determined by other data.

3.4.2 Reduction by Rotations

Recall from the previous section that the configuration space after reduction to the center of mass frame is

$$Q \cong \underbrace{(S^1 \times \cdots \times S^1)}_{N \ times},$$

and so the cotangent space is $T^*\underbrace{(S^1 \times \cdots \times S^1)}_{N \ times}$.

There exists a rotational symmetry group S^1 which acts on the cotangent space as follows :

$$
\begin{aligned}
\theta \cdot ((\theta_1, \mu_1), \cdots, (\theta_N, \mu_N)) &= ((\theta_1 + \theta, \mu_1), \cdots, (\theta_N + \theta, \mu_N)) \\
&= ((\theta_1, \mu_1), \cdots, (\theta_N, \mu_N)).
\end{aligned}
$$

To complete the reduction, we reduce by the diagonal action of S^1 on the configuration space $\underbrace{S^1 \times \cdots \times S^1}_{N \ times}$ that was obtained in Section 3.2.1. The momentum map for this action is found next. We know that S^1 is diffeomorphic to $SO(2)$ (the special orthogonal group of (2×2) matrices i.e., $A \in SO(2)$, $AA^T = I$, and $\det(A) = 1$). The Lie algebra of $SO(2)$ is $so(2)$ (skew-symmetric matrices with determinant equal to k, k¿0), i.e., $T_e SO(2) = so(2)$.

30

For

$$\xi \; = \; \begin{bmatrix} 0 & 1 \\ -1 & 0 \end{bmatrix},$$

where $\xi \in so(2)$, the *exponential* of ξ is

$$\exp(t\xi) \; = \; \exp\left(t\begin{bmatrix} 0 & 1 \\ -1 & 0 \end{bmatrix}\right)$$

$$= \; \begin{bmatrix} \cos(t) & \sin(t) \\ -\sin(t) & \cos(t) \end{bmatrix},$$

So $\exp(t\xi) \in O(2)$.

The *infinitesimal generator* $\xi_Q(q)$ can now be calculated as follows :

$$\xi_Q(q) \; = \; \frac{d}{dt}\Phi(\exp(t\xi), q) \;|_{t=0}$$

$$= \; \frac{d}{dt}\Phi(\begin{bmatrix} \cos(t) & \sin(t) \\ -\sin(t) & \cos(t) \end{bmatrix}, \; (\theta_1, \ldots, \theta_N) \;) \;|_{t=0}$$

$$= \; \frac{d}{dt}(\theta_1 + t, \ldots, \theta_N + t) \;|_{t=0}$$

$$= \; (1, \ldots, 1).$$

The *momentum map* is given by

$$J : T^*Q \; \rightarrow \; \mathbf{g}^* \; = \; so^*(2),$$

with the *momentum* $P : TQ \rightarrow \mathbf{R}$

$$P(v_q) \; = \; \hat{J}(\xi)(v_q)$$

$$= \; FL(v_q) \cdot \xi_Q(q)$$

$$= \; \langle v_Q, \xi_Q(q) \rangle \quad \text{on } \mathbf{TQ}.$$

Note that the metric here is the Reimannian metric and the inner product '$\langle , \rangle$' is given by $\langle \underline{x}, \underline{y} \rangle = \underline{x}^T J \underline{y}$.

$$P(v_q) \; = \; \langle (\omega_1, \ldots, \omega_N) \;, \; (1, \cdots, 1) \rangle$$

$$= \; [1, \ldots, 1] J \underline{\omega} \quad \text{on } \mathbf{TQ},$$

31

or on T^*Q, for $\alpha_q \in T^*Q$ we have

$$P(\alpha_q) \;=\; \mu_1 \;+\; \cdots \;+\; \mu_N.$$

i.e.,

$$J((\theta_1, \mu_1), \ldots, (\theta_N, \mu_N)) \;=\; \mu_1 \;+\; \cdots \;+\; \mu_N. \qquad (4.8)$$

For purposes of later stability calculations, we shall find it convenient to form the Poisson reduced space

$$P \;:=\; T^*(\underbrace{S^1 \times \cdots \times S^1}_{N\ times})/S^1 \qquad (4.9)$$

whose symplectic leaves are the reduced symplectic manifolds

$$P_\mu \;=\; J^{-1}(\mu)/S^1 \subset P \qquad (4.10)$$

We coordinatize P by $\theta_{k,J(k)}$, $k = 2, \ldots, N$, and μ_j, $j = 1, \ldots N$; topologically,

$$P \;=\; \underbrace{S^1 \times \cdots \times S^1}_{(N-1)\ times} \times \mathbb{R}^N. \qquad (4.11)$$

The Poisson structure on P is computed in the standard way: take two functions $F(\theta_{k,J(k)}, k = 1, \ldots, N, \mu_1, \ldots, \mu_N)$ and $H(\theta_{k,J(k)}, k = 2, \ldots, N, \mu_1, \ldots, \mu_N)$. Regard them as functions of $\theta_1, \ldots, \theta_N, \mu_1, \ldots, \mu_N$ by substituting $\theta_{k,J(k)} = \theta_k - \theta_{J(k)}$ and compute the canonical bracket.

Lemma 3.4.1 : The Poisson structure on P is given by the non-canonical bracket

$$\{f, g\} \;=\; \sum_{k=2}^{N} \left[\left(\frac{\partial f}{\partial \mu_{J(k)}} - \frac{\partial f}{\partial \mu_k} \right) \frac{\partial g}{\partial \theta_{k,J(k)}} - \left(\frac{\partial g}{\partial \mu_{J(k)}} - \frac{\partial g}{\partial \mu_k} \right) \frac{\partial f}{\partial \theta_{k,J(k)}} \right], (4.12)$$

where $f, g : P \mapsto \mathbf{R}$.

Proof : The canonical bracket on the Poisson manifold P is given by (see Chapter 2) :

$$\{f, g\} \;=\; \sum_{k=1}^{N} \left[\frac{\partial f}{\partial \mu_k} \frac{\partial g}{\partial \theta_k} - \frac{\partial g}{\partial \mu_k} \frac{\partial f}{\partial \theta_k} \right]. \qquad (4.13)$$

Since $f, g : P \mapsto \mathbf{R}$ and P is coordinatized by $\mu_1, \ldots, \mu_N, \theta_{k,J(k)}$, $k = 2, \ldots, N$, we have f and g being functions of $\mu_1, \ldots, \mu_N, (\theta_k - \theta_{J(k)})$, $k = 2, \ldots, N$, since $\theta_{k,J(k)} = (\theta_k - \theta_{J(k)})$.

Therefore,

$$\frac{\partial f}{\partial \theta_k} = \frac{\partial f}{\partial \theta_{k,J(k)}}, \tag{4.14}$$

$$\frac{\partial f}{\partial \theta_{J(k)}} = -\frac{\partial f}{\partial \theta_{k,J(k)}}. \tag{4.15}$$

Substituting (4.14) and (4.15) in (4.13) and combining suitable terms results in the non-canonical bracket (4.12). Q.E.D..

CASIMIRS

The Casimirs on P are obtained by composing J with Casimirs on the dual of the Lie algebra of S^1; i.e. with arbitrary functions of one variable; thus

$$C = \Phi(\mu_1 + \ldots + \mu_N), \tag{4.16}$$

results. This can of course be checked directly.

The cotangent bundle reduction theorem asserts in this case that the reduction of $T^*(\underbrace{S^1 \times \cdots \times S^1}_{N \ times})$ by S^1 is symplectically diffeomorphic to

$$T^*(\underbrace{S^1 \times \cdots \times S^1}_{N \ times})/S^1 \cong T^*(\underbrace{S^1 \times \cdots \times S^1}_{(N-1) \ times}).$$

Remark 3.4.2: The reduced bracket on $T^*(S^1 \times \cdots \times S^1)/S^1$ can also be obtained from the general formula for the bracket on $(P \times T^*G)/G \cong P \times g^*$ found in Krishnaprasad and Marsden [34].

The reduced Hamiltonian on P is just (3.10) regarded as a function of $\mu_1, \ldots, \mu_N$ and $\theta_{k,J(k)}$, $k = 2, \ldots, N$. We therefore know that the Euler-Lagrange equations (2.3) are equivalent to $\dot{F} = \{F, H\}$ for the reduced bracket (4.12).

Reduced Hamiltonian

The reduced Hamiltonian is given by

$$H = \frac{1}{2}\underline{\mu}^T \mathbf{J}^{-1}(\underline{q})\underline{\mu} = \frac{1}{2}\underline{\mu}^T \mathbf{J}^{-1}(\underline{\theta})\underline{\mu}, \tag{4.17}$$

where the conjugate momentum vector $\underline{\mu} = [\mu_1, \ldots, \mu_N]$ and $\underline{\theta} = \left[\theta_{k,J(k)}, \; k = 2, \cdots, N\right]$.

The *momentum map J* is given by

$$J(\underline{\mu}) \;\; = \;\; \mu_1 \; + \; \cdots \; + \; \mu_N.$$

and the conjugate momenta μ_i's are given by

$$\underline{\mu} \;\; = \;\; \mathbf{J}(\underline{\theta})\underline{\omega}, \tag{4.18}$$

with $\underline{\omega}$ and $\mathbf{J}$ given by (2.27) and (2.28) respectively.

We now take a moment to review our analysis and put the results obtained so far into perspective. The reduced Poisson space P is coordinatized by $\theta_{k,J(k)}$, $k = 2, \ldots, N$ and μ_k, $k = 1, \ldots, N$; topologically $P = \underbrace{S^1 \times \cdots \times S^1}_{(N-1) \; times} \times \mathbb{R}^N$. The Poisson structure on this manifold is given by

$$\{f, g\} \;\; = \;\; \sum_{k=2}^{N} \left[\left(\frac{\partial f}{\partial \mu_{J(k)}} - \frac{\partial f}{\partial \mu_k} \right) \frac{\partial g}{\partial \theta_{k,J(k)}} - \left(\frac{\partial g}{\partial \mu_{J(k)}} - \frac{\partial g}{\partial \mu_k} \right) \frac{\partial f}{\partial \theta_{k,J(k)}} \right], \tag{4.19}$$

We summarize the results so far as a lemma.

Lemma 3.4.2 : The reduced Hamiltonian for the planar system of N rigid bodies connected in the form of a tree structure by means of frictionless revolute joints is given by :

$$H \;\; = \;\; \frac{1}{2}\underline{\mu}\mathbf{J}^{-1}\underline{\mu}, \tag{4.20}$$

where,

$$\underline{\mu} \;\; = \;\; [\mu_1, \cdots, \mu_N]^T, \tag{4.21}$$

$$\mathbf{J} \;\; = \;\; \begin{bmatrix} \tilde{I}_1 & \tilde{\lambda}_{12} & \cdots & \tilde{\lambda}_{1N} \\ \tilde{\lambda}_{12} & \tilde{I}_2 & \cdots & \tilde{\lambda}_{2N} \\ \vdots & \vdots & \ddots & \vdots \\ \tilde{\lambda}_{1N} & \tilde{\lambda}_{2N} & \cdots & \tilde{I}_N \end{bmatrix}, \tag{4.22}$$

34

$$\tilde{\lambda}_{jl}(\theta_{j,l}) = \left[\sum_{k=1}^{N} m_k(\tilde{\delta}_{kj}.\tilde{\delta}_{kl})\right]\cos(\theta_{j,l}) + \left[\sum_{k=1}^{N} m_k(|\tilde{\delta}_{kj} \times \tilde{\delta}_{kl}|.\hat{Z})\right]\sin(\theta_{j,l}), \quad (4.23)$$

$$\tilde{I}_k = I_k + \sum_{j=1}^{N} m_j \parallel \tilde{\delta}_{jk} \parallel^2 . \quad (4.24)$$

The *Legendre transform* for the reduced system maps

$$L(\theta_1, \cdots, \theta_N, \omega_1, \cdots, \omega_N) \longmapsto H(\theta_{k,J(k)}, k = 2, \ldots, N, \mu_1, \ldots, \mu_N), \quad (4.25)$$

where

$$\underline{\mu} = \mathbf{J}\underline{\omega}. \quad (4.26)$$

3.5 Hamiltonian Dynamics

3.5.1 Dynamics

The dynamics of a conservative system of an arbitrary number of rigid bodies connected in the form of a tree structure, is formulated by mapping the Euler-Lagrange equations into Hamilton's equations with the help of the *Legendre transformation*. The resulting equations are consolidated in the following theorem.

Theorem 3.5.1 : The Hamiltonian dynamics for the planar, rigid N body system with the bodies connected to each other by revolute joints is given by :

$$\dot{\mu}_i = \sum_{\forall j, \, s.t. \, J(j)=i} \frac{\partial H}{\partial \theta_{j,i}} - \frac{\partial H}{\partial \theta_{i,J(i)}} \quad \text{for } i = 1, \ldots, N, \quad (5.1)$$

$$\dot{\theta}_{i,J(i)} = \frac{\partial H}{\partial \mu_i} - \frac{\partial H}{\partial \mu_{J(i)}} \quad \text{for } i = 2, \ldots, N, \quad (5.2)$$

where H is as given by Lemma 3.4.2.

Proof : The Lagrangian dynamics in the absence of any external torques or forces is given by

$$\frac{d}{dt}\left(\frac{\partial L}{\partial \underline{\dot{q}}}\right) - \frac{\partial L}{\partial \underline{q}} = 0, \quad (5.3)$$

35

with

$$L = \frac{1}{2}\underline{\omega}^T \mathbf{J} \underline{\omega}, \tag{5.4}$$

and $\underline{q} = [\theta_1, \dots, \theta_N]$.

The dynamics in the Hamiltonian setting can be derived using the Lagrangian formulation with the appropriate transformation

$$\underline{\mu} = \mathbf{J}.\underline{\omega}. \tag{5.5}$$

Simple computation using (5.3) – (5.5) shows that,

$$\underline{\dot{\mu}} = \frac{d\mathbf{J}}{dt}\underline{\omega} + \mathbf{J}\underline{\dot{\omega}} = \frac{d}{dt}\left(\frac{\partial L}{\partial \underline{\dot{q}}}\right). \tag{5.6}$$

Also

$$\frac{\partial L}{\partial \theta_k} = -\sum_{j=1}^{k-1} \tilde{\lambda}'_{jk}\omega_k\omega_j + \sum_{j=k+1}^{N} \tilde{\lambda}'_{kj}\omega_j\omega_k, \tag{5.7}$$

where

$$\tilde{\lambda}'_{ji} = \left[\frac{\partial \tilde{\lambda}_{ji}}{\partial \theta_i}\right]. \tag{5.8}$$

Differentiating (4.20) with respect to $\theta_{i,J(i)}$ and using (5.5) we get,

$$\begin{aligned}
\frac{\partial H}{\partial \theta_{i,J(i)}} &= -\frac{1}{2}\underline{\mu}^T \mathbf{J}^{-1} \frac{d\mathbf{J}}{d\theta_{i,J(i)}} \mathbf{J}^{-1}\underline{\mu} \\
&= -\frac{1}{2}\underline{\omega}^T \frac{d\mathbf{J}}{d\theta_{i,J(i)}}\underline{\omega} \\
&= -\sum_{J(i),i \in S_{k-1,l}} \tilde{\lambda}'_{kl}\omega_k\omega_l.
\end{aligned}$$

$$k < l, \ k,l = 1, \cdots, N$$

Consider,

$$\begin{aligned}
\sum_{\forall j \ s.t. \ i=J(j)} \frac{\partial H}{\partial \theta_{j,i}} - \frac{\partial H}{\partial \theta_{i,J(i)}} &= -\sum_{\forall j \ s.t. \ J(j)=i} \sum_{\forall k<l \ s.t. i,j \in S_{k-1,l}} \tilde{\lambda}'_{kl}\omega_k\omega_l \\
&\quad + \sum_{\forall k<l, \ s.t. \ J(i),i \in S_{k-1,l}} \tilde{\lambda}'_{kl}\omega_k\omega_l \\
&= \sum_{l=i+1}^{N} \tilde{\lambda}'_{il}\omega_i\omega_l - \sum_{l=1}^{i-1} \tilde{\lambda}'_{li}\omega_i\omega_l.
\end{aligned}$$

36

But this is the same as (5.7), therefore,

$$\frac{\partial L}{\partial \theta_i} = \sum_{\forall j \ s.t. \ J(j)=i} \frac{\partial H}{\partial \theta_{j,i}} - \frac{\partial H}{\partial \theta_{i,J(i)}}. \tag{5.9}$$

It is obvious from comparing (5.6), (5.9) and (5.3) that

$$\dot{\mu}_i = \sum_{\forall j \ s.t. J(j)=i} \frac{\partial H}{\partial \theta_{j,i}} - \frac{\partial H}{\partial \theta_{i,J(i)}} \quad \forall i = 1,\ldots,N. \tag{5.10}$$

Finally,

$$\underline{\omega} = \mathbf{J}^{-1}\underline{\mu} = \frac{dH}{d\underline{\mu}},$$

or,

$$\begin{aligned}
\dot{\theta}_{i,J(i)} &= \dot{\theta}_i - \dot{\theta}_{J(i)} \\
&= \omega_i - \omega_{J(i)} \\
&= \frac{dH}{d\mu_i} - \frac{dH}{d\mu_{J(i)}}
\end{aligned} \tag{5.11}$$

Q.E.D..

Corollary 3.5.1 : The dynamics of a multibody system evolves over a reduced Poisson space P coordinatized by $\theta_{k,J(k)}$, $k = 2,\ldots,N$ and μ_k, $k = 1,\ldots N$. Topologically P is $\underbrace{S^1 \times \cdots \times S^1}_{N-1 \ times} \times \mathbb{R}^N$. The system is Hamiltonian in the Poisson structure of P with the bracket given by :

$$\{f,g\} = \sum_{k=2}^{N} \left[\left(\frac{\partial f}{\partial \mu_{J(k)}} - \frac{\partial f}{\partial \mu_k} \right) \frac{\partial g}{\partial \theta_{k,J(k)}} - \left(\frac{\partial g}{\partial \mu_{J(k)}} - \frac{\partial g}{\partial \mu_k} \right) \frac{\partial f}{\partial \theta_{k,J(k)}} \right], \tag{5.12}$$

where $f,g : \mathbb{R}^{2N-1} \to \mathbb{R}$.

The corresponding dynamics represented in terms of the bracket are

$$\dot{\mu}_k = \{\mu_k, H\} \quad k = 1,\cdots,N, \tag{5.13}$$

$$\dot{\theta}_{k,J(k)} = \left\{ \theta_{k,J(k)}, H \right\} \quad k = 2,\cdots,N. \tag{5.14}$$

Proof : Use Lemma 3.4.2 and Theorem 3.5.1.

Corollary 3.5.2 : The sum of all the conjugate momentum variables μ_k, $k = 1,\ldots,N$ is equal to the angular momentum of the multibody system.

Proof : The angular momentum of the multibody system along the Z axis at the center of mass is given by :

$$\text{system angular momentum} = \sum_{k=1}^{N} \left[I_k \omega_k + (\mathbf{r}_k^o \times m_k \dot{\mathbf{r}}_k^o) \right]. \qquad (5.15)$$

From (2.16) and (2.17) we have

$$\mathbf{r}_k^o = \sum_{l=1}^{N} R(\theta_l) \tilde{\delta}_{k,l},$$

$$\dot{\mathbf{r}}_k^o = \sum_{j=1}^{N} \dot{R}(\theta_j) \tilde{\delta}_{k,j}.$$

Substituting for $R(\theta_l)$, $\dot{R}(\theta_j)$ and $\tilde{\delta}_{k,l}$ as given by (1.2), (2.19) and (2.18) respectively, we have

$$
\begin{aligned}
(\mathbf{r}_k^o \times \dot{\mathbf{r}}_k^o) &= \sum_{j=1}^{N} \sum_{l=1}^{N} \left(R(\theta_l) \tilde{\delta}_{k,l} \right) \times \left(\dot{R}(\theta_j) \tilde{\delta}_{k,j} \right) \\
&= \sum_{j=1}^{N} \sum_{l=1}^{N} \left\{ \left[\tilde{\delta}_{k,l} \cdot \tilde{\delta}_{k,j} \right] \cos(\theta_j - \theta_l) \right. \\
&\quad \left. + \left[|\tilde{\delta}_{k,l} \times \tilde{\delta}_{k,j}| \right] \sin(\theta_j - \theta_l) \right\} \omega_k.
\end{aligned}
\qquad (5.16)
$$

Therefore from (5.15) and (5.16) we have

$$
\begin{aligned}
\text{system angular momentum} &= \sum_{k=1}^{N} I_k \omega_k + \sum_{k=1}^{N} m_k \sum_{j=1}^{N} \sum_{l=1}^{N} \left\{ \left[\tilde{\delta}_{k,l} \cdot \tilde{\delta}_{k,j} \right] \cos(\theta_j - \theta_l) \right. \\
&\quad \left. + \left[|\tilde{\delta}_{k,l} \times \tilde{\delta}_{k,j}| \right] \sin(\theta_j - \theta_l) \right\} \omega_j \\
&= \sum_{k=1}^{N} \left[I_k + \sum_{j=1}^{N} m_j \parallel \tilde{\delta}_{j,k} \parallel^2 \right] \omega_k \\
&\quad + \sum_{k=1}^{N} m_k \sum_{j=1}^{N} \omega_j \sum_{\substack{l=1 \\ l \neq j}}^{N} \left\{ \left[\tilde{\delta}_{k,l} \cdot \tilde{\delta}_{k,j} \right] \cos(\theta_j - \theta_l) \right. \\
&\quad \left. + \left[|\tilde{\delta}_{k,l} \times \tilde{\delta}_{k,j}| \right] \sin(\theta_j - \theta_l) \right\} \\
&= \sum_{k=1}^{N} \tilde{I}_k \omega_k \\
&\quad + \sum_{k=1}^{N} m_k \sum_{j=1}^{N} \omega_j \sum_{\substack{l=1 \\ l \neq j}}^{N} \left\{ \left[\tilde{\delta}_{k,l} \cdot \tilde{\delta}_{k,j} \right] \cos(\theta_j - \theta_l) \right. \\
&\quad \left. + \left[|\tilde{\delta}_{k,l} \times \tilde{\delta}_{k,j}| \right] \sin(\theta_j - \theta_l) \right\}.
\end{aligned}
\qquad (5.17)
$$

But from Lemma 3.4.2 we have that

$$\sum_{k=1}^{N} \mu_k = [1, 1, \ldots, 1] \begin{bmatrix} \tilde{I}_1 & \tilde{\lambda}_{1,2} & \cdots & \tilde{\lambda}_{1,N} \\ \tilde{\lambda}_{1,2} & \tilde{I}_1 & \cdots & \tilde{\lambda}_{2,N} \\ \vdots & \vdots & \ddots & \vdots \\ \tilde{\lambda}_{1,N} & \tilde{\lambda}_{2,N} & \cdots & \tilde{I}_N \end{bmatrix} \cdot \begin{bmatrix} \omega_1 \\ \omega_2 \\ \vdots \\ \omega_N \end{bmatrix}$$

$$= \sum_{k=1}^{N} \left[\tilde{I}_k + \sum_{j=1,\; j\neq k}^{N} \tilde{\lambda}_{k,j} \omega_k \right].$$

Substituting for $\tilde{\lambda}_{j,l}$'s from (2.30) in the above equation and noting that $\tilde{\lambda}_{k,j} = \tilde{\lambda}_{j,k}$ we get

$$\sum_{k=1}^{N} \mu_k = \sum_{k=1}^{N} \tilde{I}_k + \sum_{k=1}^{N}\sum_{j=1}^{N}\sum_{l=1,\; l\neq j}^{N} m_k \left\{ \left[\tilde{\delta}_{k,l} \cdot \tilde{\delta}_{k,j} \right] \cos(\theta_j - \theta_l) \right.$$
$$\left. + \left[|\tilde{\delta}_{k,l} \times \tilde{\delta}_{k,j}| \right] \sin(\theta_j - \theta_l) \right\} \omega_j.$$

Rearranging the summations we have

$$\sum_{k=1}^{N} \mu_k = \sum_{k=1}^{N} \tilde{I}_k + \sum_{k=1}^{N} m_k \sum_{j=1}^{N} \omega_j \sum_{l=1\; l\neq j}^{N} \left\{ \left[\tilde{\delta}_{k,l} \cdot \tilde{\delta}_{k,j} \right] \cos(\theta_j - \theta_l) \right.$$
$$\left. + \left[|\tilde{\delta}_{k,l} \times \tilde{\delta}_{k,j}| \right] \sin(\theta_j - \theta_l) \right\}. \tag{5.18}$$

Comparing (5.17) and (5.18) we see that

$$\sum_{k=1}^{N} \mu_k = \text{system angular momentum about the } Z \text{ axis. Q.E.D.}.$$

3.6 Internal and External Torques

A multibody system in space can experience *internal* and *external* torques. An internal torque at a joint acting on one of the bodies produces an equal and opposite (reaction) torque on the body to which it is connected to (at the joint). Torque due to a motor at a joint, is an example of internal torque.

For a multibody system if the angular momentum is conserved, the dynamics evolve on a given symplectic leaf of the Poisson manifold P. In other words the symplectic leaf is determined by assigning a particular value to the system angular

momentum. Since internal torques change the energy of the system but leave the system angular momentum invariant, the corresponding motion will be confined to a single leaf.

External torques on a multibody system change the energy as well as the angular momentum of the system. The evolution of dynamics switches from one symplectic leaf to another on the application of external pulse torques. Examples of external torques are, torques induced by gas jets, gravity gradient torque , solar radiation pressure, solar wind, etc. Actuators may be used to create internal and external torques for control purposes.

We are interested in studying the effect of these torques on the dynamics of the system. The following theorem gives the dynamics when internal and external torques are applied to the multibody system.

Theorem 3.6.1 : The dynamics of the planar multibody system, under the application of external and internal torques are given by:

$$\dot{\mu}_i = \sum_{\forall j, \ s.t. \ J(j)=i} \frac{\partial H}{\partial \theta_{j,i}} - \frac{\partial H}{\partial \theta_{i,J(i)}} + \sum_{\forall j, \ s.t. \ J(j)=i} T_{j-1} - T_{i-1} + T_i^{ext}, \qquad (6.1)$$

$$\text{for } i = 1, \ldots, N$$

$$\dot{\theta}_{i,J(i)} = \frac{\partial H}{\partial \mu_i} - \frac{\partial H}{\partial \mu_{J(i)}} \qquad \text{for } i = 2, \ldots, N, \qquad (6.2)$$

where T_{i-1} is the internal (reaction) torque acting at joint $i-1$ ($T_0 \cong 0$), and T_i^{ext} is the external torque acting on body i.

Proof : The Lagrangian dynamics in the presence of any internal and external torques is given by

$$\frac{d}{dt}\left(\frac{\partial L}{\partial \dot{\underline{q}}}\right) - \frac{\partial L}{\partial \underline{q}} = \mathbf{F}, \qquad (6.3)$$

where,

$$L = \frac{1}{2}\underline{\omega}^T \mathbf{J}\underline{\omega},$$

$$\mathbf{F} = [F_1, \ldots, F_N],$$

and F_i's are the generalized force acting on body i.

40

We know that

$$\text{virtual work} = (\text{generalized force}) \cdot (\text{displacement}).$$

Now, the total infinitesimal virtual work done by the internal torques acting on the system, δW_{int} is given by,

$$\delta W_{int} = \sum_{k=2}^{N} T_{k-1}(\delta\theta_{J(k)} - \delta\theta_k). \tag{6.4}$$

Similarly, the total infinitesimal virtual work done by the external torques acting on the system, δW_{ext} is

$$\delta W_{ext} = \sum_{i=1}^{N} T_i^{ext}\delta\theta_i. \tag{6.5}$$

Thus from (6.4) and (6.5), the total infinitesimal virtual work done by both internal and external torques δW is,

$$\begin{aligned}
\delta W &= \delta W_{int} + \delta W_{ext} \\
&= \sum_{k=2}^{N} T_{k-1}(\delta\theta_{J(k)} - \delta\theta_k) + \sum_{i=1}^{N} T_i^{ext}\delta\theta_i.
\end{aligned}$$

By definition the generalized force F_i is given by,

$$\begin{aligned}
F_i &= \frac{\partial W}{\partial\theta_i} \\
&= \sum_{\forall j \ s.t. \ J(j)=i} T_{j-1} - T_{i-1} + T_i^{ext}. \tag{6.6}
\end{aligned}$$

From Theorem 3.5.1 and (6.3) we have,

$$\dot\mu_i = \frac{d}{dt}\left(\frac{\partial L}{\partial\dot q_i}\right) = \frac{\partial L}{\partial q_i} + F_i, \tag{6.7}$$

and

$$\frac{\partial L}{\partial q_i} = \sum_{\forall j \ s.t. \ i=J(j)} \frac{\partial H}{\partial\theta_{j,i}} - \frac{\partial H}{\partial\theta_{i,J(i)}}, \tag{6.8}$$

Substituting (6.6), (6.8) in (6.7) we get,

$$\dot\mu_i = \sum_{\forall j, \ s.t. \ J(j)=i} \frac{\partial H}{\partial\theta_{j,i}} - \frac{\partial H}{\partial\theta_{i,J(i)}} + \sum_{\forall j \ s.t. \ J(j)=i} T_{j-1} - T_{i-1} + T_i^{ext},$$

$$i = 1,\dots,N$$

Also from Theorem 3.5.1 we have,

$$\dot{\theta}_{i,J(i)} \;=\; \frac{\partial H}{\partial \mu_i} \;-\; \frac{\partial H}{\partial \mu_{J(i)}} \quad \text{for } i = 2,\ldots,N.$$

Q.E.D..

Remark **3.6.1** : In the last result some special things happen because we are in the *plane* and deal with pure torques. As a consequence the torques seen by an observer fixed on to a body is equal to the torque seen by an observer fixed in the inertial frame.

42

FOUR

FEW-BODY EXAMPLES

In this chapter we consider some interesting examples of multibody systems in space. We begin by specializing our results of Chapter three to the case of two-body and three-body systems. Applications of our formalism to terrestrial multibody systems, in particular to ground based robot manipulators, is discussed. We illustrate this extension procedure for a planar two-link manipulator on ground. Dynamics of a system of planar N bodies in space connected in the form of an open chain is given. The notation used in this chapter is the same as in the general tree connected N body problem (Chapter three).

4.1 Planar Two-Body System

A system of two bodies in space, connected together by a one degree of freedom joint occurs in many contexts. Consider a two-body system where the bodies are of comparable mass and inertia, relative to each other. One of the bodies may represent a large space based sensor. Rapid reorientation of the sensor from one stationary position to another may be desirable. Such a "step-stare" maneuver would require thorough knowledge of the dynamics and thus a good mathematical model to formulate the necessary control [46].

We start with a planar two-body system as shown in Figure 4.1. The bodies are
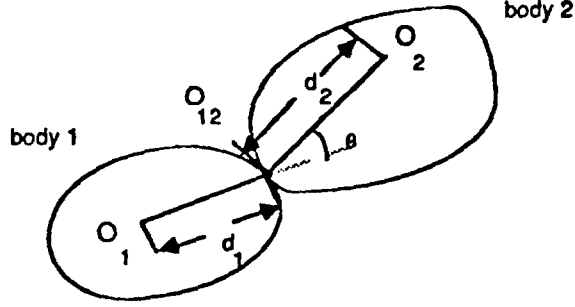
Figure 4.1: Planar two body system

connected together by a frictionless revolute joint. The system is conservative with no external or internal torques acting on it. The centers of mass of the bodies are chosen to be the origins of the respective local frames of reference. Without loss of generality, the x-axes of the local frames of reference of the bodies is chosen to be parallel to the line joining the body center of mass and O_{12}.

The Lagrangian dynamical equations are as given below.

$$\dot{\omega}_1 = -\gamma(\tilde{I}_2\omega_2^2 + \tilde{\lambda}_{12}(\theta_{2,1})\omega_1^2)$$

$$\dot{\omega}_2 = -\gamma(\tilde{I}_1\omega_1^2 + \tilde{\lambda}_{12}(\theta_{2,1})\omega_2^2)$$

$$\dot{\theta}_1 = \omega_1$$

$$\dot{\theta}_2 = \omega_2$$

where,

$$\gamma = \frac{\tilde{\lambda}'_{12}(\theta_{2,1})}{(\tilde{I}_1\tilde{I}_2 - \epsilon^2\tilde{\lambda}_{12}(\theta_{2,1}))}, \tag{1.1}$$

44

$$\begin{aligned}
\tilde{I}_1 &= (I_1 + \epsilon d_1^2), \\
\tilde{I}_2 &= (I_2 + \epsilon d_2^2), \\
\epsilon &= \frac{m_1 m_2}{m_1 + m_2} \\
\tilde{\lambda}'_{12}(\theta_{2,1}) &= \frac{\partial \tilde{\lambda}_{12}}{\partial \theta_{2,1}} \\
\tilde{\lambda}_{12}(\theta_{2,1}) &= \epsilon d_1 d_2 \cos(\theta_{2,1})
\end{aligned} \right\} \tag{1.2}$$

Remark 4.1.1 : Here ϵ is known as the 'reduced mass' and is different from our earlier notation (in Chapter two) that $\epsilon_i = \frac{m_i}{m_1 + m_2}$ for $i = 1, 2$, which is a dimensionless quantity.

4.1.1 Hamiltonian Formulation

We now use Hamilton's principle and present the dynamics of the two-body system in this new setting. We use Lemma 3.4.2 and Theorem 3.5.1 with $N = 2$, $\tilde{\beta}_2 = [d_1, 0]$ and $\tilde{\alpha}_2 = [d_2, 0]$ to compute the dynamics. The Hamiltonian for this system is simply the total kinetic energy of the system.

Lemma 4.1.1 : For the planar two-body problem the Hamiltonian is given by

$$H = \frac{1}{2} \underline{\mu}^T . \mathbf{J}^{-1} . \underline{\mu} \tag{1.3}$$

where,

$$\underline{\mu} = [\mu_1, \mu_2]^T, \tag{1.4}$$

$$\mathbf{J} = \begin{bmatrix} \tilde{I}_1 & \tilde{\lambda}_{12}(\theta_{2,1}) \\ \tilde{\lambda}_{12}(\theta_{2,1}) & \tilde{I}_2 \end{bmatrix}, \tag{1.5}$$

μ_1 and μ_2 are the conjugate momentum variables and are related to the angular velocities ω_1 and ω_2 as below:

$$\underline{\mu} = \mathbf{J} . [\omega_1, \omega_2]^T, \tag{1.6}$$

$\tilde{I}_1$ and $\tilde{I}_2$ are pseudo inertia constants given by (1.2) (similar to the 'aguemented' body inertias used by Wittenburg [59]).

Proof : Use Lemma 3.4.2 with $N = 2$.

Theorem 4.1.1: The dynamics of a planar two-body system in the $(\theta_{2,1}, \mu_1, \mu_2)$ space is given by

$$\dot{\mu}_1 \;=\; \frac{\partial H}{\partial \theta_{2,1}} \tag{1.7}$$

$$\dot{\mu}_2 \;=\; -\frac{\partial H}{\partial \theta_{2,1}} \tag{1.8}$$

$$\dot{\theta}_{2,1} \;=\; \frac{\partial H}{\partial \mu_2} - \frac{\partial H}{\partial \mu_1} \tag{1.9}$$

Proof : Use Theorem 3.5.1 with $N = 2$.

In Chapter 5 we will discuss the numerical simulation results of the dynamics of a planar two-body system with suitable initial conditions, and find the system equilibria. We analyze the stability of these equilibria using the *Energy-Casimir* method and show that this agrees with the simulation results.

Remark 4.1.2: The sum of conjugate momentum variables (i.e., $\mu_1 + \mu_2$), is equal to the system angular momentum – constant in the absence of external torques.

4.1.2 Poisson Bracket

The phase space for the evolution of the dynamics is on a Poisson reduced space

$$\mathcal{P} := T^*(S^1 \times S^1)/S^1 \tag{1.10}$$

The phase space $\mathcal{P}$ is coordinatized by $(\theta_{2,1}, \mu_1, \mu_2)$. The Poisson structure on the $\mathcal{P}$ space is given by:

$$\{f, g\} = \left(\frac{\partial f}{\partial \mu_1} - \frac{\partial f}{\partial \mu_2} \right) \frac{\partial g}{\partial \theta_{2,1}} - \left(\frac{\partial g}{\partial \mu_1} - \frac{\partial g}{\partial \mu_2} \right) \frac{\partial f}{\partial \theta_{2,1}} \tag{1.11}$$

where,

$$f, g : \mathcal{P} \longrightarrow \mathbb{R}. \tag{1.12}$$

46
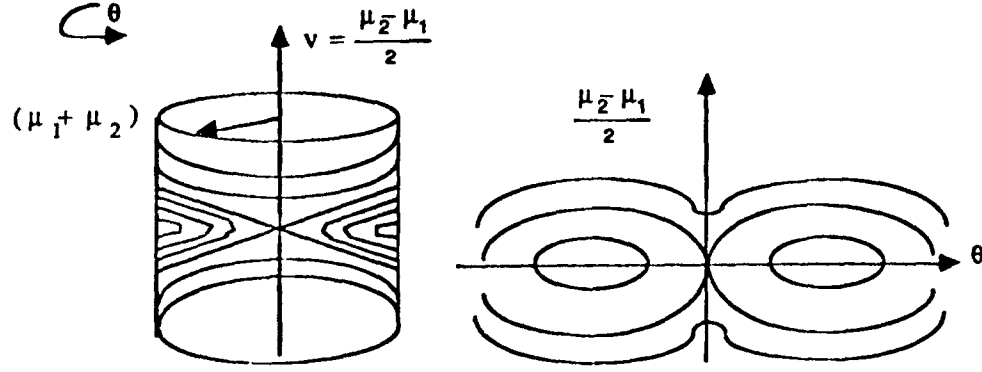
Figure 4.2: Dynamics of a two-body system

Corollary **4.1.1** : The dynamics rewritten in terms of the Poisson brackets are:

$$\dot{\mu}_1 = \{\mu_1, H\} \tag{1.13}$$

$$\dot{\mu}_2 = \{\mu_2, H\} \tag{1.14}$$

$$\dot{\theta}_{2,1} = \{\theta_{2,1}, H\} \tag{1.15}$$

Proof : See Corollary 3.5.1 with $N = 2$.

4.1.3 Control & Disturbance Torques

We are interested to study the effect of external and internal torques on the dynamics of the system. These torques may be applied as a form of control. It is to be noted here that internal torques change the energy of the system but the system angular momentum itself is conserved i.e., the symplectic leaf is left invariant. External torques acting on the system however change the system angular momentum as well as the energy; in other words the evolution of dynamics shift from one symplectic leaf to another on the application of such torques.

The dynamics of a planar two-body system evolves on the surface of a "cylinder" (see Figure 4.2). Internal torques leave the "cylinder" invariant. On the other hand

47

the external torques change the evolution of dynamics from one "cylinder" to another. The following Corollary illustrates the dynamics when these torques are present. It is important to observe the linear way in which the torques appear.

Corollary 4.1.2 : The dynamics of a planar two-body system in the $(\theta_{2,1}, \mu_1, \mu_2)$ space under the action of an internal control (reaction) torque T at the joint, and an external torque T_1^{ext} on body 1 is given by :

$$\dot{\mu}_1 = \frac{\partial H}{\partial \theta_{2,1}} + T + T_1^{ext}, \tag{1.16}$$

$$\dot{\mu}_2 = -\frac{\partial H}{\partial \theta_{2,1}} - T, \tag{1.17}$$

$$\dot{\theta}_{2,1} = \frac{\partial H}{\partial \mu_2} - \frac{\partial H}{\partial \mu_1}. \tag{1.18}$$

4.2 Three-Body Problem

A logical extension of the two-body problem is the three-body problem. A satellite with symmetrically placed solar arrays on either side of the main satellite body, may be modeled by such a system. The results presented in Section 4.1 with respect to the Hamiltonian formulation can be extended to the planar three body case. A planar, three-body system, with the bodies being connected in the form of a open chain with frictionless revolute joints is considered. It is assumed that there are no external torques or forces acting on the system.

Lemma 4.2.1 : The Hamiltonian of the planar three-body problem is given by (1.3) with the conjugate momentum vector $\underline{\mu}$ and the pseudo Inertia matrix J being defined as below:

$$\underline{\mu} = [\mu_1, \mu_2, \mu_3]^T, \tag{2.1}$$

$$
\mathbf{J} = \begin{bmatrix} \tilde{I}_1 & \tilde{\lambda}_{12}(\theta_{2,1}) & \tilde{\lambda}_{13}(\theta_{2,1} + \theta_{3,2}) \\ \tilde{\lambda}_{12}(\theta_{2,1}) & \tilde{I}_2 & \tilde{\lambda}_{23}(\theta_{3,2}) \\ \tilde{\lambda}_{13}(\theta_{2,1} + \theta_{3,2}) & \tilde{\lambda}_{23}(\theta_{3,2}) & \tilde{I}_3 \end{bmatrix}, \qquad (2.2)
$$

with

$$
\left.
\begin{aligned}
\tilde{I}_1 &= I_1 + (\epsilon_{12} + \epsilon_{31}) \parallel \tilde{\beta}_2 \parallel^2, \\
\tilde{I}_2 &= I_2 + \epsilon_{12} \parallel \tilde{\alpha}_2 \parallel^2 + \epsilon_{23} \parallel \tilde{\beta}_3 - \tilde{\alpha}_2 \parallel^2 + \epsilon_{31} \parallel \tilde{\beta}_3 \parallel^2, \\
\tilde{I}_3 &= I_3 + (\epsilon_{23} + \epsilon_{31}) \parallel \tilde{\alpha}_3 \parallel^2, \\
\tilde{\lambda}_{12}(\theta_{2,1}) &= \epsilon_{12}\lambda_{\tilde{\alpha}_2,\tilde{\beta}_2}(\theta_{2,1}) + \epsilon_{31}\lambda_{\tilde{\beta}_3,\tilde{\beta}_2}, \\
\tilde{\lambda}_{13}(\theta_{2,1} + \theta_{3,2}) &= \epsilon_{31}\lambda_{\tilde{\alpha}_3,\tilde{\beta}_2}(\theta_{2,1} + \theta_{3,2}), \\
\tilde{\lambda}_{23}(\theta_{3,2}) &= \epsilon_{31}\lambda_{\tilde{\alpha}_3,\tilde{\beta}_3 - \tilde{\alpha}_2}(\theta_{2,1}) + \epsilon_{31}\lambda_{\tilde{\alpha}_3,\tilde{\beta}_3}, \\
\lambda_{\underline{a},\underline{b}}(\theta_{i,j}) &= (\underline{a} \cdot \underline{b})\cos(\theta_{i,j}) + |\underline{a} \times \underline{b}|\sin(\theta_{i,j}), \\
\epsilon_{ij} &= \frac{m_i m_j}{m_1 + m_2 + m_3} \quad i \neq j \quad i,j = 1,2,3,
\end{aligned}
\right\} \qquad (2.3)
$$

$\underline{a}$ and $\underline{b}$ are any (2×1) vectors. $\theta_{2,1}$ and $\theta_{3,2}$ are the relative angles between body 2 and body 1, and, body 3 and body 2, respectively.

Proof : Use Lemma 3.4.2, with $N = 3$.

Theorem 4.2.1: The dynamics of a planar, three-body system in the Hamiltonian setting is given by:

$$
\dot{\mu}_1 = \frac{\partial H}{\partial \theta_{2,1}}, \qquad (2.4)
$$

$$
\dot{\mu}_2 = -\frac{\partial H}{\partial \theta_{2,1}} + \frac{\partial H}{\partial \theta_{3,2}}, \qquad (2.5)
$$

$$
\dot{\mu}_3 = -\frac{\partial H}{\partial \theta_{3,2}}, \qquad (2.6)
$$

$$
\dot{\theta}_{2,1} = \frac{\partial H}{\partial \mu_2} - \frac{\partial H}{\partial \mu_1}, \qquad (2.7)
$$

$$
\dot{\theta}_{3,2} = \frac{\partial H}{\partial \mu_3} - \frac{\partial H}{\partial \mu_2}. \qquad (2.8)
$$

Proof : See Theorem 3.5.1, with $N = 3$.

Remark 4.2.1: The sum of conjugate momentum variables (i.e., $\mu_1 + \mu_2 + \mu_3$) is a constant.

The phase space for the evolution of the dynamics is a Poisson reduced space $\mathcal{P}$, and is coordinatized by $(\theta_{2,1}, \theta_{3,2}, \mu_1, \mu_2, \mu_3)$. The Poisson structure on the $\mathcal{P}$ space $\{.,.\}$ for this case is given by:

$$\{f,g\} = \left(\frac{\partial f}{\partial \mu_1} - \frac{\partial f}{\partial \mu_2}\right) \frac{\partial g}{\partial \theta_{2,1}} - \frac{\partial f}{\partial \theta_{2,1}} \left(\frac{\partial g}{\partial \mu_1} - \frac{\partial g}{\partial \mu_2}\right)$$
$$+ \left(\frac{\partial f}{\partial \mu_2} - \frac{\partial f}{\partial \mu_3}\right) \frac{\partial g}{\partial \theta_{3,2}} - \frac{\partial f}{\partial \theta_{3,2}} \left(\frac{\partial g}{\partial \mu_2} - \frac{\partial g}{\partial \mu_3}\right), \qquad (2.9)$$

where f,g $: \mathcal{P} \to R$

Corollary 4.2.1 : The dynamics of the three-body system could also be written in terms of the brackets as below,

$$\left.\begin{array}{rcl}\dot{\mu}_i &=& \{\mu_i, H\} \quad i = 1, 2, 3 \\ \dot{\theta}_{2,1} &=& \{\theta_{2,1}, H\} \\ \dot{\theta}_{3,2} &=& \{\theta_{3,2}, H\}\end{array}\right\}, \qquad (2.10)$$

Proof : See Corollary 3.5.1, with $N = 3$.

4.3 N-Body Problem (Chain)

In Chapter 3 we have given the Hamiltonian formulation of a planar rigid N-body system, connected in the form of a tree structure. The equations for a open chain of rigid, planar, N body system, can be realized as a particular case of the tree structure (see Figure 4.3). Note that $J(i) = i - 1 \ \forall i = 2, \ldots, N$.

Lemma 4.3.1 : The Hamiltonian for an open chain of planar, N rigid bodies connected together by revolute joints is given by

$$\mathbf{H} = \frac{1}{2}\underline{\mu}^T.\mathbf{J}^{-1}.\underline{\mu}, \qquad (3.1)$$

50
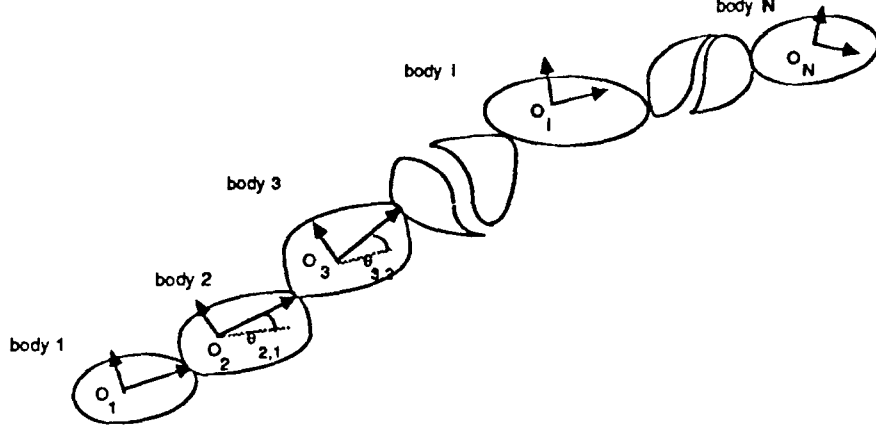
Figure 4.3: Planar N-body satellite connected in the form of a open chain

where, $\underline{\mu} = [\mu_1, \mu_2, \ldots, \mu_N]$ is the conjugate momentum vector and $\mathbf{J}$ is an $N \times N$ pseudo-inertia matrix,

$$
\mathbf{J} = \begin{bmatrix}
\tilde{I}_1 & \tilde{\lambda}_{12} & \cdots & \tilde{\lambda}_{1N} \\
\tilde{\lambda}_{12} & \tilde{I}_2 & \cdots & \tilde{\lambda}_{2N} \\
\vdots & \vdots & \ddots & \vdots \\
\tilde{\lambda}_{1N} & \tilde{\lambda}_{2N} & \cdots & \tilde{I}_N
\end{bmatrix} .
\tag{3.2}
$$

Proof : See Lemma 3.4.2.

Theorem 4.3.1: For a system of planar N rigid bodies connected in the form of a chain, the dynamics in the Hamiltonian setting under the application of internal torques T_i, $i = 1, \ldots N - 1$ and external torques T_i^{ezt}, $i = 1, \ldots N$, is given by:

$$
\dot{\mu}_1 = \frac{\partial H}{\partial \theta_{2,1}} + T_1 + T_1^{ezt},
$$

$$
\dot{\mu}_2 = \frac{\partial H}{\partial \theta_{3,2}} - \frac{\partial H}{\partial \theta_{2,1}} + T_2 - T_1 + T_2^{ezt},
$$

$$\vdots \qquad \vdots$$

$$\dot{\mu}_i = \frac{\partial H}{\partial \theta_{i+1,i}} - \frac{\partial H}{\partial \theta_{i,i-1}} + T_i - T_{i-1} + T_i^{ext},$$

$$\vdots \qquad \vdots$$

$$\dot{\mu}_{N-1} = \frac{\partial H}{\partial \theta_{N,N-1}} - \frac{\partial H}{\partial \theta_{N-1,N-2}} + T_{N-1} - T_{N-2} + T_{N-1}^{ext},$$

$$\dot{\mu}_N = -\frac{\partial H}{\partial \theta_{N,N-1}} - T_{N-1} + T_N^{ext},$$

$$\dot{\theta}_{i+1,i} = \frac{\partial H}{\partial \mu_{i+1}} - \frac{\partial H}{\partial \mu_i} \quad \text{for i=1,..,N-1},$$

where, $\theta_{i+1,i}$ is the angle between body $i+1$ and body i, for $i = 1, \dots, N$.

Proof : Note $J(i) = i - 1$, $\forall i = 2, \dots, N$ and use Theorem 3.6.1.

Poisson Structure

The Poisson reduced space P on which the dynamics evolve is coordinatized by $(\theta_{2,1}, \dots, \theta_{N,N-1}, \mu_1, \dots, \mu_N)$. The Poisson structure is given by,

$$\{f, g\} = \{f, g\}_1 + \cdots + \{f, g\}_{N-1}, \tag{3.3}$$

where

$$\{f, g\}_i = \left(\frac{\partial f}{\partial \mu_i} - \frac{\partial f}{\partial \mu_{i+1}}\right) \frac{\partial g}{\partial \theta_{i+1,i}} - \frac{\partial f}{\partial \theta_{i+1,i}} \left(\frac{\partial g}{\partial \mu_i} - \frac{\partial g}{\partial \mu_{i+1}}\right), \tag{3.4}$$

and $f, g : P \longrightarrow \mathbb{R}$.

Corollary 4.3.1 : The dynamics in terms of the Poisson bracket under the absence of external and internal torques, are given below,

$$\dot{\mu}_i = \{\mu_i, H\} \quad \text{for } i = 1, \dots, N, \tag{3.5}$$

$$\dot{\theta}_{i+1,i} = \{\theta_{i+1,i}, H\} \quad \text{for } i = 2, \dots, N, \tag{3.6}$$

Proof : See Corollary 3.5.1.
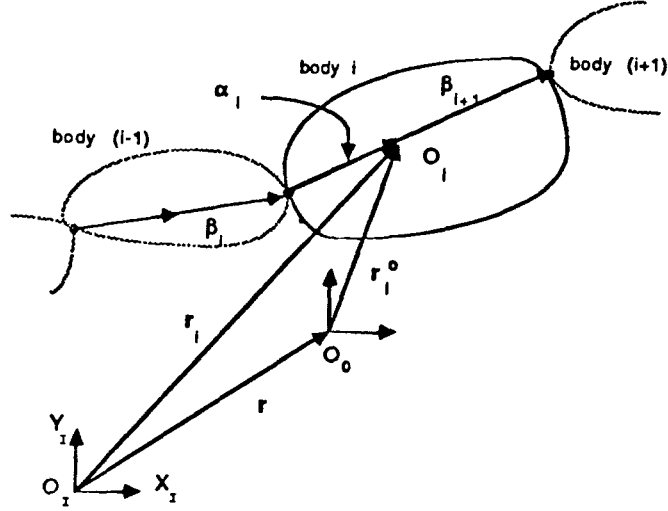
Figure 4.4: N-body (chain) example : special case

4.3.1 N-Body (Chain) : Special Case

Consider a special case of the N-body chain example wherein the center of mass of a generic body i is along the line joining the two joints (see Figure 3.5). Symbolically we have,

$$\tilde{\alpha}_i = \kappa_i \tilde{\beta}_{i+1} \quad i = 2, \ldots, N - 2 \tag{3.7}$$

where $\kappa_i \in \mathbb{R}$. By proper choice of the local frames of reference we have

$$\tilde{\beta}_{i+1} = d_i \begin{bmatrix} 1 \\ 0 \end{bmatrix} \quad i = 2, \ldots, N. \tag{3.8}$$

$$\tilde{\alpha}_1 = d_1 \begin{bmatrix} 1 \\ 0 \end{bmatrix}. \tag{3.9}$$

$$\tilde{\alpha}_N = d_N \begin{bmatrix} 1 \\ 0 \end{bmatrix}. \tag{3.10}$$

To find the dynamics of this system we first find the Hamiltonian of the system as given by Lemma 4.3.1.

Thus we get

$$\tilde{I}_k = I_k + \sum_{j=1}^{N} m_j \parallel \tilde{\delta}_{jk} \parallel^2,$$

53

$$\tilde{\lambda}_{jl} = \sum_{k=1}^{N} m_k \tilde{\delta}_{kj} \cdot \tilde{\delta}_{kl} \cos(\theta_{j,l}),$$

and

$$\tilde{\delta}_{1j} = \begin{cases} -(1 - \epsilon_1) d_1 [1,0]^T & j = 1 \\ -\left(\sum_{l=j+1}^{N} \epsilon_l + \epsilon_j \kappa_j\right) d_j [1,0]^T & j = 2,\ldots,N-1 \\ -\epsilon_N d_N [1,0]^T & j = N \end{cases} \qquad (3.11)$$

$$\tilde{\delta}_{kj} = \begin{cases} \tilde{\delta}_{1j} + d_j [1,0]^T & 1 \le j \le k-1 \\ \tilde{\delta}_{1k} + d_k [1,0]^T & j = k \\ \tilde{\delta}_{1j} & k+1 \le j \le N \end{cases} \qquad (3.12)$$

The dynamical equations are as given by Theorem 3.5.1.

Symmetrical N-Body Case

For the particular case of a planar N-body problem wherein the bodies have equal mass, inertia and other physical parameters, and with the center of mass of a generic body at the center of the line connecting the joints, we have

$$m_i = m' \quad \forall i = 1,\ldots,N$$
$$d_i = d \quad \forall i = 2,\ldots,N-1$$
$$d_1 = d_N = 0.5d$$
$$\kappa_i = 0.5 \quad \forall i = 2,\ldots,N-1,$$

the $\tilde{\delta}_{kj}$'s are given by

$$\tilde{\delta}_{1j} = \begin{cases} -\left(\frac{N-1}{2N}\right) d[1,0]^T & j = 1 \\ -\left(\frac{2N-2j+3}{2N}\right) d[1,0]^T & j = 2,\ldots,N-1 \\ -\frac{1}{2N} d[1,0]^T & j = N \end{cases}$$

$$\tilde{\delta}_{kj} = \begin{cases} \tilde{\delta}_{1j} + \frac{d}{2}[1,0]^T & 1 \le j \le k-1 \\ \tilde{\delta}_{1k} + d[1,0]^T & j = k \\ \tilde{\delta}_{1j} & k+1 \le j \le N \end{cases} \qquad .$$

4.4 Terrestrial Multibody Systems : An Example

The dynamics of a planar multibody system on ground connected in the form of tree could be derived from the general multibody system dynamics in the following way. Consider a multibody satellite system where the main satellite body is of infinite mass. This could be easily modeled in the Hamiltonian setting. The resulting equations for such a case are equivalent to the dynamics of a planar ground based multibody system, with the earth playing the role of a body with *infinite* mass. We give the following procedure for such a derivation.

The dynamics of a $N + 1$ body system is computed first. The limiting set of dynamical equations as the body 1 mass (and so its inertia) tends to *infinity* gives the dynamics of the N body system on ground - with the absence of the gravity term. The effect of gravity on the system can be modeled separately as an external torque. The procedure is illustrated with a simple example of a planar two-link robot manipulator.

We derive the dynamical equations of a planar two-link manipulator on ground as a limiting case (as described above) of a planar three-body satellite system and verify it using an example in Horn[21]. The dynamical equations of a three body system in space is given by (2.2)-(2.8). As $m_1 \rightarrow \infty$ so $\tilde{I}_1 \rightarrow \infty$ we have from (2.3),

$$\epsilon_{1,2,\infty} = \lim_{m_1 \to \infty} \frac{m_1 m_2}{m_1 + m_2 + m_3} = m_2,$$

$$\epsilon_{3,1,\infty} = \lim_{m_1 \to \infty} \frac{m_1 m_3}{m_1 + m_2 + m_3} = m_3,$$

$$\epsilon_{2,3,\infty} = \lim_{m_1 \to \infty} \frac{m_2 m_3}{m_1 + m_2 + m_3} = 0,$$

$$\tilde{I}_{2\infty} = \left[I_2 + m_3 \parallel \tilde{\alpha}_2 \parallel^2 + m_3 \parallel \tilde{\beta}_3 \parallel^2 \right],$$

$$\tilde{I}_{3\infty} = \left[I_3 + m_3 \parallel \tilde{\alpha}_3 \parallel^2 \right],$$

$$\tilde{\lambda}_{12\infty} = m_2 \lambda_{\tilde{\alpha}_2, \tilde{\beta}_2}(\theta_{2,1}) + m_3 \lambda_{\tilde{\beta}_3, \tilde{\beta}_2}(\theta_{2,1}),$$

$$\tilde{\lambda}_{13\infty} = m_3 \lambda_{\tilde{\alpha}_3, \tilde{\alpha}_1}(\theta_{3,1}),$$

$$\tilde{\lambda}_{23\infty} = m_3 \lambda_{\tilde{\alpha}_3, \tilde{\beta}_3}(\theta_{3,2}).$$

Substituting so in (2.2) we get,

$$
\begin{aligned}
\mathbf{J}_\infty^{-1} &= \lim_{\tilde{I}_1 \to \infty} \mathbf{J}^{-1} \\
&= \lim_{\tilde{I}_1 \to \infty}
\begin{bmatrix}
\tilde{I}_1 & \tilde{\lambda}_{12} & \tilde{\lambda}_{12} \\
\tilde{\lambda}_{12} & \tilde{I}_2 & \tilde{\lambda}_{23} \\
\tilde{\lambda}_{23} & \tilde{\lambda}_{23} & \tilde{I}_3
\end{bmatrix}^{-1} \\
&= \frac{1}{\Delta_\infty}
\begin{bmatrix}
0 & 0 & 0 \\
0 & \tilde{I}_{3\infty} & \tilde{\lambda}_{23\infty} \\
0 & \tilde{\lambda}_{23\infty} & \tilde{I}_{2\infty}
\end{bmatrix},
\end{aligned}
\tag{4.1}
$$

where, $\Delta_\infty = (\tilde{I}_{2\infty}\tilde{I}_{3\infty} - \tilde{\lambda}_{23\infty}^2)$.

From Lemma 4.2.1 and (4.1), the Hamiltonian for such a system can be calculated as,

$$
\begin{aligned}
H_\infty &= \lim_{\tilde{I}_1 \to \infty} \frac{1}{2}\underline{\mu}^T \mathbf{J}\underline{\mu} \\
&= \frac{1}{2\Delta_\infty} [\mu_2, \mu_3]
\begin{bmatrix}
\tilde{I}_{3\infty} & -\tilde{\lambda}_{23\infty} \\
-\tilde{\lambda}_{23\infty} & \tilde{I}_{2\infty}
\end{bmatrix}
\begin{bmatrix}
\mu_2 \\
\mu_3
\end{bmatrix}.
\end{aligned}
\tag{4.2}
$$

The dynamical equations of the ground based planar two-link manipulator in the Hamiltonian setting computed using Theorem 4.2.1 are,

$$
\dot{\mu}_1 = \frac{\partial H_\infty}{\partial \theta_{2,1}} = 0,
\tag{4.3}
$$

$$
\dot{\mu}_2 = \frac{\partial H_\infty}{\partial \theta_{3,2}},
\tag{4.4}
$$

$$
\dot{\mu}_3 = -\frac{\partial H_\infty}{\partial \theta_{3,2}},
\tag{4.5}
$$

$$
\dot{\theta}_{2,1} = \frac{\partial H_\infty}{\partial \mu_2},
\tag{4.6}
$$

$$
\dot{\theta}_{3,2} = \frac{\partial H_\infty}{\partial \mu_3} - \frac{\partial H_\infty}{\partial \mu_2},
\tag{4.7}
$$

where, H_∞ is given by (4.2).

Remark 4.4.1 : It is to be noted here that $\dot{\mu}_1 = 0$ could be interpreted as that any movement of other bodies has no effect on the main satellite body (i.e., the ground).
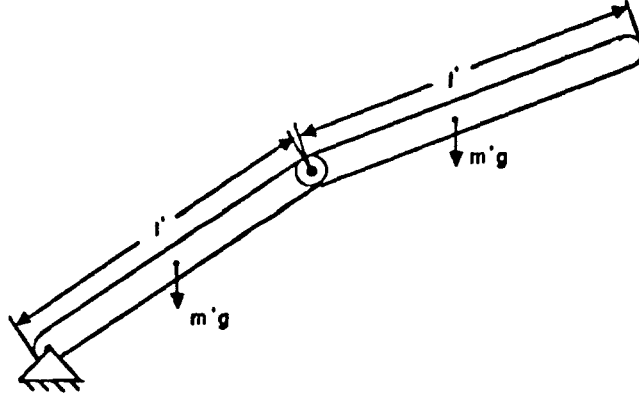
Figure 4.5: Planar two-link manipulator in Horn's example

Horn's Example : Consider a particular case of a planar two-link manipulator as in Figure 4.4. The links are in the form of two thin, similar rods of length l' and mass m' with the centers of mass of each link at the center of the rod. The Hamiltonian for such a case from (4.2) is given by,

$$
\begin{aligned}
H_\infty &= \frac{1}{2}\,[\mu_2,\mu_3]\begin{bmatrix} \frac{4m'l'^2}{3} & \frac{m'l'^2}{2}\cos(\theta_{3,2}) \\ \frac{m'l'^2}{2}\cos(\theta_{3,2}) & \frac{m'l'^2}{3} \end{bmatrix}^{-1}\begin{bmatrix} \mu_2 \\ \mu_3 \end{bmatrix} \\
&= \frac{m'l'^2}{2}\,[\omega_2,\omega_3]\begin{bmatrix} \frac{4}{3} & \frac{1}{2}\cos(\theta_{3,2}) \\ \frac{1}{2}\cos(\theta_{3,2}) & \frac{1}{3} \end{bmatrix}\begin{bmatrix} \omega_2 \\ \omega_3 \end{bmatrix}.
\end{aligned}
\tag{4.8}
$$

We know that in the absence of internal and external torques for the above system, the Lagrangian L is equal to the Hamiltonian H_∞ (as given by (4.8)). The Lagrangian dynamics are given by,

$$
\frac{d}{dt}\frac{\partial L}{\partial \dot{q}} = \frac{\partial L}{\partial q},
$$

where $q = [\theta_1,\theta_2,\theta_3]$.

Simplifying the above equation we get,

$$
\begin{bmatrix} \ddot{\theta}_{2,1} \\ \ddot{\theta}_{3,2} \end{bmatrix} = \frac{1}{\Delta}\begin{bmatrix} -9\cos(\theta_{3,2})\sin(\theta_{3,2})\dot{\theta}_{2,1}^2 - 6\sin(\theta_{3,2})(\dot{\theta}_{2,1}+\dot{\theta}_{3,2})^2 \\ \left\{[24+9\cos(\theta_{3,2})]\,\dot{\theta}_{2,1}^2 + [9\cos(\theta_{3,2})+6]\,(\dot{\theta}_{2,1}+\dot{\theta}_{3,2})^2\right\}\sin(\theta_{3,2}) \end{bmatrix},
$$

$$\Delta \;=\; (9\cos^2(\theta_{3,2}) - 16),$$

which can be easily verified to be the time evolution equations of a two-link manipulator in the example in Horn[21].

RELATIVE EQUILIBRIA & THEIR STABILITY

Stability of relative equilibria for the multibody problem is of interest. Study of equilibria and their stability is essential for a better understanding of the phase portrait of the system. Stability of equilibria of rigid spacecraft with multiple rotors has been studied by Krishnaprasad and Berenstein [33] in the Hamiltonian setting. Holm, Marsden, Ratiu and Weinstein, [18] have studied the stability of a heavy top under this setting, using the energy-Casimir method. We use Arnold's [1] energy-Casimir method, as is summarized in Holm, Marsden, Ratiu and Weinstein [18] and Krishnaprasad and Marsden [34] to determine the equilibria and to assess their stability. An equivalent alternative to this method is to look for the critical points of the Hamiltonian H restricted to the symplectic leaves and test for definiteness of d^2H at these equilibria. The equilibria are not trivial to find since they involve the solution of a set of nonlinear algebraic equations with trignometric polynomials. The solution of these equations is a difficult task and as such no general analytical methods exist. Numerical techniques like the continuation methods which in the past have been used to solve inverse kinematics of robot manipulators [53], could be used to solve these equations.

Definition : Consider a dynamical system Σ:

$$\underline{\dot{x}} = f(\underline{x})$$

with $\underline{x} \in P$ and P is the phase space. The equilibria $\underline{x}_e$ are defined as the points $\underline{x}_e \in P$ such that

$$\underline{\dot{x}}_e = f(\underline{x}_e) = 0.$$

The energy-Casimir technique is introduced along with a simple free rigid body example. General formulae to determine the Casimir functions and to find the Hessian $(d^2 H)$ are given, for a general multibody system. The equilibria for a two-body system are computed. Their stability is analyzed and the results confirmed by numerical simulation. Even though an upper bound on the number of equilibria for a three-body problem can be found, the equilibria themselves are difficult to find. So, a special kinematic case of the three-body problem is considered and the corresponding equilibria are given explicitly. The energy-Casimir technique is applied successfully to the case of N-symmetrical bodies wherin the bodies are rotating with constant angular velocity in an extended position.

5.1 Energy-Casimir Method

We present the energy-Casimir method as given in Holm, Marsden, Ratiu and Weinstein [18] and illustrate it for a simple example of a free rigid body. The procedure to be followed regarding the method is outlined in three steps.

Step 1: Consider the system Σ with the equilibrium point $\underline{x}_e$ whose Liapunov stability we wish to ascertain. Find the conserved energy H: $P \rightarrow R$, i.e.,

$$\frac{dH}{dt} = 0. \tag{1.1}$$

Consider a family of conserved quantities $F : P \rightarrow R$. These conserved quantities are typically Casimirs (generated by symmetry groups). The bracket of a Casimir function with any other function g, where $g : P \rightarrow R$, should be identically equal to zero.

Step 2: (First Variation) Find all F in step 1 s.t. $H_F = H + F$ has a critical point at $\underline{x}_e$:

$$d(H + F)(\underline{x}_e) = 0. \tag{1.2}$$

Step 3: (Second Variation) The second derivative $d^2 H_F(\underline{x}_e)$ is computed. If it is definite then the system is Liapunov stable. The test is inconclusive if the above computed value is indefinite.

We give here an application of the above method for the case of a free rigid body (see Holm, Marsden, Ratiu, and Weinstein [18]).

Example 5.1.1 : Free Rigid Body

The free rigid body equations are

$$\dot{\underline{m}} = \underline{m} \times \underline{\omega}, \tag{1.3}$$

where $\underline{m}, \underline{\omega} \in \mathbb{R}^3$, $\underline{\omega}$ is the angular velocity and $\underline{m}$ is the angular momentum. $\underline{m}$ is related to $\underline{\omega}$ by $\underline{m} = \mathbf{I} \cdot \underline{\omega}$ where $\mathbf{I} = \mathrm{diag}(I_1, I_2, I_3)$ is the diagonalized moment of inertia tensor. The system is Hamiltonian in the Lie-Poisson structure on $\mathbb{R}^3$ considered as a dual of the Lie algebra of the special orthogonal rotation group $SO(3)$. The Lie-Poisson bracket is given by,

$$\{F, G\} = -\underline{m} \left(\underline{\nabla} F(\underline{m}) \times \underline{\nabla} G(\underline{m}) \right), \tag{1.4}$$

where $F, G : \mathbb{R}^3 \mapsto \mathbb{R}$.

It can be easily verified that for the bracket the system is Hamiltonian in the sense of $\dot{m}_i = \{m_i, H\}$, $i = 1, 2, 3$, where $\underline{m} = [m_1, m_2, m_3]^T$. The Hamiltonian H is simply the kinetic energy of the system and is given by

$$H = \frac{1}{2} \underline{m}^T \cdot \mathbf{I}^{-1} \cdot \underline{m}. \tag{1.5}$$

The Casimir function for the bracket (1.4) is any smooth function $\phi : \mathbb{R} \mapsto \mathbb{R}$ such that

$$C_\phi = \phi(\frac{|\underline{m}|^2}{2}). \tag{1.6}$$

61

An easy computation shows that the bracket of ϕ with any other function G is zero. Application of the energy-Casimir method follows.

Step 1 : The equilibria of (1.3) occur when $\underline{m}$ and $\underline{\omega}$ are parallel to one another. Without loss of generality the direction of $\underline{m}$ can be taken as the x axis. Further $\underline{m}$ could be normalized as $\underline{m}_e = [1, 0, 0]$.

Step 2 : (First Variation)

The derivative of

$$H_{C_\phi} = \frac{1}{2} \underline{m}^T \mathbf{I}^{-1} \underline{m} + \phi(\frac{|m|^2}{2}) \tag{1.7}$$

is

$$dH_{C_\phi} \cdot \delta \underline{m} = (\underline{\omega} + \underline{m} \phi'(\frac{|m|^2}{2})) \cdot \delta \underline{m}, \tag{1.8}$$

For the first variation dH_{C_ϕ} to be zero we have

$$\phi'(\frac{|m|^2}{2}) = -\frac{1}{I_1}. \tag{1.9}$$

Step 3 : (Second Variation)

The second derivative of (1.7) at equilibrium point $\underline{m}_e = [1, 0, 0]$ from (1.8) and (1.9) is,

$$
\begin{aligned}
d^2 H_{C_\phi} \cdot \delta \underline{m} &= \delta \underline{\omega} \cdot \delta \underline{m} + \phi'(\frac{|m|^2}{2}) \cdot |\delta \underline{m}|^2 + (\underline{m}_e \cdot \delta \underline{m})^2 \phi''(\frac{|m|^2}{2}) \\
&= \sum_{i=1}^{3} \frac{(\delta m_i)^2}{I_i} - \frac{(\delta \underline{m})^2}{I_1} + \phi''(\frac{|m|^2}{2}) \delta m_1^2 \\
&= \left(\frac{1}{I_2} - \frac{1}{I_1}\right)(\delta m_2)^2 + \left(\frac{1}{I_3} - \frac{1}{I_1}\right)(\delta m_3)^2 + \phi''(\frac{|m|^2}{2}) \delta m_1^2 (1.10)
\end{aligned}
$$

The various conditions for the definitiveness of (1.10) are as given below.

(i) The quadratic form is positive definite if and only if

$$\phi'' > 0,$$

$$I_1 > I_2, \quad I_1 > I_3.$$

The function

$$\phi(|\underline{m}|) = -\frac{2}{I_1}|\underline{m}| + \left(|\underline{m} - \frac{1}{2}\right)^2, \tag{1.11}$$

makes $d^2 H_{C_{\bullet}}$ positive definite at the equilibrium point $[1, 0, 0]$. So any stationary rotation along the *longest* axis is Liapunov stable.

(ii) The quadratic form is negative definite if and only if

$$\phi'' < 0,$$

$$I_1 < I_2, \quad I_1 < I_3.$$

An example of the function ϕ which satisfies the above condition is

$$\phi(|\underline{m}|^2) = -\frac{2}{I_1}|\underline{m}|^2 - \left(\frac{|\underline{m}|^2}{2} - \frac{1}{2}\right)^2, \tag{1.12}$$

which makes $d^2 H_{C_{\bullet}}$ positive definite at $[1, 0, 0]$. This proves that the rotation around the *short* axis is (Liapunov) stable.

(iii) The quadratic form is indefinite if

$$I_1 > I_2, \quad I_1 < I_3,$$

so we cannot prove by this method that the middle axis is unstable.

In summary the motion of a *free rigid body* along the *long* and *short* axes is stable.

5.2 Stability of Equilibria - A General Formulation

For a general multibody system we know that the Hamiltonian (which is nothing but the system kinetic energy), as given by Lemma 3.4.2 is

$$H = \frac{1}{2}\underline{\mu}^T \mathbf{J}^{-1} \underline{\mu}, \tag{2.1}$$

where $\mathbf{J} = \mathbf{J}(\theta_{k,J(k)}, \ k = 2, \ldots, N)$ and the conjugate momentum vector $\underline{\mu} = [\mu_1, \ldots, \mu_N]$. Also

$$\underline{\mu} = \mathbf{J}\underline{\omega}, \tag{2.2}$$

where $\underline{\omega}$ is the vector of angular velocities.

Step 1 : The equilibria for the system can be determined by setting the dynamical equations in Theorem 3.5.1 to zero, i.e.,

$$\dot{\mu}_k = \sum_{\forall j \; s.t. i = J(j)} \frac{\partial H}{\partial \theta_{j,i}} - \frac{\partial H}{\partial \theta_{i,J(i)}} = 0 \quad k = 1, \ldots, N, \quad (2.3)$$

$$\dot{\theta}_{k,J(k)} = \frac{\partial H}{\partial \mu_k} - \frac{\partial H}{\partial \mu_J(k)} = 0 \quad k = 2, \ldots, N. \quad (2.4)$$

This results in

$$\left[\frac{\partial H}{\partial \mu_i}\right]_e = \left[\frac{\partial H}{\partial \mu_j}\right]_e = \omega_o(\text{say}) \quad \forall i, j = 1, \ldots N, \quad (2.5)$$

so

$$\omega_1 = \omega_2 = \cdots = \omega_N = \omega_o, \quad (2.6)$$

and

$$\left[\frac{\partial H}{\partial \theta_{k,J(k)}}\right]_e = 0 \quad k = 2, \ldots, N, \quad (2.7)$$

where the subscript e indicates that the expression is evaluated at the equlibrium point.

From (2.1) and (2.2) we have

$$H = \frac{1}{2}\underline{\mu} \cdot \underline{\omega}. \quad (2.8)$$

At any equilibrium, using (2.6) in the above equation we get,

$$H = \frac{1}{2}\underline{\mu} \cdot \underline{r} \, \omega_o$$

$$= \frac{1}{2}\mu_s \omega_o, \quad (2.9)$$

where,

$$\underline{r} = [1, \cdots, 1]^T, \quad (2.10)$$

and

$$\mu_s = (\mu_1 + \cdots + \mu_N). \quad (2.11)$$

Here μ_s is the system angular momentum.

The constant angular velocity with which the bodies rotate when the system is at any equilibrium is

$$\omega_o = \frac{2H}{\mu_s}. \tag{2.12}$$

Step 2 : For the noncanonical bracket in Corollary 3.5.1, the Casimirs are any smooth functions of the form $\phi = \phi(\mu_s^2)$ where, $\mu_s = (\mu_1 + \cdots + \mu_N)$. It is easy to check that the bracket of ϕ with any other function $g : \mathbb{R}^{2N-1} \mapsto \mathbb{R}$ is equal to zero. Using (2.5) - (2.7), the first variation of (2.1) at any equilibrium point can be computed as

$$
\begin{aligned}
d(H + C_\phi)_e &= \left[\frac{\partial(H + C_\phi)}{\partial\underline{\mu}}\right]_e \delta\underline{\mu} + \left[\frac{\partial H}{\partial\underline{\theta}}\right]_e \delta\underline{\theta} \\
&= \left[\frac{\partial H}{\partial\underline{\mu}}\right]_e \delta\underline{\mu} + \sum_{i=1}^{N} 2\mu_s \phi'\left(\mu_s^2\right)\delta\mu_i \\
&= \sum_{i=1}^{N} \left[\omega_o + 2\mu_s\phi'(\mu_s^2)\right]\delta\mu_i. \tag{2.13}
\end{aligned}
$$

Setting the first variation in (2.13) to zero would result in a constraint on the Casimir function

$$\phi'(\mu_s^2) = -\frac{\omega_o}{2\mu_s}. \tag{2.14}$$

Step 3 : (Second variation) We initially calculate the Hessian (d^2H) and then find the second variation - $d^2(H + C_\phi)$. Using the first variation as in (2.13) we find

$$
d^2 H = \begin{bmatrix} \frac{\partial^2 H}{\partial\underline{\mu}^2} & \frac{\partial^2 H}{\partial\underline{\mu}\partial\underline{\theta}} \\ \frac{\partial^2 H}{\partial\underline{\theta}\partial\underline{\mu}} & \frac{\partial^2 H}{\partial\underline{\theta}^2} \end{bmatrix}. \tag{2.15}
$$

Now from (2.1) we have

$$\frac{\partial^2 H}{\partial\underline{\mu}^2} = \mathbf{J}^{-1}. \tag{2.16}$$

Taking partial derivatives of (2.1) as below and using (2.6) we get,

$$\left[\frac{\partial^2 H}{\partial\theta_{k,J(k)}\partial\underline{\mu}}\right]_e = -\left[\mathbf{J}^{-1}\frac{\partial\mathbf{J}}{\partial\theta_{k,J(k)}}\mathbf{J}^{-1}\underline{\mu}\right]_e \tag{2.17}$$

$$= -\left[\mathbf{J}^{-1}\frac{\partial\mathbf{J}}{\partial\theta_{k,J(k)}}\right]_e \underline{r}\omega_o, \tag{2.18}$$

65

where the $N \times 1$ vector $\underline{r}$ is as given by (2.10), and,

$$\left[\frac{\partial^2 H}{\partial\theta_{k,J(k)}\partial\theta_{l,J(l)}}\right] = -\frac{1}{2}\frac{\partial}{\partial\theta_{k,J(k)}}\left[\underline{\mu}^T J^{-1}\frac{\partial J}{\partial\theta_{l,J(l)}}J^{-1}\underline{\mu}\right]$$

$$= -\frac{1}{2}\underline{\mu}^T J^{-1}\left[\frac{\partial^2 J}{\partial\theta_{k,J(k)}\partial\theta_{l,J(l)}} - 2\frac{\partial J}{\partial\theta_{k,J(k)}}J^{-1}\frac{\partial J}{\partial\theta_{l,J(l)}}\right]J^{-1}\underline{\mu}.$$

The above equation along with (2.2) and (2.6) gives

$$\left[\frac{\partial^2 H}{\partial\theta_{k,J(k)}\partial\theta_{l,J(l)}}\right]_e = -\frac{\omega_o^2}{2}\underline{r}^T\left[\frac{\partial^2 J}{\partial\theta_{k,J(k)}\partial\theta_{l,J(l)}} - 2\frac{\partial J}{\partial\theta_{k,J(k)}}J^{-1}\frac{\partial J}{\partial\theta_{l,J(l)}}\right]\underline{r}, (2.19)$$

with $\underline{r}$ as in (2.10).

Assembling the second variation from the Hessian in (2.15) and, (2.16), (2.18) and (2.19) we get

$$d^2(H + C_\phi)_e = \begin{bmatrix} J^{-1} + (4\mu_s^2\phi'' + 2\phi')R & -\omega_o\left[J^{-1}\frac{\partial J}{\partial\theta_{k,J(k)}}\underline{r}\right]_e \\ & k = 2,\dots,N \\ -\omega_o\left[J^{-1}\frac{\partial J}{\partial\theta_{k,J(k)}}\underline{r}\right]_e^T & \left[\frac{\partial^2 H}{\partial\theta_{k,J(k)}\partial\theta_{l,J(l)}}\right]_e \\ k = 2,\dots,N & \forall k,l = 2,\dots,N \end{bmatrix}, \qquad (2.20)$$

where

$$R = \begin{bmatrix} 1 & 1 & \cdots & 1 \\ 1 & 1 & \cdots & 1 \\ \vdots & \vdots & \ddots & \vdots \\ 1 & 1 & \cdots & 1 \end{bmatrix}. \qquad (2.21)$$

5.3 Equilibria: Two-Body Case

We refer to the two-body example discussed in Chapter 4. The equilibria for the system are found and their stability analyzed. To search for the equilibria we look directly at the Hamilton's equations on P, as given in Theorem 4.1.1, by setting them equal to zero.

The first two equations turn out to be

$$\dot{\mu}_1 = -\dot{\mu}_2 = \left[\frac{\partial H}{\partial\theta_{2,1}}\right]$$

$$= -\tilde{\lambda}'_{12}(\theta_{2,1})$$

$$= \epsilon d_1 d_2 \sin(\theta_{2,1}) = 0, \qquad (3.1)$$

whereas, the equilibrium condition $\dot{\theta}_{2,1} = 0$ becomes

$$\left[\frac{\partial H}{\partial \mu_1}\right] = \left[\frac{\partial H}{\partial \mu_2}\right] = 0, \tag{3.2}$$

so, $\tilde{I}_1 \mu_1 - \epsilon \lambda \mu_2 = \tilde{I}_2 \mu_2 - \epsilon \lambda \mu_1$, or

$$\omega_1 = \omega_2 = \omega_o (\text{constant}). \tag{3.3}$$

From the above equations (3.1 and 3.3) we get the equilibrium conditions:

1. $\mu_1 = $ constant,

2. $\mu_2 = $ constant,

3. $\theta_{2,1} = 0$ or π

We are interested to study the non-degenerate equilibria, i.e., the system angular velocity $\omega_o \neq 0$. Degenerate equilibria occur when $\omega_o = 0$. For notational simplicity we will call the (non-degenerate) equilibrium points with θ equal to 0 and π as "equilibrium points 1 and 2" respectively. Equilibrium point 1 physically corresponds to the uniform rotation of the bodies in an extended position (Figure 5.1a). In a similar way the equilibrium point 2 corresponds to the bodies rotating uniformly in a folded position (Figure 5.1b).

5.3.1 Stability

Energy-Casimir Method Applied to the Two-Body System:

First Variation : Let a Casimir $C_\phi \in F$ be chosen as below :

$$C_\phi = \phi(\mu_s^2),$$

where, $\mu_s = (\mu_1 + \mu_2)$. Then the first variation of the Hamiltonian H (see Lemma 4.1.1) when computed taking into account (3.1 - 3.3) would result in,

$$
\begin{aligned}
d(H + C_\phi) &= \left(\frac{\partial H}{\partial \mu_1} + 2\mu_s \phi'\right) d\mu_1 + \left(\frac{\partial H}{\partial \mu_2} + 2\mu_s \phi'\right) d\mu_2 + \left(\frac{\partial H}{\partial \theta}\right) d\theta \\
&= \left(\frac{\partial H}{\partial \mu_1} + 2\mu_s \phi'\right) d\mu_1 + \left(\frac{\partial H}{\partial \mu_2} + 2\mu_s \phi'\right) d\mu_2.
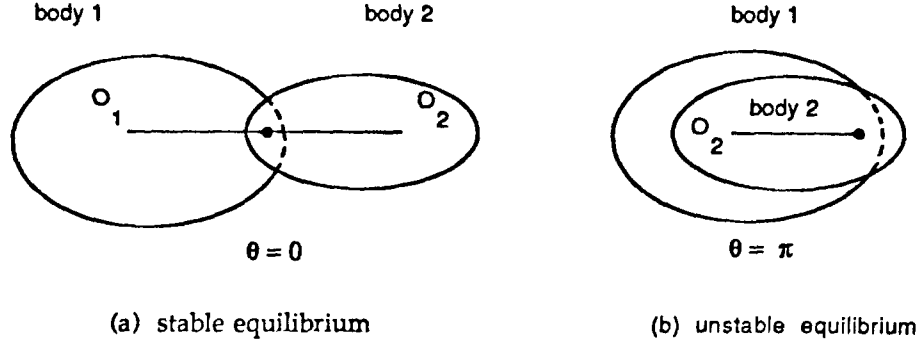\end{aligned} \tag{3.4}
$$

67

body 1   body 2   body 1

$\theta = 0$ $\theta = \pi$

(a) stable equilibrium   (b) unstable equilibrium

Figure 5.1: Equilibrium positions for a Two-Body Problem

Applying (1.2) along with (3.4) we get

$$d(H + C_\phi)_e = 0 \quad \Longrightarrow \quad \phi'(\mu_s) = -\left[\frac{\partial H}{\partial \mu_1}\right]_e$$
$$= -\frac{\omega_o}{2\mu_s},$$

where $\mu_s = (\mu_1 + \mu_2)$,

Second Variation : The second variation of H can be computed either from the general formula (2.20) <u>or</u> directly,

$$d^2(H + C_\phi) = \begin{bmatrix} \frac{\partial^2 H}{\partial \mu_1{}^2} + (4\mu_s^2\phi'' + 2\phi') & \frac{\partial^2 H}{\partial \mu_1 \partial \mu_2} + (4\mu_s^2\phi'' + 2\phi') & \frac{\partial^2 H}{\partial \mu_1 \partial \theta_{2,1}} \\ \frac{\partial^2 H}{\partial \mu_1 \partial \mu_2} + (4\mu_s^2\phi'' + 2\phi') & \frac{\partial^2 H}{\partial \mu_1{}^2} + (4\mu_s^2\phi'' + 2\phi') & \frac{\partial^2 H}{\partial \mu_2 \partial \theta_{2,1}} \\ \frac{\partial^2 H}{\partial \mu_1 \partial \theta_{2,1}} & \frac{\partial^2 H}{\partial \mu_2 \partial \theta_{2,1}} & \frac{\partial^2 H}{\partial \theta_{2,1}{}^2} \end{bmatrix}.$$
$$(3.5)$$

Evaluating all the terms and choosing $(2\mu_s^2\phi'' + \phi') = 0$ we get,

$$d^2(H + C_\phi)_e = \frac{1}{\Delta_e} \begin{bmatrix} \widetilde{I}_2 & -\widetilde{\lambda}_{12}(\theta_{2,1}) & 0 \\ -\widetilde{\lambda}_{12}(\theta_{2,1}) & \widetilde{I}_1 & 0 \\ 0 & 0 & \Delta\omega_1\omega_2 d_1 d_2 \cos(\theta_{2,1}) \end{bmatrix}_e. \quad (3.6)$$

68

where $\Delta_e = \left[\tilde{I_1}\tilde{I_2} - \epsilon^2 \lambda_{12}^2(\theta) \right]$.

From (3.6), we see that the principal minors of $d^2(H + C_\phi)$ are,

$$\frac{\tilde{I_2}}{\Delta_e}, \quad \frac{1}{\Delta_{e,}} \quad \text{and} \quad \frac{\omega_o^2 d_1 d_2 \cos(\theta_{2,1})}{\Delta_e}.$$

Since $\tilde{I_2} > 0$ and $\Delta_e > 0$ we can see that the definiteness of $d^2(H + C_\phi)$ depends on $\omega_o^2 d_1 d_2 \cos(\theta_{2,1})$. The following table gives the stability of the non-degenerate equilibria for various conditions.

Item	$\theta_{2,1} = 0$	$\theta_{2,1} = \pi$
$d_1 d_2 > 0$	Stable	Unstable
$d_1 d_2 < 0$	Unstable	Stable

If $\omega_o = 0$ (degenerate equilibria) then H is not definite and the energy-Casimir test fails. In fact for $\omega_o = 0$ the number of equilibria are *infinite*.

5.3.2 Simulation: Two-Body Case

Numerical simulation of the dynamics of a planar, rigid, two-body problem, was carried out to supplement our knowledge of the phase space and also to confirm the results from the application of the energy-Casimir method. The simulation code was written in FORTRAN and run on a VAX 11/785 under UNIX[1]. The results were displayed on a IRIS 2400 Graphics work-station. The initial conditions were generated separately for a particular value of the kinetic energy H and for a fixed value of the conjugate momentum sum. A set of output data was taken for sufficient problem time.

From Lemma 4.1.1 we have

$$H = \frac{1}{2}[\omega_1, \omega_2] \begin{bmatrix} \tilde{I_1} & \tilde{\lambda}_{12}(\theta_{2,1}) \\ \tilde{\lambda}_{12}(\theta_{2,1}) & \tilde{I_2} \end{bmatrix} \begin{bmatrix} \omega_1 \\ \omega_2 \end{bmatrix}$$

$$= \frac{1}{2} \left[\tilde{I_1}\omega_1^2 + 2\epsilon b_1 c_1 \omega_1 \omega_2 \cos(\theta_{2,1}) + \tilde{I_2}\omega_2^2 \right]. \tag{3.7}$$

---

[1] UNIX is the trademark of Bell Labs. NJ.

69

Now the system angular momentum μ_s (equal to the sum of the conjugate momentum variables) is,

$$\mu_s = (\mu_1 + \mu_2)$$

$$= [\mu_1, \mu_2] \begin{bmatrix} 1 \\ 1 \end{bmatrix}.$$

But from Lemma 4.1.1 we know that $\underline{\mu} = \mathbf{J}\underline{\omega}$, so

$$\mu_s = [\omega_1, \omega_2].\mathbf{J}^T.\begin{bmatrix} 1 \\ 1 \end{bmatrix}$$

$$= \left(\tilde{I}_1 + \epsilon d_1 d_2 \cos(\theta_0)\right)\omega_1 + \left(\tilde{I}_2 + \epsilon d_1 d_2 \cos(\theta_0)\right)\omega_2.$$

i.e.,

$$\omega_2 = \frac{\mu_s - (\tilde{I}_1 + \epsilon d_1 d_2 \cos(\theta_0))\omega_1}{(\tilde{I}_2 + \epsilon d_1 d_2 \cos(\theta_0))}, \tag{3.8}$$

where, θ_0 is the angle $\theta_{2,1}$ at time zero. Substituting for ω_2 in (3.8) from (3.7), we get an equation of the form,

$$a\omega_1^2 + b\omega_1 + c = 0, \tag{3.9}$$

where,

$$a = \frac{1}{2}\left[\tilde{I}_1 + \frac{(\tilde{I}_1 + \epsilon d_1 d_2 \cos(\theta_0))^2}{(\tilde{I}_2 + \epsilon d_1 d_2 \cos(\theta_0))^2}\tilde{I}_2 - \frac{(\tilde{I}_1 + \epsilon d_1 d_2 \cos(\theta_0))}{(\tilde{I}_2 + \epsilon d_1 d_2 \cos(\theta_0))}\epsilon d_1 d_2 \cos(\theta_0)\right],$$

$$b = \left[\frac{(\tilde{I}_1 + \epsilon d_1 d_2 \cos(\theta_0))}{(\tilde{I}_2 + \epsilon d_1 d_2 \cos(\theta_0))}\tilde{I}_2\mu_s + \frac{\epsilon d_1 d_2 \cos(\theta_0)}{(\tilde{I}_2 + \epsilon d_1 d_2 \cos(\theta_0))}\right],$$

$$c = \frac{\tilde{I}_2\mu_s^2}{(\tilde{I}_2 + \epsilon d_1 d_2 \cos(\theta_0))^2} - H.$$

A set of physical parameters [2] and a fixed value of the conjugate momentum sum $\mu_s = (\mu_1 + \mu_2)$ were assumed. For a given value of H, from (3.9) and (3.8), we get two sets of values for the $[\omega_1, \omega_2]^T$ vector and so for the $[\mu_1, \mu_2]^T$ vector. Simulations were carried out for each pair of these initial conditions by assuming a initial value of $\pi/2$ for $\theta_{2,1}$ i.e., $\theta_o = \pi/2$.

---

[2]$m_1 = 125$, $m_2 = 100$, $d_1 = 0.8$, $d_2 = 0.6$, $I_1 = 70$, $I_2 = 50$, and $\mu_s = 50$. (SI units).

A coordinate frame consisting of $x = (\mu_1 + \mu_2)\cos(\theta_{2,1})$, $y = (\mu_1 + \mu_2)\sin(\theta_{2,1})$ and $z = (\mu_1 - \mu_2)$ was chosen to display the results. The trajectories were found to live on a cylinder with the generators parallel to the z axis. The radius of the cylinder (as expected) was equal to the conjugate momentum sum. For a given value of the kinetic energy and $\theta_{2,1}$ at time zero the trajectories were closed. The trajectories around the equilibrium point 1 were elliptical in nature with the ellipse being laid out on the surface of the cylinder (see Figure 5.2). The major axes of these closed trajectories (orbits) were along the circumference of the cylinder. The opposite ends of the major axis ultimately met at a saddle point, which is the equilibrium point 2 (see Figure 5.3). From then on the trajectories were closed around the cylinder. From Figure 5.3 we can see that there are two homoclinic orbits from the unstable equilibrium (equilibrium point 2) and back onto itself.

Application of internal torque (this changes the energy level in the system) resulted in the trajectory jumping from one orbit to another but still remaining on the surface of the 'cylinder' one started with. Application of an external torque would result in the trajectory jumping from one concentric 'cylinder' to another depending on whether angular momentum was added (bigger radius 'cylinder') or subtracted (smaller radius 'cylinder').

One can expect that, when an additional third body is attached or if the system is forced (by means of a joint torque) there will be splitting of these homoclinic orbits resulting in chaotic dynamics. Melnikov's method may be used (see Holmes and Marsden[19]) for such analysis. The whole process of these evolving trajectories suggests that the existence of a 'energy ellipsoid' which gradually emerges out, from inside the cylinder, and the trajectories being formed by the points where this 'energy ellipsoid' intersects the momentum cylinder.

5.4 Equilibria : Three-Body Case

Consider a planar satellite composed of three rigid bodies connected by revolute joints in the form of an open chain (for details on notation refer to Chapter 4, Section 4.3). The local coordinate system for body 1 is chosen such that the x-axis is parallel
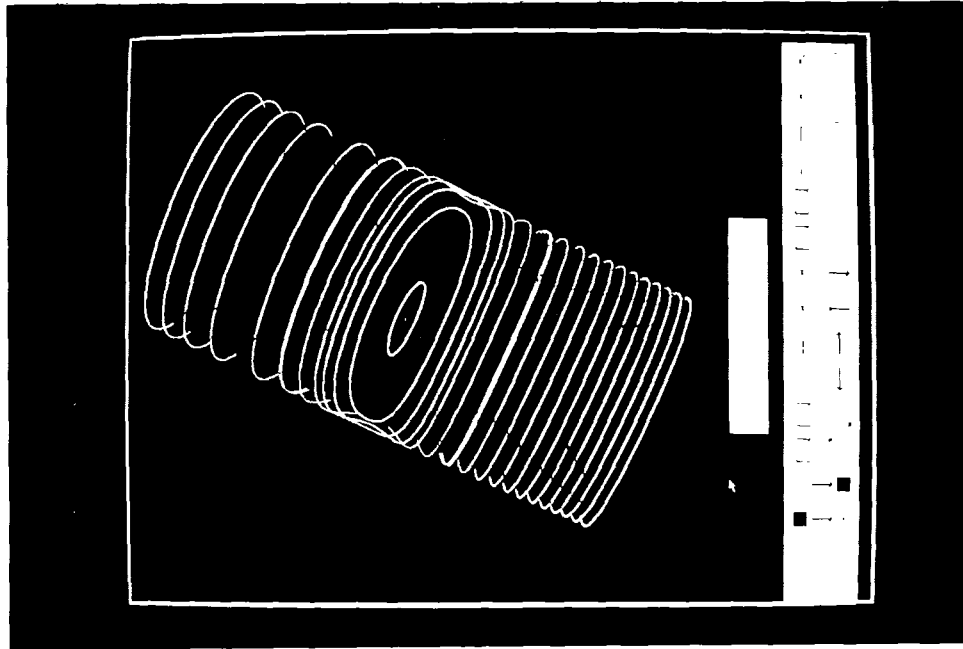
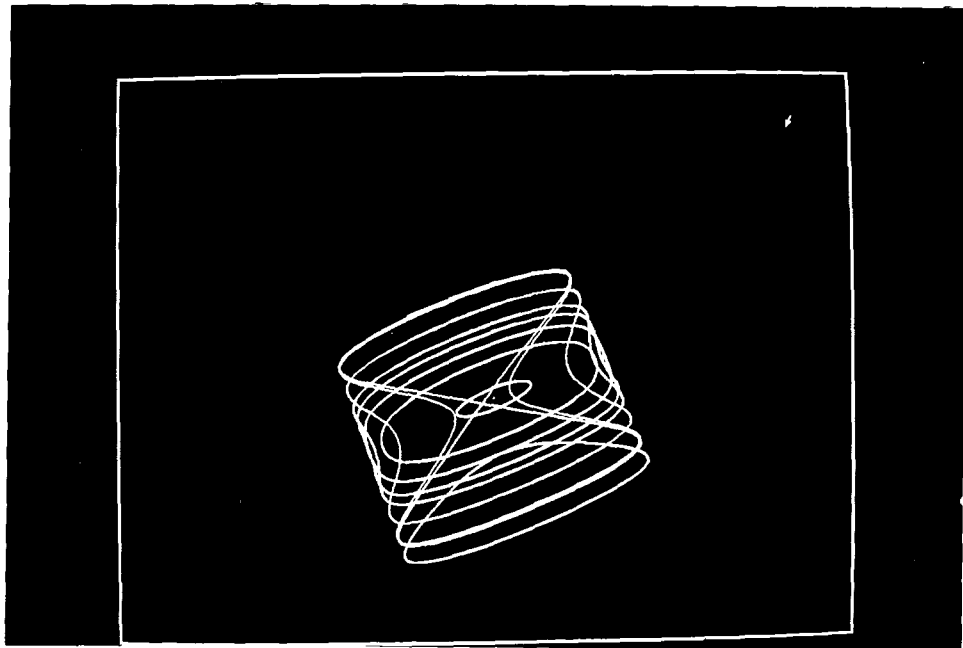Figure 5.2: Planar Two-Body Simulation - Equilibrium Point 1

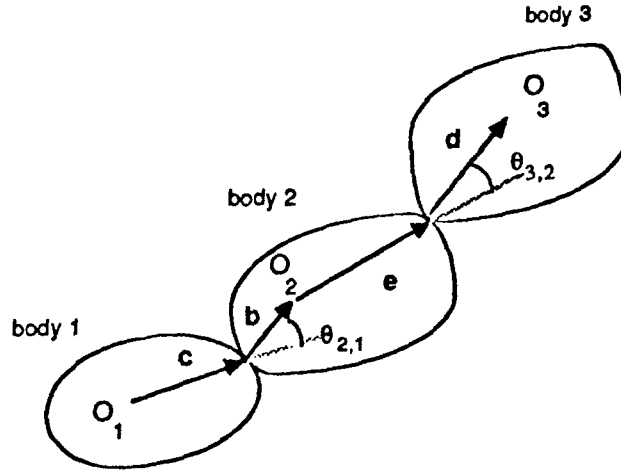Figure 5.3: Planar Two-Body Simulation - Equilibrium Point 2

Figure 5.4: Planar Three-Body System

to the line joining O_1 and O_{12} . Similarly the coordinate systems for body 2 and body 3 are chosen to be parallel to the line joining O_2 and O_{12}, and, the line joining O_3 and O_{23} respectively.

With such preliminaries taken care of, we define the vectors $\tilde{\alpha}_2, \tilde{\alpha}_3, \tilde{\beta}_2, \tilde{\beta}_3$, in their respective local coordinate systems to be : $\tilde{\alpha}_2 = [b_1, 0]^T$, $\tilde{\alpha}_3 = [d_1, 0]^T$, $\tilde{\beta}_2 = [c_1, 0]^T$, $\tilde{\beta}_3 = \tilde{\alpha}_2 + [e_1, e_2]^T$,

The equilibria for the three-body system can be found by setting the dynamical equations (in Theorem 4.2.1) to be zero. This results in the following equations :

$$\frac{\partial H}{\partial \theta_{2,1}} = \frac{\partial H}{\partial \theta_{3,2}} = 0, \tag{4.1}$$

$$\dot{\theta}_{2,1} = \omega_2 - \omega_1 = 0, \tag{4.2}$$

$$\dot{\theta}_{3,2} = \omega_3 - \omega_2 = 0. \tag{4.3}$$

From the above equations it can be seen that

$$\omega_1 = \omega_2 = \omega_3 = \omega_o(\text{constant}). \tag{4.4}$$

73

The system angular momentum μ_s, and the Hamiltonian H are given by

$$\mu_s = \omega_o \left[\sum_{i=1}^{3} \tilde{I}_i + 2(\tilde{\lambda}_{12}(\theta_{2,1}) + \tilde{\lambda}_{23} + \tilde{\lambda}_{31}(\theta_{2,1} + \theta_{3,2})) \right], \qquad (4.5)$$

$$H = \frac{1}{2}\omega_o^2 \left[\sum_{i=1}^{3} \tilde{I}_i + 2(\tilde{\lambda}_{12}(\theta_{2,1}) + \tilde{\lambda}_{23}(\theta_{3,2}) + \tilde{\lambda}_{31}(\theta_{2,1} + \theta_{3,2})) \right]$$

$$= \frac{1}{2}\omega_o \mu_s, \qquad (4.6)$$

or,

$$\omega_o = \frac{2H}{\mu}. \qquad (4.7)$$

Keeping in mind Lemma 4.2.1 we get,

$$\left[\frac{\partial H}{\partial \theta_{2,1}} \right]_e = \frac{1}{2} \frac{\partial}{\partial \theta_{2,1}} \left(\mu^T \mathbf{J}^{-1} \mu \right) \Big|_e$$

$$= -\frac{1}{2} \mu^T \mathbf{J}^{-1} \frac{\partial \mathbf{J}}{\partial \theta_{2,1}} \mathbf{J}^{-1} \mu \Big|_e$$

$$= -\frac{1}{2} \underline{\omega}^T \frac{\partial \mathbf{J}}{\partial \theta_{2,1}} \underline{\omega} \Big|_e$$

$$= -\frac{\omega_o^2}{2(m_1 + m_2 + m_3)} [A_1 \sin(\theta_{2,1} + \theta_{3,2}) + B_1 \sin(\theta_{2,1}) + C_1 \cos(\theta_{2,1})]$$

$$= 0,$$

or, for the non-degenerate case $(\omega_o \neq 0)$,

$$A_1 \sin(\theta_{2,1} + \theta_{3,2}) + B_1 \sin(\theta_{2,1}) + C_1 \cos(\theta_{2,1}) = 0, \qquad (4.8)$$

where,

$$A_1 = m_1 m_3 c_1 d_1, \qquad (4.9)$$

$$B_1 = [m_3(b_1 + e_1) + m_2 b_1] m_1 c_1, \qquad (4.10)$$

$$C_1 = m_1 m_3 c_1 e_2. \qquad (4.11)$$

Similarly, for $\frac{\partial H}{\partial \theta_{3,2}}$ we get,

$$\frac{\partial H}{\partial \theta_{3,2}} = \frac{\omega_o^2}{2(m_1 + m_2 + m_3)} [A_1 \sin(\theta_{2,1} + \theta_{3,2}) + B_2 \sin(\theta_{3,2}) + C_3 \cos(\theta_{3,2})] = 0, \qquad (4.12)$$

74

where,

$$B_2 = [m_1(b_1 + e_1) + m_2 e_1] m_3 d_1, \qquad (4.13)$$

$$C_2 = (m_1 + m_2) m_3 d_1 e_2. \qquad (4.14)$$

From (4.8) and (4.12) we assemble the final equilibrium equations:

$$\left. \begin{array}{l} A_1 \sin(\theta_{2,1} + \theta_{3,2}) + B_1 \sin(\theta_{2,1}) + C_1 \cos(\theta_{2,1}) = 0 \\ A_1 \sin(\theta_{2,1} + \theta_{3,2}) + B_2 \sin(\theta_{3,2}) + C_2 \cos(\theta_{3,2}) = 0 \end{array} \right\}. \qquad (4.15)$$

We now use a polar transformation on the above equations.

Let,

$$\left. \begin{array}{ll} \eta = e^{i\theta_{2,1}} & \text{so} \quad \sin(\theta_{2,1}) = \frac{1}{2i}\left[\eta - \frac{1}{\eta}\right] \quad ; \quad \cos(\theta_{2,1}) = \frac{1}{2}\left[\eta + \frac{1}{\eta}\right] \\ \xi = e^{i(\theta_{2,1} + \theta_{3,2})} & \text{so} \quad \sin(\theta_{2,1} + \theta_{3,2}) = \frac{1}{2i}\left[\xi - \frac{1}{\xi}\right] \quad ; \quad \cos(\theta_{2,1} + \theta_{3,2}) = \frac{1}{2}\left[\xi + \frac{1}{\xi}\right] \end{array} \right\}. \qquad (4.16)$$

Substituting from (4.16) for the trignometric terms in (4.15) and simplifying we get,

$$\left(\xi - \frac{1}{\xi}\right) A_1 + (B_1 + iC_1)\eta + (-B_1 + iC_1)\frac{1}{\eta} = 0, \qquad (4.17)$$

$$-\left(\xi - \frac{1}{\xi}\right) A_1 + (B_2 + iC_2)\frac{\xi}{\eta} + (-B_2 + iC_2)\frac{\eta}{\xi} = 0. \qquad (4.18)$$

Further manipulation of the above equations yield,

$$(p_7 + iq_7)\eta^7 + (p_6 + iq_6)\eta^6 + \cdots + (p_1 + iq_1)\eta + (p_0 + iq_0) = 0, \qquad (4.19)$$

$$\xi = \pm\sqrt{\frac{A_1 + (-B_1 + iC_1)\eta}{-(B_2 + iC_2) + A_1\eta}} \, \eta, \qquad (4.20)$$

where p_i's and q_i's are real constants, and i is the imaginary operator.

From the fundamental theorem of algebra we see that the polynomial equation (4.19) should have exactly seven roots subject to the condition $p_7 + iq_7 \neq 0$. From (4.20) we know that for every value of η we have two values of ξ.

Therefore in total we have 14 solutions of the (η, ξ) pair

The obvious question is whether all the above fourteen solutions of (4.19) are feasible, since we have not taken into account the constraints $\mid \eta \mid = 1$ and $\mid \xi \mid = 1$. Several approaches have been tried, to answer this question satisfactorily . Since the solutions have to lie on a unit circle an analogy to the stability of a discrete time control system whose characteristic equation is (4.19), can be considered. This has not led us to any conclusive result since the resulting expressions are horrendous.

Another approach is the following. If the ratio of the magnitudes of the coefficients of η^0 to η^7 is equal to one, then all the solutions have to lie on the unit circle, otherwise, we know that there are only an even number of solutions which are less than fourteen.

Yet another approach would be that of restricting ourselves to a sub-class of problems with simple kinematics, solving them and hope to gain some insight about the number of feasible solutions.

With this motivation, the following special case of the three body system wherein the joints and the centers of mass of the bodies lie in a straight line was considered and solved. It was found that there may be 4 or 6 solutions of the $(\theta_{2,1}, \theta_{3,2})$ pair for this special kinematic case of the three body system.

5.5 Three-Body System : Special Kinematic Case

We consider here a case of the three-body system with a special kinematic structure where the centers of mass of the bodies are aligned with the joints in a straight line when the bodies are in a stretched out position. It follows that $\tilde{\beta}_3 - \tilde{\alpha}_2 = [e_1, 0]^T$. So from (4.11) and (4.14)

$$e_2 = 0 \implies C_1 = C_2 = 0.$$

Thus (4.15) reduces to,

$$A_1 \sin(\theta_{2,1} + \theta_{3,2}) + B_1 \sin(\theta_{2,1}) = 0, \tag{5.1}$$

$$A_1 \sin(\theta_{2,1} + \theta_{3,2}) + B_2 \sin(\theta_{3,2}) = 0, \tag{5.2}$$

with

$$A_1 = c_1 d_1 m_1 m_3, \tag{5.3}$$

$$B_1 = [(b_1 + e_1)m_3 + b_1 m_2]c_1 m_1, \tag{5.4}$$

$$B_2 = [(b_1 + e_1)m_1 + e_1 m_2]d_1 m_3. \tag{5.5}$$

Subtracting (5.1) and (5.2) we get

$$\sin(\theta_{3,2}) = \kappa \sin(\theta_{2,1}), \tag{5.6}$$

where

$$\kappa = \frac{B_1}{B_2}. \tag{5.7}$$

Expanding (5.1) and substituting (5.6), we get

$$A_1 \sin(\theta_{2,1})[\cos(\theta_{3,2}) + \kappa \cos(\theta_{2,1}) + \tau] = 0, \tag{5.8}$$

where

$$\tau = \frac{B_1}{A_1}. \tag{5.9}$$

Consequently from (5.6) and (5.8) we have

$$\sin(\theta_{2,1}) = 0 \quad \text{and} \quad \sin(\theta_{3,2}) = 0, \tag{5.10}$$

or,

$$\sin(\theta_{3,2}) = \kappa \sin(\theta_{2,1}), \tag{5.11}$$

$$\cos(\theta_{3,2}) + \kappa \cos(\theta_{2,1}) + \tau = 0. \tag{5.12}$$

It is obvious from considering (5.10) that the following four roots of the $\{\theta_{2,1}, \theta_{3,2}\}$ pair could be readily identified :

$$\left.\begin{array}{c} \{0,0\} \\ \{0,\pi\} \\ \{\pi,0\} \\ \{\pi,\pi\} \end{array}\right\}. \tag{5.13}$$
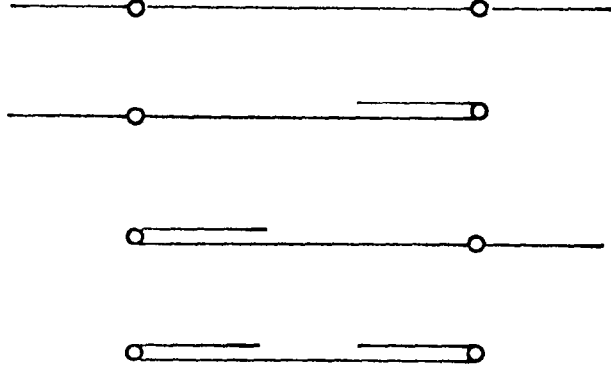
Figure 5.5: Fundamental equilibria

We label these equilibria as the *fundamental equilibria*. A stick figure representation (Figure 5.5) helps in bringing out the symmetrical way in which these equilibria occur.

The remaining equilibria for this system are computed as the solutions to (5.11) and (5.12). Since the equilibrium equations are nonlinear and parameter dependent, one needs to exercise care while solving them. The parameter dependence of the equilibrium solutions can be summarized by two sets of constraints – *parameter-sign* and *parameter-value* constraints respectively. It was found that two *extra equilibria* (other than the *fundamental equilibria*) can exist at a time, subject to the existence of suitable values of κ and τ satisfying these constraints. The maximum number of equilibria for a general three-body system (special kinematic case) is thus, 6. For some values of κ and τ not satisfying these constraints and for the cases with κ and/or τ being zero these *extra equilibria* merge with the *fundamental equilibria* to give a total of four equilibria.

5.5.1 Parameter-Sign Constraints

This constraint set restricts the existence of values of $\{\theta_{2,1}, \theta_{s,2}\}$ pair depending
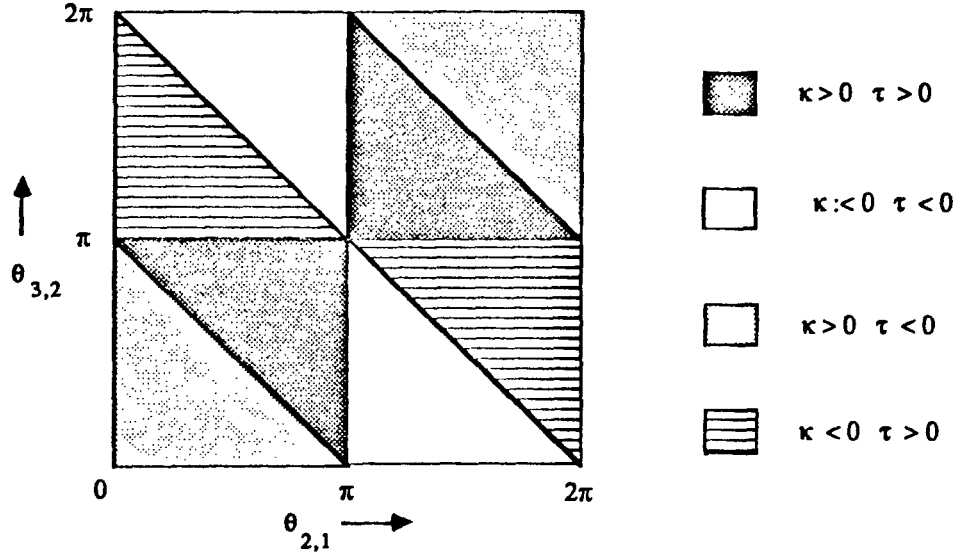
Figure 5.6: Parameter-Sign Constraints

on the signs of κ and τ.

Using (5.9) in (5.1) we get

$$\sin(\theta_{2,1} + \theta_{3,2}) = -\tau \sin(\theta_{2,1}). \qquad (5.14)$$

Taking into account the signs of κ and τ, from (5.11) and (5.14) we get Figure 5.6, which illustrates the feasible regions of the solution pair $\{\theta_{2,1}, \theta_{3,2}\}$ to form the *parameter-sign* constraints.

5.5.2 Parameter-Value Constraints

The existence of solutions of (5.11) and (5.12) is also dependent on the actual values of κ and τ (which are constants for a given three-body system). The *parameter-value* dependence of the solutions can be formulated by squaring and adding (5.11) and (5.12), and simplifying to get

$$\cos(\theta_{2,1}) = \frac{1 - \kappa^2 - \tau^2}{2\kappa\tau}, \qquad (5.15)$$

$$\cos(\theta_{3,2}) = \frac{\kappa^2 - \tau^2 - 1}{2\tau}, \qquad (5.16)$$

79
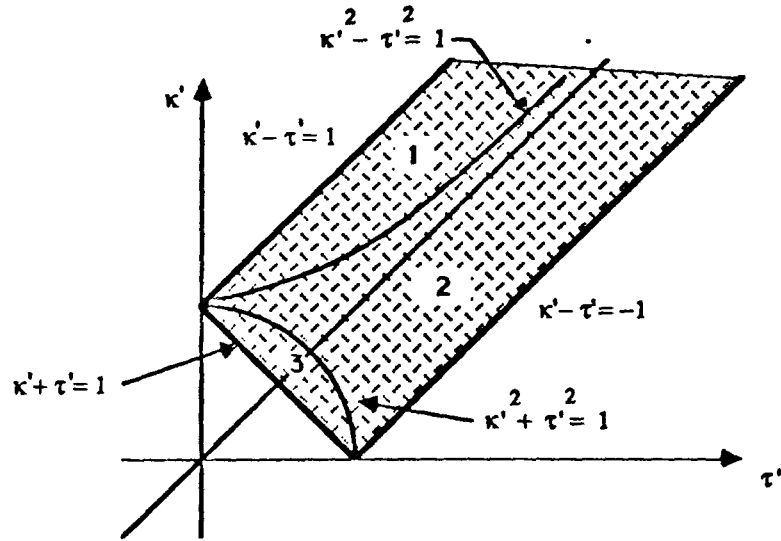
Figure 5.7: Parameter-Value Constraints

$$1 \; < \; \frac{1 - \kappa^2 - \tau^2}{2\kappa\tau} < 1, \tag{5.17}$$

$$1 \; < \; \frac{\kappa^2 - \tau^2 - 1}{2\tau} < 1. \tag{5.18}$$

These equations could be represented in the form of a graph as in Figure 5.7. The graph has been drawn for $\kappa' > 0$ and $\tau' > 0$, where

$$\kappa' \; = \; |\kappa|,$$

$$\tau' \; = \; |\tau|.$$

5.5.3 Local Frames of Reference

It is necessary to choose a local frame of reference for each of the bodies in order to parameterize the system and study the system equilibria. Refer to Figure 5.8. Proper choice of the local frames of reference for bodies 1 and 3 results in the vectors $\tilde{\beta}_2 = [c_1, 0]^T$ and $\tilde{\alpha}_3 = [d_1, 0]^T$, where both c_1 and d_1 are positive. In general, the

Figure 5.8: Reference Configuration

local frame of reference of body 2 could be chosen in such a way that $\tilde{\beta}_3 - \tilde{\alpha}_2 = [e_1, e_2]^T = [e_1, 0]^T$, where e_1 is positive. Note that if $\tilde{\alpha}_2 = [b_1, 0]^T$, the kinematic parameter b_1 could be either negative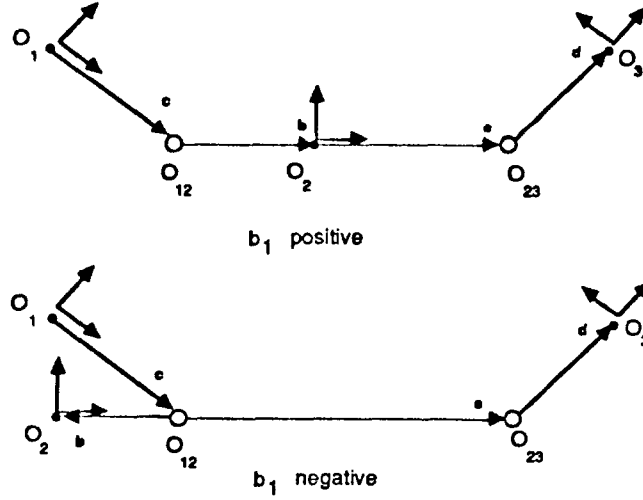 or positive. The two cases of the signs of b_1 represent whether the center of mass of body 2 is inside the line segment joining the joints O_{12} and O_{23} or outside it. If any of the kinematic parameters c_1 or d_1 is equal to zero then the three body problem decomposes into a two-body problem and a one-body problem. It is also important to observe that with this choice of local frames of reference, A_1 is positive (see (5.3)).

5.5.4 Parameter-Dependent Equilibria

We now delve into particular cases of the signs of parameters κ and τ and establish the solutions to the equilibrium equations. We constantly refer to (5.3)-(5.9) while formulating the necessary conditions.

In all the cases we consider, we first ascertain that there exist physically realizable values of the kinematic parameters - c_1, b_1, e_1 and d_1, before finding the actual solutions. The equilibria are evaluated based on the signs of $\cos(\theta_{2,1})$, and, $\cos(\theta_{3,2})$

81

(see (5.15) and (5.16)), and according to the *parameter-sign* and *parameter-value* constraints. The results are presented in the form of a table for each case. The graphs under the column *parameter-sign* constraints have to be read with $\theta_{2,1}$ as the X-axis and $\theta_{3,2}$ being the Y-axis (see Figure 5.6 for more details). The shaded regions represent the valid regions of existence of the $\{\theta_{2,1}, \theta_{3,2}\}$ pair. In the column of the *parameter-value* constraints, the regions referred to are the regions of Figure 5.7.

Given values of κ and τ, one can identify the corresponding table depending on the signs of these parameters, and determine which region they belong to with regard to Figure 5.7. The two *extra equilibria*, if any, could then be read off from the table.

CASE 1 : $\kappa > 0 \; \tau > 0$

For κ and τ to be greater than zero, A_1, B_1 and B_2 should be greater than zero. By choice of the local frames of reference we have from (5.4) and (5.5) :

$$(b_1 + e_1)m_3 + b_1 m_2 > 0 \quad \text{so} \quad e_1 > -\left(1 + \frac{m_2}{m_3}\right)b_1,$$

$$(b_1 + e_1)m_1 + e_1 m_2 > 0 \quad \text{so} \quad e_1 > -\left(\frac{m_1}{m_1 + m_2}\right)b_1,$$

i.e.,

$$e_1 > -\left(1 + \frac{m_2}{m_3}\right)b_1. \tag{5.19}$$

This is automatically satisfied if $b_1 > 0$.

The equilibrium solutions are given in a compact form in Table 5.1.

CASE 2 : $\kappa < 0, \; \tau < 0$

The case $\kappa < 0$ and $\tau < 0$ can be realized if and only if $B_1 < 0$, and $B_2 > 0$ (since $A_1 > 0$ always).

Simplifying so from (5.4) and (5.5) we have

$$-\left(1 + \frac{m_2}{m_3}\right)b_1 > e_1 > -\left(\frac{m_1}{m_1 + m_2}\right)b_1. \tag{5.20}$$

Naturally, the above equation indicates that this case is possible only if b_1 is negative (since $e_1 > 0$).

Case	$\cos(\theta_{2,1})$	$\cos(\theta_{3,2})$	Parameter-sign constraints	Parameter-value constraints	Equilibria
1.1	> 0	> 0		not satisfied	
1.2	< 0	< 0		region 2	
1.3	< 0	> 0		region 1	
1.4	> 0	< 0		region 3	

TABLE 1 : $\kappa > 0 \; \tau > 0$
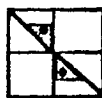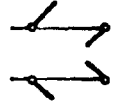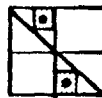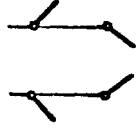
Case	$\cos(\theta_{2,1})$	$\cos(\theta_{3,2})$	Parameter-angle constraints	Parameter-value constraints	Equilibria
2.1	> 0	> 0		region 3	
2.2	< 0	< 0		region 1	
2.3	< 0	> 0		region 2	
2.4	> 0	< 0		not satisfied	

TABLE 5.2 : $\kappa < 0 \; \tau < 0$

83
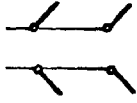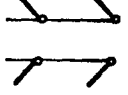
Case	$\cos(\theta_{2,1})$	$\cos(\theta_{3,2})$	Parameter-sign constraints	Parameter-value constraints	Equilibria
3.1	> 0	> 0		region 2	
3.2	< 0	< 0	not satisfied		
3.3	< 0	> 0		region 3	
3.4	> 0	< 0		region 1	

TABLE 5.3 : $\kappa > 0 \ \tau < 0$

Table 5.2 gives the equilibria associated with this case if (5.20) is satisfied.

CASE 3 : $\kappa > 0, \tau < 0$

For this case since $A_1 > 0$ we have to have B_1, $B_2 < 0$ i.e.,

$$e_1 \ < \ -\left(1 + \frac{m_2}{m_3}\right) b_1,$$

$$< \ -\left(\frac{m_1}{m_1 + m_2}\right) b_1.$$

With the choice of local frames of reference, $e_1 > 0$ so this case is possible only if b_1 is negative and

$$e_1 \ < \ -\left(\frac{m_1}{m_1 + m_2}\right) b_1. \tag{5.21}$$

The equilibria are as given in Table 5.3.

CASE 4 : $\kappa < 0, \tau > 0$

The necessary condition for this case is

$$-b_1 \left(1 + \frac{m_2}{m_3}\right) < \ e_1 \ < -b_1 \left(\frac{m_1}{m_1 + m_2}\right). \tag{5.22}$$

But $e_1 > 0$, so b_1 has to be negative. Then from (5.22) $\frac{e_1}{|b_1|}$ is greater than 1 but less than a fraction − which is impossible.

So kinematic parameters satisfying $\kappa < 0$ and $\tau > 0$ can never exist.

5.6 Equilibria of N-Body (Chain) : Special Case

We consider the special case of the N-body (chain) discussed in Chapter 4.3.1 with no internal or external torques. The dynamical equations given by Theorem 4.3.1 are,

$$
\dot{\mu}_1 = \frac{\partial H}{\partial \theta_{2,1}},
$$

$$
\dot{\mu}_2 = \frac{\partial H}{\partial \theta_{3,2}} - \frac{\partial H}{\partial \theta_{2,1}},
$$

$$
\vdots \qquad \vdots
$$

$$
\dot{\mu}_i = \frac{\partial H}{\partial \theta_{i+1,i}} - \frac{\partial H}{\partial \theta_{i,i-1}},
$$

$$
\vdots \qquad \vdots
$$

$$
\dot{\mu}_{N-1} = \frac{\partial H}{\partial \theta_{N,N-1}} - \frac{\partial H}{\partial \theta_{N-1,N-2}},
$$

$$
\dot{\mu}_N = -\frac{\partial H}{\partial \theta_{N,N-1}},
$$

$$
\dot{\theta}_{i+1,i} = \frac{\partial H}{\partial \mu_{i+1}} - \frac{\partial H}{\partial \mu_i} \quad \text{for i=1,..,N-1},
$$

where μ_i 's are the conjugate momentum variables.

Setting

$$
\dot{\mu}_i = 0, \; i = 1, \ldots, N
$$

$$
\dot{\theta}_{i+1,i} = 0, \; i = 1, \ldots, N - 1
$$

we get the *relative equilibrium* conditions.

Considering *non-degenerate* equilibrium solutions $(\omega_o \neq 0)$ we have on simplification,

$$
\underline{\omega} = [1, \ldots, 1]^T \omega_o,
$$

where ω_o is the constant angular velocity with which all the bodies rotate when the system is at equilibrium. Also

$$\frac{\partial H}{\partial \theta_{i+1,i}} = \omega_o^2 \sum_{j=1}^{i} \sum_{k=i+1}^{N} \tilde{\lambda}_{jk} \sin(\theta_{k,j}) = 0. \qquad (6.1)$$

It is clear from 6.1 that

$$\theta_{i+1,i} = n\pi, \quad i = 1,\dots,N-1,$$

$$n = 0,1,2,\dots$$

gives a set of solutions.

Further it is obvious that

$$\theta_{i+1,i} = 0, \quad i = 1,\dots,N-1, \qquad (6.2)$$

i.e., the case wherein the bodies are in a stretched out position and rotating with constant angular velocity is definitely an equilibrium solution.

We now study the stability of this equilibrium solution for the case of symmetrical bodies (bodies with same mass, inertia and physical parameters, and, with the center of mass at the center of the line connecting the joints, see Chapter 4.3.1) using energy-Casimir method.

By suitable choice of the second derivative of the Casimir function i.e.,

$$2\mu_s^2 \phi'' + \phi' = 0, \qquad (6.3)$$

we have from (2.20) the Hessian at the equilibrium given by (6.2) as

$$d^2(H + C_\phi)_e = \begin{bmatrix} \mathbf{J}^{-1} & \underline{O}_{N,N-1} \\ \underline{O}_{N-1,N} & \left[\frac{\partial^2 H}{\partial \theta_{k,k-1} \partial \theta_{l,l-1}}\right]_e \\ & \forall k,l = 2,\dots,N \end{bmatrix}. \qquad (6.4)$$

We need to establish the definiteness of the above matrix at the equilibrium point to prove stability. Since $\mathbf{J}$ is positive definite we need to find the definiteness of the remaining part in (6.4), which on simplification yields

$$\left[\frac{\partial^2 H}{\partial \theta_{k,k-1} \partial \theta_{l,l-1}}\right]_e = -\frac{1}{2}\omega_o^2 \left[\underline{r}^T \frac{\partial^2 \mathbf{J}}{\partial \theta_{k,k-1} \partial \theta_{l,l-1}} \underline{r}\right]_e \qquad (6.5)$$

86

where

$$\mathbf{r}^T \left.\frac{\partial^2 \mathbf{J}}{\partial \theta_{k,k-1} \partial \theta_{l,l-1}}\mathbf{r}\right|_e = \sum_{i=1}^{l} \sum_{j=l+1}^{N} \tilde{\lambda}_{i,j}(0) \text{ for } l \geq k, \; l = 2,\ldots,N. \qquad (6.6)$$

and $\tilde{\lambda}$'s is given in terms of $\tilde{\delta}$'s (see Chapter 4.3.1 and Theorem 3.4.2).

The expressions for $\tilde{\delta}$'s involve inequalities and it is hard to prove in general the definiteness of the matrix given by (6.5). A numerical experiment was conducted for such systems, with the number of bodies varying from two to ten. In all cases the matrix was found to be positive definite. These results are given in Appendix 1.

This conclusively proves that multibody systems consisting of two and upto ten bodies have a *stable equilibrium when all the bodies are rotating with a constant angular velocity, in an extended position.*

SIX

CONTROL & STABILIZATION

We have so far addressed the modeling aspects of multibody systems in space as well as on ground. The equilibria of these dynamical systems have been looked into and their stability for particular cases examined by means of rigorous analysis as well as simulations. This leads to the next logical step which is the study of control of multi-body systems.

The issues involved in the control of spacecraft can be divided into three categories: sensing, control and actuation. Sensing of control and state variables is essential for feedback control and supervisory purposes. Control of spacecraft could be done by either passive (e.g. gravity gradient methods) or active means (e.g. momentum wheels, gas jets, etc.) [58]. Actuation of control signals could be achieved by methods which conserve mass and momentum of the system or by the ones which do not. Techniques which make use of the former concept are based on the use of momentum and reaction wheels, while the use of gas jets, magnetic torquers etc. do not preserve angular momentum. The control strategy itself is dictated by the goal specifications, system dynamics, external and internal disturbances, workspace limitations, and lastly the available technology. A certain amount of analysis and understanding of the control theoretic aspects greatly helps in devising such strategies.

In this chapter we prove global controllability as applicable to such multibody

systems connected in the form of a tree structure. We also prove that these multibody systems are linearizable in the Input/Output (henceforth referred to as I/O) sense by means of a nonlinear state feedback. Differential geometric methods are made use of to achieve this "exact linearization" and the I/O map of the linearized system is also given. Finally we conclude the chapter with a discussion of stabilizability of these systems and prove a feedback stabilization theorem. In each section we will go through examples which amply illustrate the control problem being tackled with reference to multibody systems – particularly multibody spacecraft and terrestrial and space-based robots.

6.1 Controllability

Consider a robot arm mounted on a satellite. The commanded motions of this robot arm induce motions of the satellite constituting the robot base. As a result the robot joint angles that would normally be commanded (on a stationary base) to produce the desired robot end-effector motion, would result in a missed target. A simple example illustrates this. Consider a space shuttle of mass $m_S = 100,000$ kgs. with a maximum payload of $m_L = 30,000$ kgs on the shuttle remote manipulator arm. We desire to move the payload by say $r = 10$ m. in inertial space. Making use of standard kinematic relations, with a point mass model, the invariance of center of mass position indicates that the payload has moved only

$$\frac{r}{1 + \frac{m_L}{m_S}} = 7.5m. \tag{1.1}$$

This would result in the end-effector missing the target by a large margin. Further if the base of the shuttle arm is uncontrolled, the final end-effector state is not function of the terminal joint angles alone, but is determined by the entire joint angle history. Thus the control of these special kinds of dynamical systems is made difficult since the kinematics and the dynamics are coupled in these systems.

The reaction torques and forces on the Space Station due to the movement of the MRMS could be minimized if the MRMS presents a low inertia profile when traversing the space station keel. Similarly, for an open chain of bodies in space, it is of interest

to us to study how using articulation control we could get this system of bodies –
which presents a larger inertia profile, to form a closed chain – which presents a
relatively smaller inertia profile for the dynamics. We may also want to conduct this
maneuver in an optimal way with respect to time and fuel.

Similar problems are also encountered in other applications involving robotics in
space. The Telerobotic Work System (TWS) [1] as envisioned by NASA [28], is to be
used in conjunction with the Orbital Maneuvering Vehicle (OMV). The function of
the TWS will be the servicing of satellites; satellite repair; assembly and construction;
payload handling, and contingency repair of spacecraft. Imagine the TWS already
docked with the satellite to be repaired or serviced, and has now formed an 'open'
chain along with the satellite. The manipulator arms on the TWS are now to be
used to repair the satellite. Commanded movement of the arm produces undesirable
reaction forces on the remaining (connected) bodies including the satellite. These
forces may move the position of center of mass of the satellite and may rotate the
body about its center of mass, resulting in the end-effector missing the target.

Thus the problem of closing an open chain of bodies in space appears to be generic.

Rapid reorientation of large space-based sensors from one stationary orientation
to another is a problem of continuing concern [46]. Such a "step-stare" maneuver is
rendered difficult due to the interaction of dynamics of the connected bodies. For
example consider a space based telescope which is connected to the main satellite
body by means of a revolute joint. Reorientation of the telescope may be necessary
while keeping the antennae on the main satellite body oriented towards the earth.

All the above examples require that a suitable control input be found to drive the
system from any initial state to a given final state in finite time. In other words we
are interested in controllability questions.

6.1.1 Multibody System Controllability

The Hamiltonian dynamics of a planar multibody system connected in the form
of a tree structure with joint (internal) torques T_k, $k = 1, \ldots, N - 1$ and an external

---

[1]recent telerobotic literature refers to this as Flight Telerobotic Servicer (FTS) [63]

torque T_1^{ext} on body 1 is given by Theorem 3.6.1 to be

$$\dot{\mu}_1 = \sum_{\forall j,\ s.t.\ J(j)=1} \frac{\partial H}{\partial \theta_{j,1}} + \sum_{\forall j,\ s.t.\ J(j)=1} T_{j-1} + T_1^{ext}, \tag{1.2}$$

$$\vdots \qquad \vdots$$

$$\dot{\mu}_i = \sum_{\forall j,\ s.t.\ J(j)=i} \frac{\partial H}{\partial \theta_{j,i}} - \frac{\partial H}{\partial \theta_{i,J(i)}} + \sum_{\forall j,\ s.t.\ J(j)=i} T_{j-1} - T_{i-1}, \tag{1.3}$$

$$\text{for } i = 2,\ldots,N-1,$$

$$\vdots \qquad \vdots$$

$$\dot{\mu}_N = -\frac{\partial H}{\partial \theta_{N,J(N)}} - T_{N-1}, \tag{1.4}$$

$$\dot{\theta}_{i,J(i)} = \frac{\partial H}{\partial \mu_i} - \frac{\partial H}{\partial \mu_{J(i)}} \quad \text{for } i = 2,\ldots,N. \tag{1.5}$$

The above equations could be also written as,

$$\left.\begin{array}{rcl} \dot{\underline{x}} &=& f(\underline{x}) + \underline{g}\underline{u} \\ \underline{y} &=& h(\underline{x}) \end{array}\right\}, \tag{1.6}$$

where the state vector $\underline{x}$ and control (input) vector $\underline{u}$ are given by

$$\underline{x} = \left[\mu_1,\ldots,\mu_N,\theta_{k,J(k)},\ k = 2,\ldots,N\right], \tag{1.7}$$

$$\underline{u} = \left[T_1,\ldots,T_{N-1},T_1^{ext}\right]^T, \tag{1.8}$$

and

$$f(\underline{x}) = \begin{bmatrix} \sum_{\forall j,\ s.t.\ J(j)=1} \frac{\partial H}{\partial \theta_{j,1}} \\ \sum_{\forall j,\ s.t.\ J(j)=i} \frac{\partial H}{\partial \theta_{j,i}} - \frac{\partial H}{\partial \theta_{i,J(i)}} \\ i=2,\ldots,\text{N-1} \\ -\frac{\partial H}{\partial \theta_{N,J(N)}} \\ \frac{\partial H}{\partial \mu_k} - \frac{\partial H}{\partial \mu_{J(k)}}, \quad k = 2,\ldots,N \end{bmatrix}, \tag{1.9}$$

$$\underline{g} = \begin{bmatrix} \underline{Q} & | & \underline{w} \\ \underline{O}_{N-1,N} \end{bmatrix}, \tag{1.10}$$

and $\underline{Q}$ is a $N \times N - 1$ matrix whose elements are either 0, +1, or −1, $\underline{w} = [1,0,\ldots,0]^T$, and $\underline{O}_{N-1\times N}$ is the $N - 1 \times N$ *null matrix*.

91

The output $\underline{y}$ is the vector of inertial angular velocities $\underline{\omega}$ of the system and is given by :

$$\underline{y} = h(\underline{x})$$
$$= \underline{\omega}$$
$$= \left[\mathbf{J}^{-1}\underline{\mu} \right] . \tag{1.11}$$

Lemma 6.1.1 : The matrix $\underline{Q}$ is full rank.

Proof : Let us first list some of the properties of the matrix $\underline{Q}$

(i) $\underline{Q}$ is a $N \times N - 1$ matrix.

(ii) Any column of $\underline{Q}$ contains only two nonzero elements a (+1) and a (-1), the rest are all zeros.

(iii) Consequently adding all the rows of $\underline{Q}$ results in a *zero row vector*. This means that the rank of $\underline{Q}$ is less than or equal to $(N - 1)$.

(iv) Addition of any $r < N$ rows of $\underline{Q}$ results in a nonzero row vector (since $\underline{Q}$ represents a *directional vertex matrix* of a *connected graph*. For more details see Seshu and Reed [48], Lemma 5-1(b) and Theorem 5-1).

(v) The non-zero elements of the first row of $\underline{Q}$ are always 1.

Let $\underline{Q}_1, \ldots, \underline{Q}_N$, be the rows of $\underline{Q}$. Let c_k's be scalar; the equation

$$\sum_{k=1}^{N} c_k \underline{Q}_k = \underline{Q}_{1,N-1},$$

has the only non-trivial solution (modulo a scale factor),

$$c_1 = c_2 = \cdots = c_N = 1, \tag{1.12}$$

from properties (iii) and (iv).

Thus only one independent relation exists among the rows of $\underline{Q}$. Since $\underline{Q}$ has N rows the rank of $\underline{Q}$ is $N - 1$. Q.E.D.

Theorem 6.1.1 : The multibody system given by (1.6) is globally controllable., i.e., one can find an input to take the system from any initial state in the state space to any given final state in arbitrarily small time.

Proof : Differentiating (1.11) we get

$$
\begin{aligned}
\underline{\dot{y}} &= \frac{\partial h}{\partial \underline{x}} \underline{\dot{x}} \\
&= \frac{\partial h}{\partial \underline{x}} \left[f(\underline{x}) + \underline{g}\underline{u} \right] \\
&= \frac{\partial h}{\partial \underline{x}} f(\underline{x}) + \frac{\partial h}{\partial \underline{x}} \underline{g}\underline{u}.
\end{aligned}
\tag{1.13}
$$

Again from (1.11) we have,

$$
\frac{\partial h}{\partial \underline{x}}\underline{g} = \left[\mathbf{J}^{-1} \;\middle|\; \begin{array}{c} -\underline{\mu}^T \mathbf{J}^{-1} \frac{\partial \mathbf{J}}{\partial \theta_{2,1}} \mathbf{J}^{-1} \\ \cdots \\ -\underline{\mu}^T \mathbf{J}^{-1} \frac{\partial \mathbf{J}}{\partial \theta_{i,J(i)}} \mathbf{J}^{-1} \\ \cdots \\ -\underline{\mu}^T \mathbf{J}^{-1} \frac{\partial \mathbf{J}}{\partial \theta_{N,J(N)}} \mathbf{J}^{-1} \end{array} \right] \cdot \left[\begin{array}{c} Q \mid \underline{w} \\ \underline{Q}_{N-1,N} \end{array} \right]
$$

$$
= \mathbf{J}^{-1} \left[\underline{Q} \mid \underline{w} \right].
\tag{1.14}
$$

Recall that $\underline{Q}$ is full rank from Lemma 6.1.1, so $\left[\underline{Q} \mid \underline{w} \right]$ is full rank and

$$
\frac{\partial h}{\partial \underline{x}}\underline{g} = \text{full rank,}
$$

i,e., from (1.13) we can choose

$$
\underline{u} = \left[\frac{\partial h}{\partial \underline{x}}\underline{g} \right]^{-1} \left[-\frac{\partial h}{\partial \underline{x}} f(\underline{x}) + \underline{v} \right],
\tag{1.15}
$$

where $\underline{v} \in \mathcal{U}$ is the new input. The block diagram (Figure 6.1) illustrates a realization by feedback.

So (1.13) becomes

$$
\underline{\dot{y}} = \underline{v},
\tag{1.16}
$$

i.e., from (1.11), the above equation becomes

$$
\underline{\dot{\omega}} = \underline{v}.
\tag{1.17}
$$

93
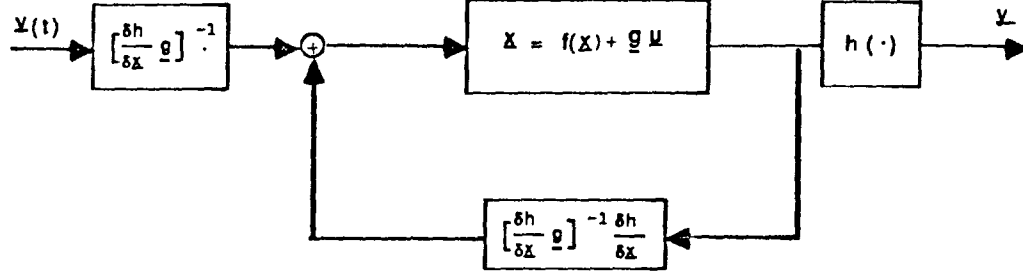
Figure 6.1: Controllable realization

Let

$$\underline{\Theta} = [\theta_1, \theta_2, \cdots, \theta_N]^T, \tag{1.18}$$

where θ_i is the angle made by the local coordinate system of body i with the inertial coordinate system. i.e.,

$$\underline{\dot{\Theta}} = \underline{\omega}. \tag{1.19}$$

From (1.17) and (1.19) we get

$$\left.\begin{array}{c}
\begin{bmatrix} \underline{\dot{\Theta}} \\ \underline{\dot{\omega}} \end{bmatrix} = \begin{bmatrix} \underline{O}_{N,N} & I_N \\ \underline{O}_{N,N} & \underline{O}_{N,N} \end{bmatrix} \begin{bmatrix} \underline{\Theta} \\ \underline{\omega} \end{bmatrix} + \begin{bmatrix} O \\ I_N \end{bmatrix} \underline{v} \\
y = \underline{\omega}
\end{array}\right\}. \tag{1.20}$$

By choosing a suitable nonlinear control as in (1.15) we have reduced the system in (1.6) to a I/O linearized system given by (1.20), which is controllable.

This means we can go from any given initial state $[\underline{\Theta}(0), \underline{\omega}(0)]^T$ to any given final (arbitrary) state, $[\underline{\Theta}(t_f), \underline{\omega}(t_f)]^T$, in arbitrary time $t_f \in \mathbb{R}$ by carefully choosing the control input $\underline{v}$.

Consequently, we can go from any given initial state $[\underline{\theta}(0), \underline{\mu}(0)]^T$ to any given final (arbitrary) state, $[\underline{\theta}(t_f), \underline{\mu}(t_f)]^T$, in arbitrary time $t_f \in \mathbb{R}$, since

$$\mu = J\underline{\omega},$$

$$\underline{\theta} \;=\; \underline{Q}^T \underline{\Theta},$$

$\Longrightarrow$ the multibody system given by (1.6) is _controllable_. Q.E.D.

Actually we can say something more than just proving the existence of an input which takes the system in (1.20) from any initial position at time zero to any final position at time T (arbitrary). Let us represent the system as

$$\begin{aligned}
\underline{\dot{z}} &= A\underline{z} + B\underline{v} \\
y &= \begin{bmatrix} \underline{Q}_{N,N} \mathbf{I}_N \end{bmatrix} \underline{z}
\end{aligned} \right\},$$
(1.21)

where $\underline{z} = [\underline{\Theta}, \underline{\omega}]^T$. The following remark gives such an input $\underline{v}^*$ which could be used as a form of an open loop control.

Remark 6.1.1 : Consider the system (1.21). One of the controls which takes the system from an initial position $\underline{z}(0) = [\underline{\Theta}(0), \underline{\omega}(0)]$ at time zero, to a position $\underline{z}(T) = [\underline{\Theta}(T), \underline{\omega}(T)]$ at time T (arbitrary) is given by

$$\underline{v}^* \;=\; -B^T e^{-A^T} \eta^*,$$
(1.22)

where η^* is any solution of

$$W(0,T)\eta \;=\; \underline{z}(0) \;-\; e^{-AT}\underline{z}(T),$$
(1.23)

and

$$W(0,t) \;=\; \int_0^t e^{-A\tau} B B^T e^{-A^T \tau} d\tau,$$
(1.24)

for $t \in [0,T]$ is the controllability grammian [30].

Remark 6.1.2 : Orientation of articulated sensors could be accomplished by first choosing a feedback as in (1.15) to I/O linearize the system and then accomplishing the orientation by means of the open loop control given by (1.22).

6.2 Exact Linearization

Exact linearization as opposed to linearization around an operating point involves the use of differential geometric methods to determine the nonlinear transformation/feedback which linearizes the system. Beginning with the work of Brockett [4] there has been considerable interest in nonlinear feedback theory to linearize a nonlinear system by using the concept of feedback equivalence among systems (characterized via necessary and sufficient Lie-algebraic conditions). Systems for which feedback equivalence could be applied and which could be linearized can then be taken to be equivalent to the linear controllable ones. Jackubczyk and Respondek [27] discovered the necessary and sufficient conditions for the (local) feedback equivalence for a nonlinear system, under a large group of equivalence transformation than considered by Brockett [4].

Transformation of a nonlinear system to an equivalent linear system has been done both in the single input case by Su [52], and in the multi-input case by Hunt, Su, and Meyer [24]. This theory provided a formal mathematical framework for the successful implementation of an automatic flight controller design for the vertical and short takeoff (VSTOL) aircraft. The nonlinear plant could be controlled by controlling the linear system, and any controller design could be done on the "linear side" of the system (i.e., on the transformed nonlinear system). An inflight testing of an automatic flight control system for a DHC-6 and an Automatic Wing Jet STOL Research aircraft have been successful, and the methodology is being used for the UH-1H helicopter. However these results are true locally only i.e., 'in the neighborhood of the origin'. Hunt, Su, and Meyer [23] have also formulated a procedure for the global transformation of nonlinear systems to linear controllable ones for the single input case.

Isidori and Krener [26] consider a multi-input multi-output system case with the inputs entering linearly, and achieved the Input/State linearization by using a combination of coordinate changes and static state feedback. The resulting transformation could be explicitly solved to achieve the desired linearization. These methods are in

general known as Input/State linearization.

Input/Output linearization as given by Isidori [25] for a class of nonlinear systems with the inputs entering linearly could be effected either by a change of coordinates or by a proper choice of nonlinear state feedback. The method uses Lie brackets extensively and along with the Volterra series expansion achieves the desired results. Here we use the Input/Output linearization procedure as delineated in Isidori[25] Chapter 5.

The rigid body dynamical model of a general multi-body system in space could be represented as ,

$$\underline{\dot{x}} = f(\underline{x}) + \underline{g}\underline{u},$$
$$y = h(\underline{x}),$$

where, $\underline{x} \in \mathbb{R}^{2N-1}$, $\underline{u} \in \mathbb{R}^m$, $\underline{y} \in \mathbb{R}^l$, $f : \mathbb{R}^{2N-1} \to \mathbb{R}^{2N-1}$, $\underline{g} : \mathbb{R}^{2N-1} \to \mathbb{R}^{2N-1} \times \mathbb{R}^m$, and $h : \mathbb{R}^{2N-1} \to \mathbb{R}^l$.

Here $\underline{x}$ denotes system state vector, $\underline{u}$ denotes the vector of control variables (internal torques only) and $\underline{y}$ is the vector of the system outputs, m and l are the number of inputs and outputs respectively. It is to be noted here that the control enters linearly in the above equations.

The technique for exact linearization basically involves three steps. Firstly we determine whether or not the system is Input/Output linearizable (here onwards referred to as I/O linearizable or simply linearizable) by a possibly nonlinear coordinate transformation. The second step is a test to determine whether or not the system is I/O linearizable by the use of a feedback of the form,

$$\underline{u} = \alpha(\underline{x}) + \beta(\underline{x})\underline{v},$$

where, $\alpha : \mathbb{R}^{2N-1} \to \mathbb{R}^m$ and $\beta : \mathbb{R}^{2N-1} \to \mathbb{R}^m \times \mathbb{R}^m$ and $\underline{v} \in \mathbb{R}^m$ is the new input.

If this test is positive, we go through the final step wherein we determine the exact nonlinear feedback necessary to make the system I/O linearizable. The resulting nonlinear representation of this I/O linearized system could also be found. It is to be noted here that the technique is to be used locally. The submanifold over which this

method works successfully could be found in the second step. *A major difference with regard to the model between this section and the previous one is that we consider only internal torques here.*

6.2.1 I/O Linearization of the Multibody System :

The dynamical equations for the multibody system with only *internal torques at the joints and no external torques*, could be represented as (see Lemma 3.4.2 and Theorem 3.6.1),

$$\left. \begin{array}{rcl} \underline{\dot{x}} & = & f(\underline{x}) + \underline{g}u \\ \underline{y} & = & h(\underline{x}) \end{array} \right\} \, , \tag{2.2}$$

where

$$\underline{x} = \left[\mu_1, \mu_2 \cdots \mu_N, \theta_{2,1}, \cdots, \theta_{k,J(k)}, \cdots, \theta_{N,J(N)} \right]^T , \tag{2.3}$$

$$\underline{u} = [T_1, T_2 \cdots T_{N-1}]^T . \tag{2.4}$$

$f(\underline{x})$ is given by (1.9) and

$$\underline{g} = \left[\begin{array}{c} \underline{Q} \\ \underline{O}_{N-1,N-1} \end{array} \right] , \tag{2.5}$$

$$\begin{array}{rcl} h(\underline{x}) & = & \left[\theta_{k,J(k)}, \ k = 2, \ldots N \right] \\ & = & \left[\underline{O}_{N-1,N} \mid \mathbf{I}_{N-1} \right] \underline{x} , \end{array} \tag{2.6}$$

where $\underline{O}_{k,j}$ is a $(k \times j)$ *zeromatrix*, and $\underline{Q}$ is a $(N \times N - 1)$ matrix with elements 0, -1 or 1. Note that by Lemma 6.1.1 the matrix $\underline{Q}$ is full rank.

LINEARIZATION :

We follow a method outlined by Isidori [25] Chapter 5, for the design of a control system to re-orient the spacecraft under consideration. We give here the following steps.

STEP I: Check whether the system given by (2.2) is linearizable by a change of coordinates.

First form

$$\mathbf{T}_k = L_g L_f^k h = \begin{bmatrix} T_{11}^k & \cdots & T_{1m}^t \\ \vdots & \ddots & \vdots \\ T_{l1}^k & \cdots & T_{lm}^k \end{bmatrix} \quad k = 0, \cdots, \infty, \tag{2.7}$$

where

$$T_{ij}^k = L_{g_j} L_f^k h_i \quad i = 1, \cdots, l \tag{2.8}$$
$$j = 1, \cdots, m,$$

and g_i and h_i are the element of $\underline{g}$ and $h(\underline{x})$ respectively. m is the number of inputs (equal to $N - 1$) and l is the number of outputs (equal to $N - 1$). The *Lie derivative* $L_f g$ is defined as

$$L_f g = \left[\frac{\partial g}{\partial \underline{x}} \right] f, \tag{2.9}$$

with the following properties easily proved by direct computation,

$$L_g L_f h = \left[\frac{\partial L_f h}{\partial \underline{x}} \right] g$$
$$L_f^k g = L_f \left[L_f^{k-1} g \right] \quad k \geq 1.$$

If $\mathbf{T}_k$, $k = 0, \cdots, \infty$ is independent of $\underline{x}$ then we can find a (possibly nonlinear) transformation to render the system I/O linearizable.

From (2.7) we calculate $\mathbf{T}_0$ to be

$$\begin{aligned} \mathbf{T}_0 &= L_g h \\ &= \left[\frac{\partial h}{\partial \underline{x}} \right] g \\ &= \left[\underline{O}_{N-1,N} \mid \mathbf{I_{N-1}} \right] \cdot \begin{bmatrix} \underline{Q} \\ \underline{O}_{N-1,N-1} \end{bmatrix} \\ &= \underline{O}_{N-1,N-1} , \end{aligned} \tag{2.10}$$

where $\underline{O}_{N-1,N-1}$ is a $(N - 1 \times N - 1)$ *zeromatrix*.

Similarly we know from (2.7) that

$$\mathbf{T}_1 = L_g L_f h . \tag{2.11}$$

99

But $L_f h$ can be calculated from (2.9 and (2.6) to be,

$$
\begin{aligned}
L_f h &= \left[\frac{\partial h}{\partial \underline{x}} \right] f(\underline{x}) \\
&= \left[\underline{O}_{N-1,N} \mid \mathbf{I}_{N-1} \right] \cdot f(\underline{x}) \\
&= \begin{bmatrix} \frac{\partial H}{\partial \mu_2} - \frac{\partial H}{\partial \mu_1} \\ \vdots \\ \frac{\partial H}{\partial \mu_k} - \frac{\partial H}{\partial \mu_{J(k)}} \\ \vdots \\ \frac{\partial H}{\partial \mu_N} - \frac{\partial H}{\partial \mu_{N,J(N)}} \end{bmatrix} \cdot \\
&= \underline{Q}^T \frac{\partial H}{\partial \underline{\mu}}.
\end{aligned}
\tag{2.12}
$$

Since from Lemma 3.4.2

$$
\begin{aligned}
\frac{\partial H}{\partial \underline{\mu}} &= \mathbf{J}^{-1} \underline{\mu} \\
&= \underline{\omega} \\
&= [\omega_1, \dots, \omega_N]^T,
\end{aligned}
$$

we have from (2.12),

$$
\begin{aligned}
L_f h(\underline{x}) &= \underline{Q}^T \underline{\omega} \\
&= \begin{bmatrix} \omega_2 - \omega_1 \\ \vdots \\ \omega_k - \omega_{J(k)} \\ \vdots \\ \omega_N - \omega_{J(N)} \end{bmatrix} \cdot \\
&= \underline{Q}^T \mathbf{J}^{-1} \underline{\mu}.
\end{aligned}
\tag{2.13}
$$

Substituting (2.13) in (2.11) we get

$$
\begin{aligned}
\mathbf{T}_1 &= L_g \left(\underline{Q}^T \mathbf{J}^{-1} \underline{\mu} \right) \\
&= \left[\frac{\partial}{\partial \underline{x}} \left(\underline{Q}^T \mathbf{J}^{-1} \underline{\mu} \right) \right] g
\end{aligned}
$$

100

$$= \left[\underline{Q}^T \mathbf{J}^{-1} \mid - \underline{Q}^T \mathbf{J}^{-1} \frac{\partial \mathbf{J}}{\partial \underline{\theta}} \mathbf{J}^{-1} \mu \right] \cdot \begin{bmatrix} \underline{Q} \\ \underline{Q}_{N-1,N-1} \end{bmatrix}$$

$$= \underline{Q}^T \mathbf{J}^{-1}(\underline{\theta}) \underline{Q}. \tag{2.14}$$

Since $\mathbf{T}_1(\underline{x})$ is dependent on the state variables, there exists no transformation to I/O linearize the system.

STEP II : Now we attempt to I/O linearize the system using nonlinear feedback of the form $\underline{u}(\underline{x}) = \alpha(\underline{x}) + \beta(\underline{x})\underline{v}$ where $\beta(\underline{x})$ is invertible and $\underline{v}$ is the new input.

To this end we construct a formal power series

$$\mathbf{T}(s, \underline{x}) = \sum_{k=0}^{\infty} \mathbf{T}_k(\underline{x}) s^{-k-1}, \tag{2.15}$$

where $\mathbf{T}_k$ is given by (2.7).

Fact 6.2.1 : There exists a solution to the I/O linearization problem <u>if and only if</u> $\mathbf{T}(s, \underline{x})$ is separable i.e.,

$$\mathbf{T}(s, \underline{x}) = \mathbf{K}(s)\mathbf{R}(s, \underline{x}), \tag{2.16}$$

where

$$\mathbf{K}(s) = \sum_{k=0}^{\infty} \mathbf{K}_k s^{k-1}, \tag{2.17}$$

and

$$\mathbf{R}(s, \underline{x}) = \mathbf{R}_{-1} + \sum_{k=0}^{\infty} \mathbf{R}_k(s) s^{-k-1}, \tag{2.18}$$

and, with the inverse of $\mathbf{R}_{-1}$ existing.

Proof : See Isidori [25] Chapter 5, Theorem (1.11).

NOTE: $\mathbf{K}_k$ is a matrix of real numbers.

Lemma 6.2.1 : The multibody system is I/O linearizable by feedback of the form $\underline{u} = \alpha(\underline{x}) + \beta(\underline{x})\underline{v}$.

Proof : We know from (2.7) and (2.15)

$$\mathbf{T}(s, \underline{x}) = \underline{Q}_{N-1,N-1} + \left[\underline{Q}^T \cdot \mathbf{J}^1 \cdot \underline{Q} \right] s^{-2} + \sum_{k=2}^{\infty} \left[L_g L_f^k h \right] s^{-k-1}$$

$$= \left[\mathbf{I}_{N-1} s^{-2} \right] \cdot \left[\underline{Q}^T \cdot \mathbf{J}^{-1} \cdot \underline{Q} + \sum_{k=2}^{\infty} \left[L_g L_f^k h \right] s^{-(k-1)} \right] \tag{2.19}$$

comparing the above equation with (2.16) we get

$$\mathbf{K}(s) \;=\; \underline{Q}_{N-1,N-1} \cdot s^{-1} + \mathbf{I}_{N-1} s^{-2} + \underline{Q}_{N-1,N-1} \cdot s^{-3} + \cdots \quad (2.20)$$

i.e., $\mathbf{K_0} = \mathbf{K_2} = \cdots = \mathbf{K_\infty} = \underline{Q}_{N-1,N-1}$ and $\mathbf{K_1} = -\mathbf{I_{N-1}}$, and

$$\mathbf{R}(s,\underline{x}) \;=\; \underline{Q}^T \cdot \mathbf{J}^{-1} \cdot \underline{Q} + \sum_{k=2}^{\infty} \left[L_g L_f^k h \right] s^{-k+1}, \quad (2.21)$$

i.e.,

$$\mathbf{R_{-1}} \;=\; \underline{Q}^T \cdot \mathbf{J}^{-1} \cdot \underline{Q}. \quad (2.22)$$

Thus we can find a feedback of the form

$$\underline{u}(\underline{x}) \;=\; \alpha(\underline{x}) + \beta(\underline{x})\underline{v},$$

if and only if $\mathbf{R_{-1}}$ is invertible $\Longleftrightarrow$ $\mathbf{R_{-1}}$ is full rank.

But from (2.21) $\mathbf{R_{-1}}$ is full rank $\Longleftrightarrow$ $\mathbf{J}^{-1}$ and $\underline{Q}$ are full rank.

It is clear from Lemma 6.1.1 that $\underline{Q}$ is full column rank. Since $\mathbf{J}$ is a pseudo inertia matrix its inverse always exists, i.e.,

$$\Longrightarrow \underline{R}_{-1} \text{ is full rank.}$$

So there exists a feedback which I/O linearizes the multibody system around any point $\underline{x}_o$. The *subspace* over which this is true is given by the subspace over $\mathbf{R_{-1}}$ exists. Since $\mathbf{R_{-1}}$ exists everywhere the system is I/O linearizable at any point in the *phase space*.

STEP III : To find $\alpha(\underline{x})$ and $\beta(\underline{x})$ using the structure algorithm.

We apply the structure algorithm as in Isidori [25] Chapter 5, to find the expression for $\alpha(\underline{x})$ and $\beta(\underline{x})$.

STEP III.1 : From (2.10) we know that

$$\mathbf{T}_o \;=\; L_g h \;=\; \underline{Q}_{N-1,N-1}, \quad (2.23)$$

$$V_1 T_o \;=\; \underline{Q}_{N-1,N-1}, \quad (2.24)$$

where

$$V_1 = \begin{bmatrix} \underline{P}_1 \\ K_1^1 \end{bmatrix},$$ (2.25)

and $\mathbf{P}_1$ is a matrix with no rows. $K_1^1 = \mathbf{I}_{N-1}$,

$$\delta_1 = 0 = r_o,$$ (2.26)

$$\gamma_1 = \underline{R}_1 h = \text{does not exist},$$

$$\overline{\gamma_1} = K_1^1 h,$$

$$= \left[\theta_{2,1}, \ldots, \theta_{k,J(k)}, \ldots, \theta_{N,J(N)} \right]^T.$$ (2.27)

STEP III.2: Now

$$\begin{bmatrix} L_g \gamma_1 \\ L_g L_f \overline{\gamma_1} \end{bmatrix} = L_g L_f h = \mathbf{R}_{-1}.$$ (2.28)

Since $\mathbf{R}_1$ has rank $l = (N-1)$ the algorithm terminates setting

$$\delta_2 = r_1 = (N-1),$$ (2.29)

$$\underline{P}_2 = \mathbf{I}_{N-1},$$

$$K_2^2 = \text{does not exist},$$

$$\gamma_2 = \underline{P}_2 L_f \gamma_1,$$

$$= L_f h.$$ (2.30)

STEP III.3: Linearizing feedback

With the introduction of the feedback input $\underline{u} = \alpha(\underline{x}) + \beta(\underline{x})\underline{v}$ the dynamical equations (2.2) becomes

$$\dot{\underline{x}} = f(\underline{x}) + \underline{g} \left[\alpha(\underline{x}) + \beta(\underline{x})\underline{v} \right]$$

$$= f(\underline{x}) + \underline{g}\alpha(\underline{x}) + \underline{g}\beta(\underline{x})\underline{v},$$

i.e.

$$\left. \begin{array}{rcl} \dot{\underline{x}} & = & \tilde{f}(\underline{x}) + \tilde{g}(\underline{x})\underline{v} \\ \underline{y} & = & h(\underline{x}) \end{array} \right\},$$ (2.31)

103

where

$$\tilde{f}(\underline{x}) \;=\; f(\underline{x}) + \underline{g}\alpha(\underline{x}), \tag{2.32}$$

$$\tilde{g}(\underline{x}) \;=\; \underline{g}\beta(\underline{x}), \tag{2.33}$$

$f(\underline{x})$, $h(\underline{x})$ and $\underline{g}$ are given by (1.9), (2.5) and (2.6) respectively.

$\alpha(\underline{x})$: For the closed loop system to be linearizable in the I/O sense we have to have

$$L_{\tilde{f}}\Gamma(\underline{x}) \;=\; \underline{O}_{N-1,N-1}, \tag{2.34}$$

where $\tilde{f}$, $\tilde{g}$ are given by (2.32) and (2.33) respectively, and,

$$\Gamma(\underline{x}) \;=\; \begin{bmatrix} \gamma_1 \\ \gamma_2 \end{bmatrix}$$
$$\;=\; L_f h, \tag{2.35}$$

i.e., (2.34) reduces to

$$[L_{\tilde{g}}\Gamma(\underline{x})]\,\alpha(\underline{x}) \;=\; -L_f\Gamma(\underline{x}),$$

or using (2.13) and (2.35),

$$[L_{\tilde{g}}L_f h]\,\alpha(\underline{x}) \;=\; -L_f\left[\underline{Q}\mathbf{J}^{-1}\underline{\mu}\right].$$

But from (2.14) we have $L_{\tilde{g}}L_f h \;=\; \underline{Q}^T\mathbf{J}^{-1}\underline{Q}$, therefore,

$$\alpha(\underline{x}) \;=\; -\left[\underline{Q}^T\mathbf{J}^{-1}\underline{Q}\right]^{-1}\left[\underline{Q}^T\mathbf{J}^{-1}\,|-\underline{Q}^T\mathbf{J}^{-1}\frac{\partial\mathbf{J}}{\partial\mu}\right]f(\underline{x}). \tag{2.36}$$

$\beta(\underline{x})$: The I/O linearizing feedback also needs to satisfy the following condition,

$$L_{\tilde{g}}\Gamma(\underline{x}) \;=\; \left[\mathbf{I}_{r_q-1}\,|\underline{O}\right], \tag{2.37}$$

where q is the number of steps it took for the algorithm to terminate (here $q = 2$). i.e.,

$$[L_{\tilde{g}}\Gamma(\underline{x})]\,\beta(\underline{x}) \;=\; \left[\mathbf{I}_{r_2-1}\,|\underline{O}\right]$$
$$\;=\; [\mathbf{I}_{r_1}\,|\underline{O}]$$
$$\;=\; \mathbf{I}_{N-1}. \tag{2.38}$$

104
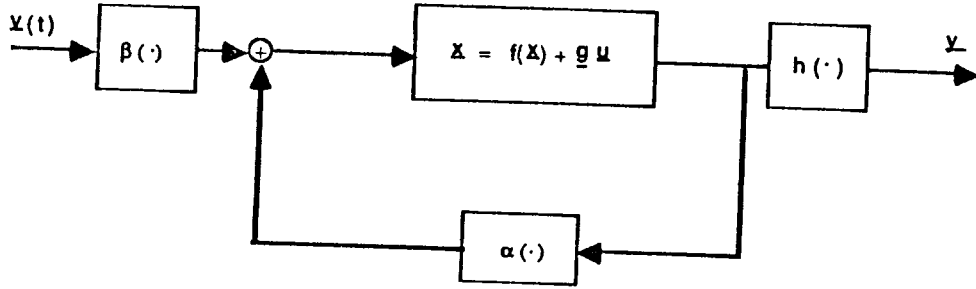
Figure 6.2: I/O linearization of the planar multibody system

From (2.14) and (2.38) we have

$$\beta(\underline{x}) = -\left[\underline{Q}^T \mathbf{J}^{-1} \underline{Q}\right]^{-1}. \tag{2.39}$$

LINEARIZED MODEL :

$$\underline{\dot{x}} = \tilde{f}(\underline{x}) + \tilde{g}(\underline{x})\underline{v}, \tag{2.40}$$

$$\underline{y} = h(\underline{x}), \tag{2.41}$$

where

$$\tilde{f}(\underline{x}) = f(\underline{x}) + \underline{g}\alpha(\underline{x}), \tag{2.42}$$

$$\tilde{g}(\underline{x}) = \underline{g}\beta(\underline{x}). \tag{2.43}$$

$f(\underline{x})$, $\underline{g}$, $h(\underline{x})$, $\alpha(\underline{x})$ and $\beta(\underline{x})$ are given by (1.9), (2.5), (2.6), (2.36) and (2.39) respectively. Figure 6.2 gives a block diagram representation of the system.

Remark 6.2.1 : Since $\mathbf{J}^{-1}\mu = \underline{\omega} = [\omega_1, \cdots \omega_N]^T$, we can rewrite (2.36) as

$$\alpha(\underline{x}) = -\left[\underline{Q}^T \mathbf{J}^{-1}(\theta)\underline{Q}\right]^{-1} \left[\underline{Q}^T \mathbf{J}^{-1}(\theta) \mid - \underline{Q}^T \mathbf{J}^{-1}(\underline{\theta}) \frac{\partial \mathbf{J}}{\partial \underline{\theta}} \mathbf{J}^{-1}(\theta)\underline{\mu}\right] f(\underline{x})$$

$$= -\left[\underline{Q}^T \mathbf{J}^{-1}(\theta)\underline{Q}\right]^{-1} \left[\underline{Q}^T \mathbf{J}^{-1}(\theta) \mid - \underline{Q}^T \mathbf{J}^{-1}(\theta) \frac{\partial \mathbf{J}}{\partial \underline{\theta}}\right] f(\underline{x}), \tag{2.44}$$

Also from (2.39) we have $\beta(\underline{x})$ as

$$\beta(\underline{x}) = \left[\underline{Q}^T \mathbf{J}^{-1}(\theta)\underline{Q}\right]^{-1}. \tag{2.45}$$

From (2.44) and (2.45) it is clear that the knowledge of the inertial angular velocities of the individual bodies $(\underline{\omega})$ along with the relative angles $(\underline{\theta})$ between the bodies is enough to find the linearizing feedback at any given instant.

6.2.2 Output in terms of new input:

We will compute $\underline{y}$ in terms of $\underline{v}$ the new input.

From Isidori chapter 5 equation (1.3) [25] we have

$$\underline{y} = W_0(t) + \int_o^t W(t,\tau)\underline{v}(\tau)d\tau, \tag{2.46}$$

and

$$W_0(t) = \sum_{n=0}^{\infty} L_{\tilde{f}}^n h(\underline{x}_o)\frac{t^n}{n!}, \tag{2.47}$$

and

$$W(t,\tau) = \sum_{n_1=0}^{\infty} \sum_{n_0}^{\infty} L_{\tilde{f}}^{n_0} L_{\tilde{g}} L_{\tilde{f}}^{n_1} h(\underline{x}_o)\frac{(t-z)^{n_1}}{n_1!}\frac{(t-z)^{n_0}}{n_0!}. \tag{2.48}$$

$\underline{x}_o$ - Point in state space around which the system is being linearized in the I/O sense. Now from (2.47)

$$\begin{aligned} W_0(t) &= h(\underline{x}_o) + \sum_{n=1}^{\infty} L_{\tilde{f}}^n h(\underline{x}_o)\frac{t^n}{n!} \\ &= h(\underline{x}_o) + L_{\tilde{f}} h(\underline{x}_o)\frac{t}{1!} + \sum_{n=2}^{\infty} L_{\tilde{f}}^n h(\underline{x}_o)\frac{t^n}{n!}, \end{aligned} \tag{2.49}$$

$$L_{\tilde{f}} h(\underline{x}_o) = L_{f+g\alpha} h(\underline{x}_o) = L_f h(\underline{x}_o) + L_g h\alpha(\underline{x}_o). \tag{2.50}$$

From (2.10) and (2.13) we have

$$L_{\tilde{f}} h(x_o) = \underline{Q}^T \mathbf{J}^{-1}\underline{\mu}(0) = \underline{Q}^T\underline{\omega}(0), \tag{2.51}$$

$$\begin{aligned} \underline{x}_o &= \left[\underline{\mu}(0),\underline{\theta}(0)\right] \\ &= \left[\mu_1(0),\cdots,\mu_N(0),\theta_{k,J(k)}(0),\ k=2,\cdots,N\right]^T, \end{aligned} \tag{2.52}$$

$$\underline{\omega}(0) = \mathbf{J}^{-1}(\underline{\theta}(0))\cdot\underline{\mu}(0). \tag{2.53}$$

106

Also from (2.13), (2.50) and (2.34) we have

$$
\begin{aligned}
L_f^2 h(\underline{x}) &= L_{\hat{f}} L_f h(\underline{x}) \\
&= L_{\hat{f}} \Gamma(\underline{x}) \\
&= \underline{O}_{N-1,N-1}.
\end{aligned}
$$

therefore,

$$
L_{\hat{f}}^n h(\underline{x}_o) = \underline{O}_{N-1,N-1} \qquad n \geq 2, \tag{2.54}
$$

and,

$$
W_0(t) = \underline{\theta}(0) + \underline{Q}^T \underline{\omega}(0) t. \tag{2.55}
$$

From (2.48) we have,

$$
W(t,\tau) = \sum_{n_0=0}^{\infty} L_{\hat{f}}^{n_0} L_{\hat{g}} L_{\hat{f}}^{n_1} h(\underline{x}_o) \frac{(t-\tau)^{n_1}}{n_1!} \frac{\tau^{n_0}}{n_0!}. \tag{2.56}
$$

Using (2.54) and (2.51) we have

$$
\begin{aligned}
W(t,\tau) &= \sum_{n_0=0}^{\infty} L_{\hat{f}}^{n_0} L_{\hat{g}} L_f h(\underline{x}_o)(t-\tau) \frac{\tau^{n_0}}{n_0!} \\
&= \sum_{n_0=0}^{\infty} L_{\hat{f}}^{n_0} \left[L_g L_f h(\underline{x}_o) \right] \beta(\underline{x})(t-\tau) \frac{\tau^{n_0}}{n_0!}. \tag{2.57}
\end{aligned}
$$

But from (2.38) $[L_g L_f h] \beta(\underline{x}) = \mathbf{I}_N$s, substituting so in (2.57) we have

$$
\begin{aligned}
W(t,\tau) &= \left[\sum_{n_0=0}^{\infty} L_{\hat{f}}^{n_0} \mathbf{I}_N \right] (t-\tau) \frac{\tau^{n_0}}{n_0!} \\
&= \mathbf{I}_{N-1}(t-\tau). \tag{2.58}
\end{aligned}
$$

Substituting (2.49) and (2.58) in (2.46) we have

$$
\underline{y} = \underline{\theta}(0) + \underline{Q}^T \underline{\omega}(0) + \int_\tau^t \int_0^{\tau_1} \tau_1 \, \underline{v}(\tau_2) d\tau_1 d\tau_2, \tag{2.59}
$$

where

$$
\begin{aligned}
\underline{\theta}(0) &= \left[\theta_{2,1}(0), \ldots, \theta_{k,J(k)}(0), \ldots, \theta_{N,J(N)}(0) \right]^T, \\
\underline{\omega}(0) &= \left[\omega_1(0), \ldots, \omega_k(0), \ldots, \omega_N(0) \right]^T,
\end{aligned}
$$

We sum the results up in the following theorem.

Theorem 6.2.1 : The multibody system given by (2.2) can be Input/Output linearized by the application of static state feedback $\underline{u} = \alpha(\underline{x}) + \beta(\underline{x})\underline{v}$ where α and β are state feedbacks given by (2.36) and (2.39) respectively, and $\underline{v}$ is the new input. The I/O map with the feedback is given by (2.59).

6.3 Stabilization - N-Body Problem

In the case of a Hamiltonian system a natural approach to stabilization is provided by Liapunov's second or direct method as noted by several authors Tsinias & Kaloupsidis [54] , Marino [40], van der Schaft [56]. The obvious reason being that the internal energy of the system H is a natural candidate for the Liapunov function, since $\frac{dH}{dt} = 0$ along any system trajectory with the input equal to zero. If H posseses a strict local minimum at the *origin this implies that the system is* locally stable [32]. However in the present context H does not possess a strict local minimum, but $H + C$ does, where C is a Casimir function. In other words if we restrict the system to the symplectic leaf of the Poisson manifold then H has a strict local minimum.

The dynamics of the multibody system with control torques at the joints (internal torques) and an output $\underline{y}$ is given by (2.2) - (2.6).

Consider a Liapunov function $V(\underline{x})$ as shown below,

$$
\begin{aligned}
V(\underline{x}) &= H + C_\phi \\
&= \frac{1}{2}\underline{\mu}^T \mathbf{J}^{-1}(\underline{\theta})\underline{\mu} + \phi(\mu_s^2)
\end{aligned}
\tag{3.1}
$$

where $\underline{x} = [\underline{\mu}^T, \underline{\theta}^T]$. Now using (2.2) – (2.6) and keeping in mind that $C_\phi = \phi(\mu_s^2)$ (μ_s is the total system angular momentum), we have

$$
\begin{aligned}
\dot{V}(\underline{x}) &= \frac{d(H + C_\phi)}{dt} \\
&= \frac{\partial H}{\partial \underline{x}}\dot{\underline{x}} + \sum_{i=1}^{N} \frac{\partial \phi(\mu_s^2)}{\partial \mu_i}\dot{\mu}_i,
\end{aligned}
\tag{3.2}
$$

But

$$\frac{\partial \phi \left(\mu_s^2 \right)}{\partial \mu_i} = \frac{\partial \phi \left(\mu_s^2 \right)}{\partial \mu_j} \quad \forall i, j = 1, \ldots, N, \tag{3.3}$$

also

$$\sum_{i=1}^{N} \dot{\mu}_i = 0, \tag{3.4}$$

from Theorem 3.5.1.

Using (3.3) and (3.4) in (3.2) we have

$$
\begin{aligned}
\dot{V}(\underline{x}) &= \frac{\partial H}{\partial \underline{x}} \dot{\underline{x}} \\
&= \left[\frac{\partial H}{\partial \underline{\mu}} \, \frac{\partial H}{\partial \underline{\theta}} \right] \cdot \left(f(\underline{x}) + \underline{g} u \right) \\
&= \sum_{i=1}^{N} \frac{\partial H}{\partial \mu_i} \left[\sum_{\forall j \; s.t. \; J(j)=i} \frac{\partial H}{\partial \theta_{j,i}} - \frac{\partial H}{\partial \theta_{i,J(i)}} + \sum_{\forall j \; s.t. \; J(j)=i} T_{j-1} - T_{i-1} \right] \\
&\quad + \sum_{i=2}^{N} \frac{\partial H}{\partial \theta_{i,J(i)}} \left[\frac{\partial H}{\partial \mu i} - \frac{\partial H}{\partial \mu_{J(i)}} \right] \\
&= \sum_{i=2}^{N} T_{i-1} \left[\frac{\partial H}{\partial \mu_{J(i)}} - \frac{\partial H}{\partial \mu_i} \right] \\
&= - \sum_{i=2}^{N} T_{i-1} \dot{\theta}_{i,J(i)}. \tag{3.5}
\end{aligned}
$$

Consider now a feedback

$$T_{i-1} = C_{i-1} \dot{\theta}_{i,J(i)},$$

on the system where, $C_i > 0$

Substituting so in (3.5) results in

$$\dot{V}(x) = - \sum_{i=2}^{N} C_{i-1} \dot{\theta}_{i,J(i)}^2.$$

Since $\dot{V}(x) < 0$ and $x = \left[\underline{\mu}^T, \underline{\theta}^T \right]$, $V(x)$ is a valid Liapunov function for the system. Further $V(x) > 0$. The system will converge to a maximal invariant set given by

$$S = \left\{ x : V(x) < C, \dot{V}(\underline{x}) = 0 \right\}.$$

109

Now

$$\dot{V}(x) \;=\; 0 \;\Longrightarrow\; \underline{\dot{\theta}} \;=\; 0$$

$$\Longrightarrow\; \underline{\theta} \;=\; \text{constant vector.}$$

But

$$\underline{\theta} \;=\; \text{constant} \Longrightarrow \omega_1 \;=\; \omega_2 \;=\; \cdots \;=\; \omega_N \;=\; \omega'$$

$$\Longrightarrow \underline{\omega}' \;=\; \text{constant (since total angular momentum is conserved).}$$

Since $\underline{\theta}$ is constant and $\underline{\omega} \;=\; [\omega_1, \omega_2, \cdots, \omega_N]^T$ is constant and $\mu \;=\; \mathbf{J}^{-1}(\theta)\underline{\omega}$, $\underline{\mu}$ is a constant. i.e.,

$$\underline{\dot{\mu}} \;=\; 0,$$

$$\underline{\dot{\theta}} \;=\; 0$$

$$\Longrightarrow\; S \;=\; \{\underline{x} : \underline{x} \;=\; \text{equilibrium points of system 1 with } T_i \;=\; 0\}$$

Since S contains only discrete set of points and no trajectories, the system given by (2.2) – (2.6) with a feedback $T_i \;=\; C_i \dot{\theta}_i$ with $C_i > 0$ is asymptotically stable.

Thus we give the following Theorem.

Theorem 6.3.1 : The planar multibody system given by (2.2) – (2.6) with a feedback $T_{i-1} \;=\; C_{i-1}\theta_{i,J(i)}$ and $C_{i-1} > 0$ converges to a maximum invariant set given by

$$S \;=\; \{\underline{x} : \underline{x} \;=\; \text{equilibrium points of the system with } T_i \;=\; 0\} \qquad (3.6)$$

110

SYMBOLIC COMPUTATION

We have used symbolic and LISP based computation as tools for generation, analysis and simulation of dynamics of multibody systems. This chapter discusses our efforts in that direction. In Section 7.1 we present **OOPSS** a system designed to generate, simulate and animate the dynamics of planar multibody system. We have also used symbolic computation in a MACSYMA [1] environment to generate the explicit dynamical equations of multibody system using augmented body method [59] and nested-body approach [13]. Software has been written and validated. Section 7.2 discusses the symbolic generation of dynamical equations.

7.1 OOPSS : Object Oriented Planar System Simulator

OOPSS - Object Oriented Planar System Simulator, is a general purpose software system architecture designed to generate the dynamical equations of a multibody system *symbolically* and to simulate the equations so generated *numerically*. **OOPSS** animates the multibody system by exploiting the high resolution graphics and windowing facilities of a LISP machine and has been implemented in Zeta-Lisp on a Symbolics 3600 series machine. A nice *user interface* is characteristic of **OOPSS**. Users can interactively :

---

[1]MACSYMA is a trademark of Symbolics Inc., Cambridge, Mass.

111

(i)   choose any kinematic or physical parameter for the system,

(ii)   change any runtime initial condition - system energy, system angular
         momentum, time step, maximum problem time, initial values of state
         and other variables (angles, conjugate momentum variables),

(iii)   select display parameters for the graphs,

(iv)   choose torque laws and gains.

OOPSS is implemented using the *Object Oriented Programming* (OOP) technique. A brief introduction to OOP follows.

Objects are entities that combine the properties of procedures and data, since they perform computation and save local state [50]. Also, objects could be linked to real world things. A program could be built using a set of *objects*. In OOP we have uniform usage of objects whereas conventional programming uses separate procedures and data. Sending *messages* between objects causes action in OOP. Message sending is a form of indirect procedure call and supports *data abstraction*.

General descriptions of objects in Zeta-Lisp are in the form of *flavors*. In Zeta-Lisp a conceptual class of objects and their operations are realized by the *Flavor System*, where part of its implementation is simply a convention in procedure calling style; part is a powerful language feature, called *Flavors*, for defining classes of abstract objects. Any particular object is an *instance* of a flavor; for example a flavor *satellite-body* may have *satellite-body-1* and *satellite-body-2* as its instances. Flavors have *inheritance* property; thus if we build a flavor using other flavors then all the properties of the latter are inherited by the former. The variables associated with a generic object are known as *instance variables*.

In a multibody system for example, a generic body i can be defined as an object with the following instance variables : a vector connecting the joint $(i-1)$ to the center of mass of body i, vector(s) connecting the joint $(i-1)$ and other joint(s) on body i, angle made by the body with respect to the inertial coordinate system and shape of the body.

112

```
        ┌─────────────┐
        │  Symbolic   │
        │    eqn.     │
        │  Generator  │
        └─────────────┘
               │
    ┌──────────┴──────────┐
    ▼                     ▼
┌───────────┐       ┌───────────┐
│ Descriptor│       │  FORTRAN  │
│           │       │ Simulator │
└───────────┘       └───────────┘
    ▲                     ▲
    └──────────┬──────────┘
               ▼
        ┌─────────────┐
        │   DISPLAY   │
        └─────────────┘
```
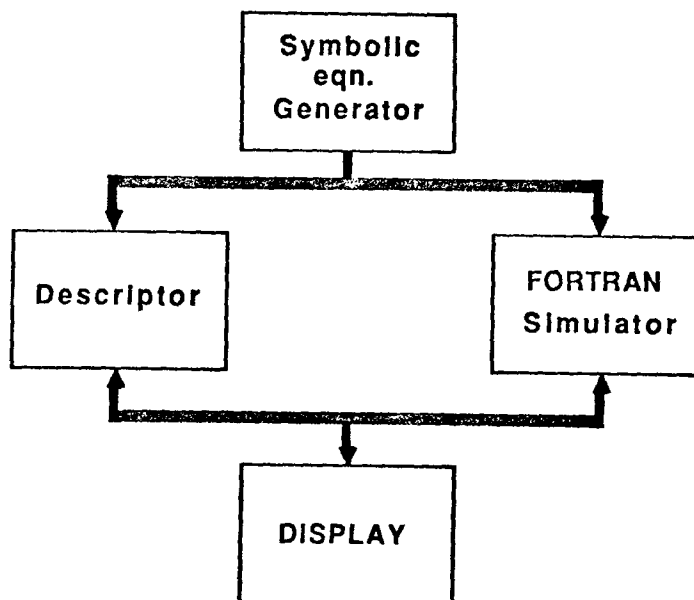
Figure 7.1: Block diagram representation of OOPSS

Specific operations could be associated with the objects using *methods*. One can create a method to define a specific operation on any instance of a flavor and attribute special properties to it. For instance one can define a method for a body which is the leaf of a tree and so has only one joint (i.e., only one body attached to it - contiguous to and inboard) where as a generic body has two or more bodies attached to it.

Functions are used to send messages to instances of flavors through the already defined methods.

OOPSS uses OOP along with *symbolic manipulation* to formulate and simulate the dynamics of a planar multibody system. Figure 7.1 shows the block diagram representation of OOPSS. A detailed description of each block is given in the following paragraphs.

7.1.1 Symbolic manipulation

The symbolic equation generator generates the dynamics of a planar multibody system connected in the form of a tree structure in the Hamiltonian setting. The formulation and the notation is the same as detailed in Chapter three. This block is implemented in MACSYMA. The input data for this block consists of the following: the label of the body contiguous and inboard of the body under consideration $J(i)$,

```
/* -*- Mode: Macsyma; Fonts: cptfontb -*- */

block(

n:3,

s0[2]:[1,2],
s0[3]:[1,2,3],

jj[2]:1,
jj[3]:2,

for i:1 thru n do inert[i]:in[i],

beta_t[2]:matrix([c_1],[0]),
beta_t[3]:matrix([b_1+e_1],[e_2]),

alpha_t[2]:matrix([b_1],[0]),
alpha_t[3]:matrix([d_1],[0])

        );█
```

Figure 7.2: Data file for the MACSYMA program

the various kinematic parameters included in the vectors $\tilde{\alpha}_i$ and $\tilde{\beta}_j$, the physical parameters like the mass and inertia of the bodies; any external and internal torques. A sample data file is as shown in Figure 7.2 for a planar three-body system. A session of the automatic equation generation is given for the above data file in Appendix 2.

7.1.2 FORTRAN simulator

The **FORTRAN** simulator simulates the dynamical equations generated by the symbolic equation generator, and has been implemented by FORTRAN-77 running on the LISP machine. The **FORTRAN** simulator needs numerical values of all parameters to be in an input data file. This input data file is generated by the **DESCRIPTOR**. The input data file contains the numerical values of all kinematic and physical parameters, the system angular momentum and system energy values, problem time, time step etc., associated with the particular example.

The state and related variables (for example, angular velocities) at any instance of time could be passed onto the **DISPLAY** block by means of *lispfunctions* to be used for animation and display purposes. For example the,

lispfunction displaybody displaybody (omega1,omega2,omega3,theta21,theta32,time) can be used as

114

$$displaybody(\omega_1, \omega_2, \omega_3, \theta_{21}, \theta_{32}, t)$$

in the FORTRAN program to pass the relevant variables to the **DISPLAY** block. The function '*displaybody*' is implemented in Zeta-Lisp in the **DISPLAY** package.

The initial condition for initiating the simulation is chosen as follows. An initial system energy H, system angular momentum μ_s, and relative angle $\theta_{2,1} = \theta$, are selected. Since the energy is quadratic in the conjugate momenta (see Lemma 3.4.2) and the system angular momentum $\mu_s = \mu_1 + \mu_2$ we get two solutions for the (μ_1, μ_2) pair. User has the choice to select either the 'First initial condition' or the 'Second initial condition' (see Figure 7.3).

7.1.4 DESCRIPTOR

The **DESCRIPTOR** consists of descriptions of various flavors to implement the display and the user interface. It also contains flavors to define a generic body in the multibody system. Using *methods* we can attribute special properties to the instances of the flavors.

The *user interface* consists of a window with many panes (Figure 7.3). Three frames of references in the corresponding window panes: inertial frame of reference and two other selectable frames (from various joint and/or body frames), have been implemented . The *message pane* where a part of runtime data for the FORTRAN program is displayed. The *simulation pane* draws various graphs of state and/or other variables as functions of time. The *menu pane* is self descriptive. Every item in this pane is *mouse sensitive* (mouse selectable). More on this in the following sections as we deal with particular examples of planar two-body and planar three-body systems. A brief online *HELP* facility exists and information can be got by clicking left using the mouse when it is highlighted.

7.1.5 DISPLAY

The **DISPLAY** block is the implementation of various functions to drive the instances of flavors by sending messages to them. **DISPLAY** keeps track of sending
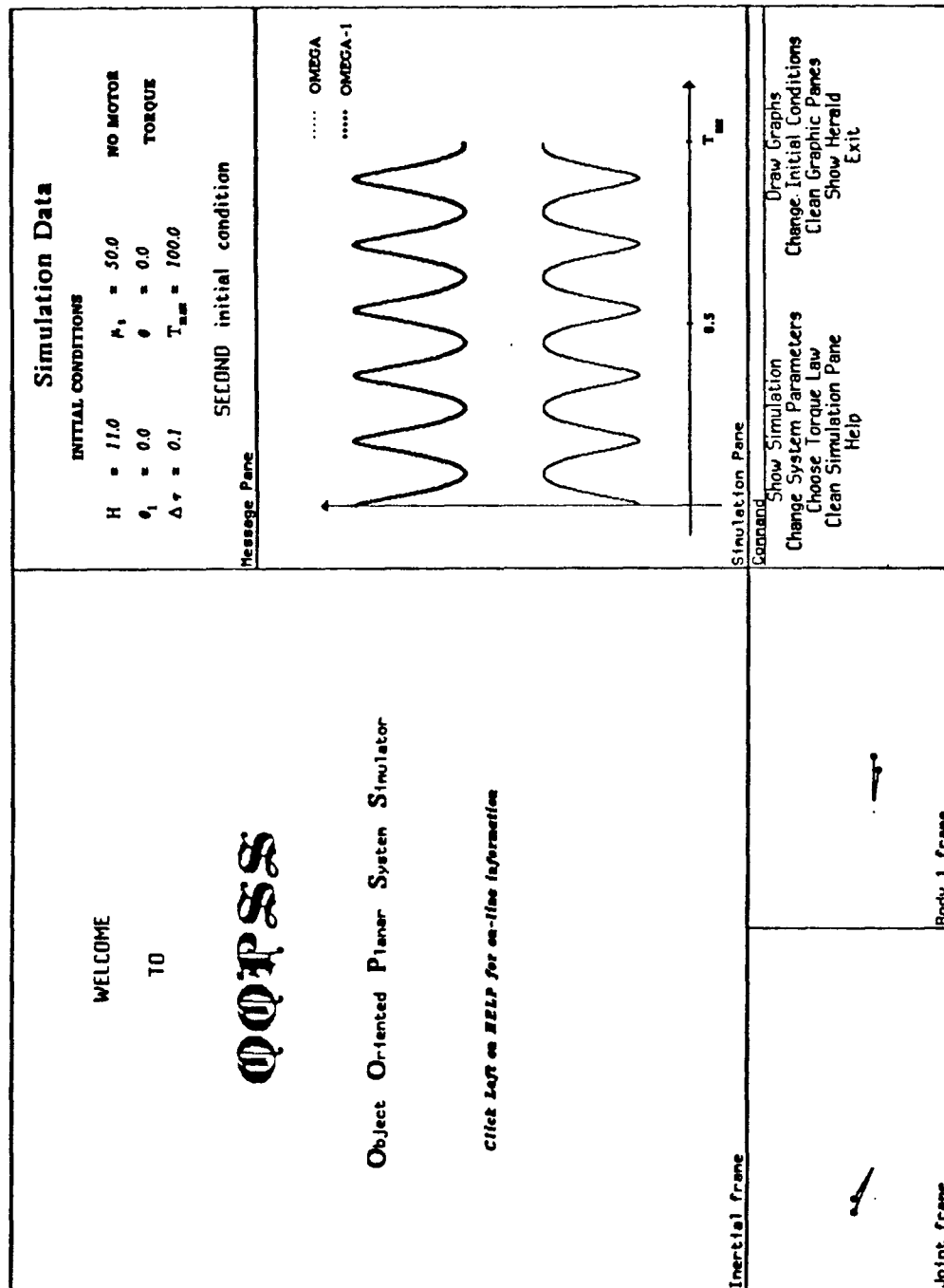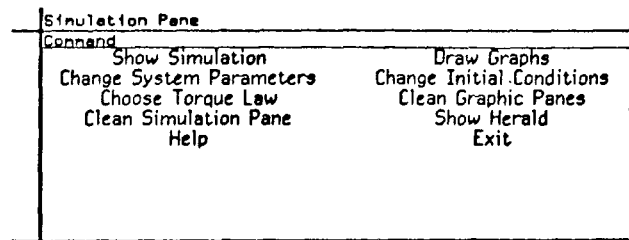
Figure 7.3: OOPSS window

proper messages to the relevant panes as and when it receives data from the **FOR-TRAN** block. **DISPLAY** is characterized by a *'tv:alu-xor'* option which helps in erasing the display at time t and creating a new display at time $t + \Delta t$. *'displaybody'* and *'cleanbody'* are functions to display the system and clean the displayed picture off the relevant pane respectively.
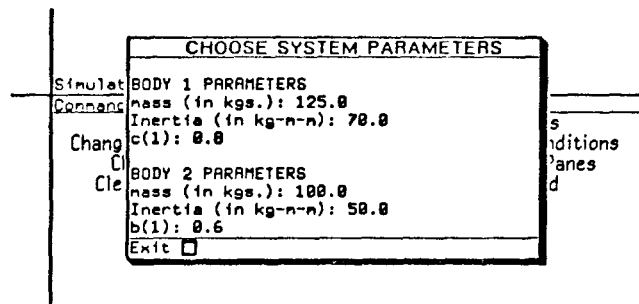
7.1.6 Implementation

Two-Body Example

Refer to Chapter four for notation and description of the problem. Figure 7.4a shows the menu pane for this example. Clicking left on the mouse when *system parameters* is highlighted gives Figure 7.4b. Clicking left on *Torque Law* results in Figure 7.4c. Further clicking on *P-D Torque Law* implements a joint torque law (internal torque) - a proportional sinusoidal biased spring plus derivative controller, i.e., $(K_p \sin(\theta_{2,1} - \theta_{\text{bias}}) + K_d \dot{\theta}_{2,1})$. Gains K_p and K_d and the *bias* angle θ_{bias} could be chosen (see Figure 7.4d) interactively by the user.

The *stable equilibrium* is displayed in Figure 7.5. The trace shown in the inertial frame is the *trace* left by the joint as it moves in space. Simple calculation shows that this trace is indeed a circle when the system is in stable equilibrium position. Figure 7.6 displays a trajectory when the system is at a point very near the *saddle* point. Figure 7.7 describes a trajectory for an arbitrary value of the system energy. If a P-D torque is introduced in the system then the resulting trajectory is as shown in Figure 7.8 - 7.9 (no bias) and Figure 7.10 - 7.11 (bias). Notice that with K_p equal to zero and K_d positive the system always goes to the stable equilibrium and confirms our 'stabilization theorem' - Theorem 6.3.1, i.e., introduction of a feedback internal torque proportional to the rate of the relative angle stabilizes the system. One could also interpret this result as follows: by introducing this torque law the energy in the system is dissipated till the system goes to a minimum energy state which is the stable (stretched out) equilibrium.

(a)

```
Simulation Pane
Command
            Show Simulation              Draw Graphs
      Change System Parameters     Change Initial Conditions
         Choose Torque Law          Clean Graphic Panes
       Clean Simulation Pane            Show Herald
               Help                        Exit
```
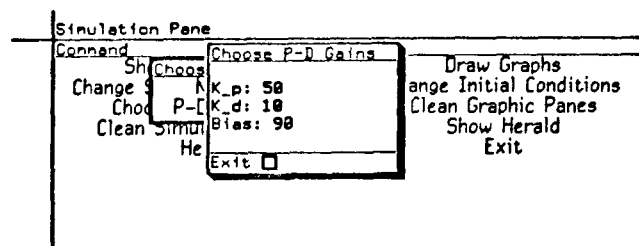
(b)

```
                CHOOSE SYSTEM PARAMETERS
    Simulat  BODY 1 PARAMETERS
    Command  mass (in kgs.): 125.0
             Inertia (in kg-n-n): 70.0                s
      Chang  c(1): 0.0                              ditions
         Cl  BODY 2 PARAMETERS                      anes
         Cle mass (in kgs.): 100.0                  d
             Inertia (in kg-n-n): 50.0
             b(1): 0.6
             Exit ☐
```

(c)

```
Simulation Pane
Command
            Show Simulation                    Draw Graphs
      Change System P Choose Torque Law  nge Initial Conditions
         Choose Torq     No Torque       lean Graphic Panes
       Clean Simulat   P-D Controller        Show Herald
               Help                            Exit
```

(d)

```
Simulation Pane
Command
          Sh Choos  Choose P-D Gains     Draw Graphs
   Change S   N   K_p: 50            ange Initial Conditions
      Cho   P-D  K_d: 10             Clean Graphic Panes
   Clean Simu    Bias: 90               Show Herald
          He                               Exit
                 Exit ☐
```

Figure 7.4: Two-body problem menu-pane

118

Three-Body Example

A general three-body example has also been implemented on OOPSS. Figure 7.12 shows a general three-body system wherein the center of mass of the middle body is not along the line joining the two joints. The *filled-in circles* represents the center of mass of each body (the first body represented by a big circle, second with a smaller circle and the third with the smallest circle). Display frames could be chosen by clicking left on the 'Choose display frames' using the mouse. Figure 7.13 displays special kinematic case of a three-body example discussed in Chapter 5.3. Joint torques of the proportional sinusoidal bias spring plus derivative type can be introduced at the joints (see Figure 7.14).

Complex Multibody Examples

Plans are underway to implement complex multibody system examples. As the complexity of the examples grow one may find oneself limited by the processing capabilities of the currently available LISP machines. One could take advantage of the existing parallelism in these problems by utilizing the processing power of parallel LISP processors. A *Connection Machine* [2] may just serve the purpose. Thus dynamics of complex multibody systems may be generated automatically, simulated and animated.

7.2 Symbolic Dynamical Equation Generation

The formulation of dynamical equations by hand is a tedious process and often prone to errors. Many researchers have taken up the possibility of computer-aided methods to generate these equations. One way of categorizing these computer-oriented methods is by the way of numerical and symbolic programs. Numerical programs are characterized by numerical digital computation whereas symbolic programs generate equations and accompanying expressions in symbolic (or alpha-numeric)

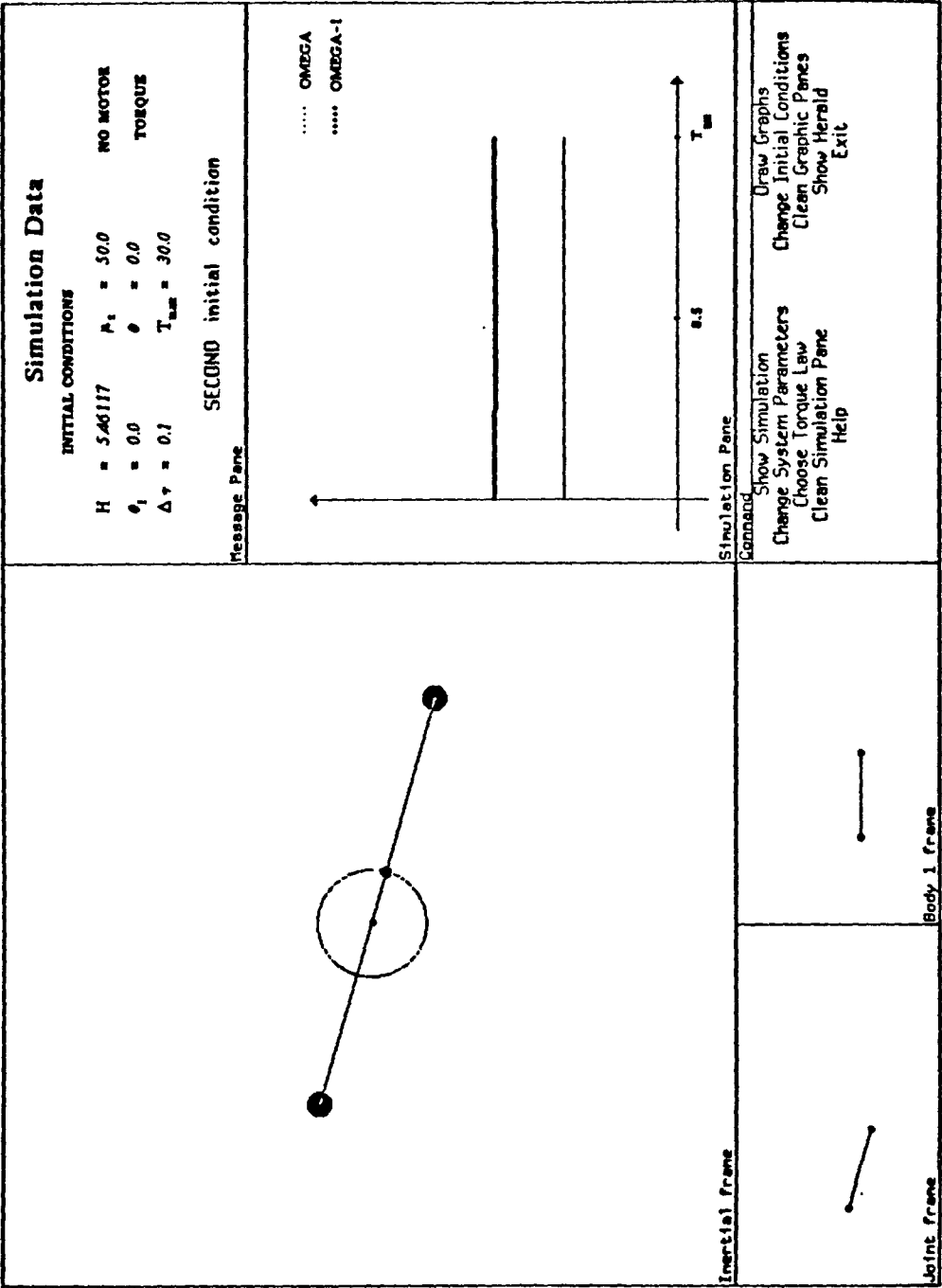[2]manufactured by Thinking Machines Inc, Cambridge, Mass.
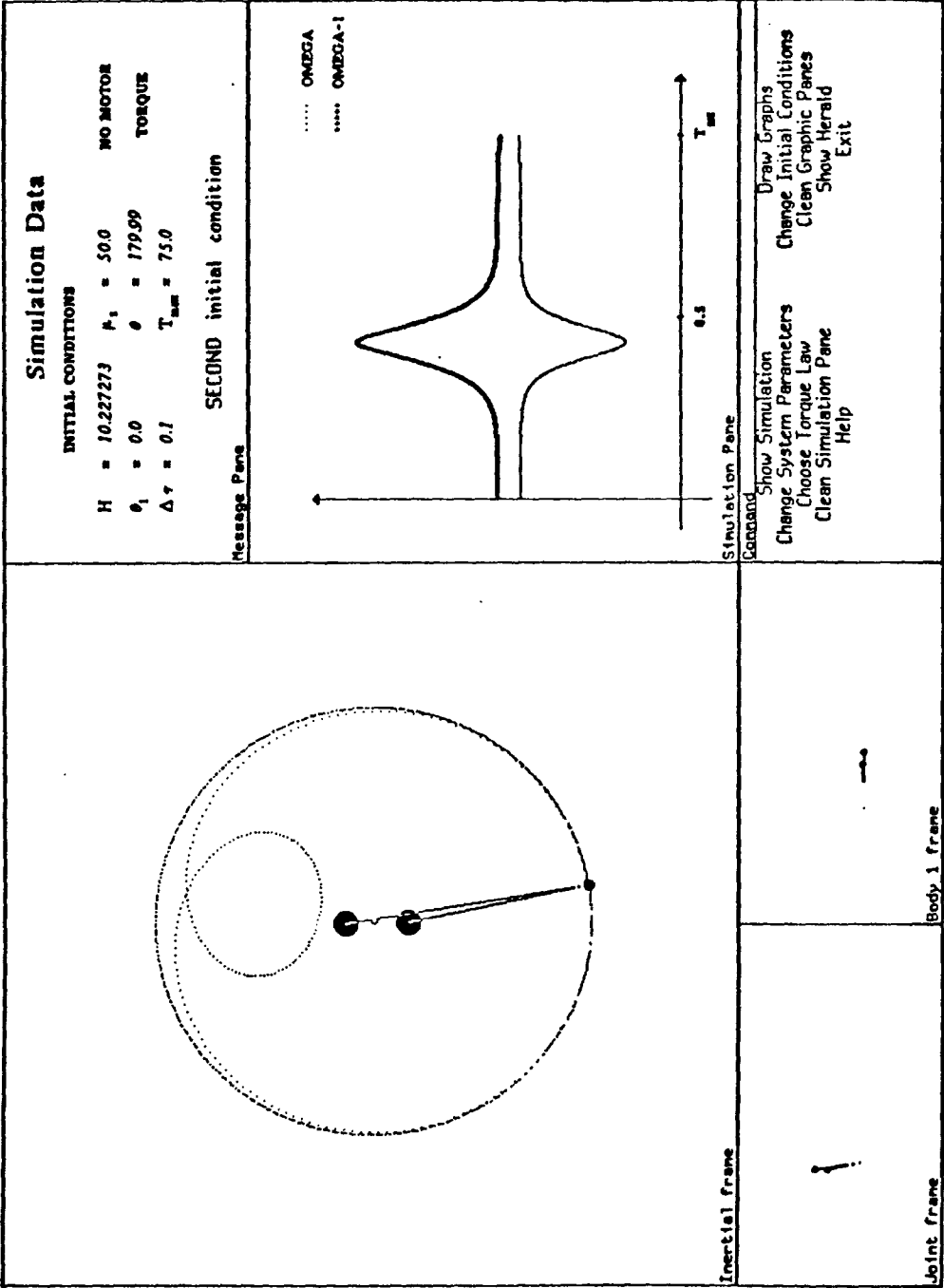
Figure 7.5: Two-body problem : stable equilibrium

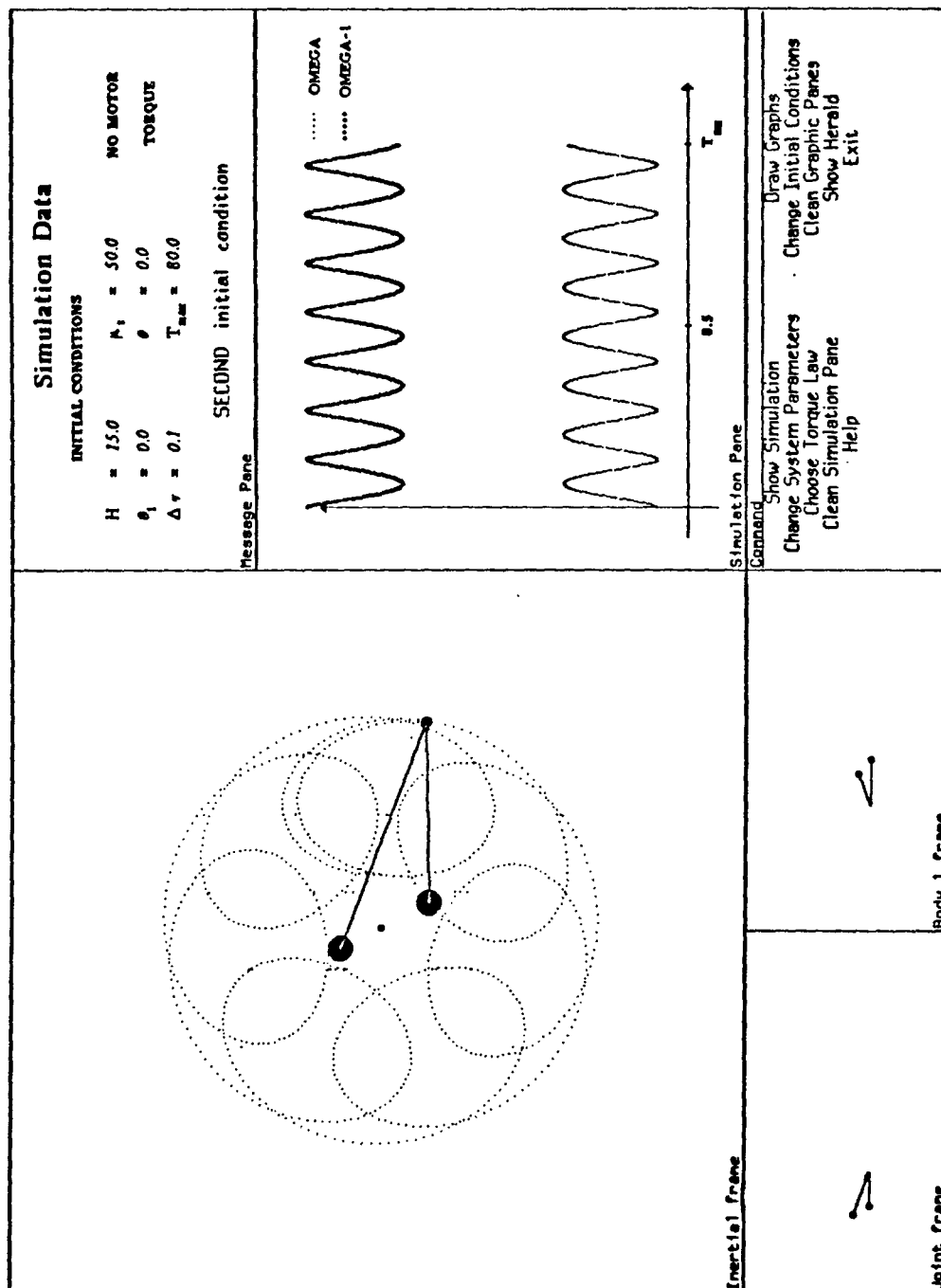Figure 7.6: Two-body problem : unstable equilibrium

Figure 7.7: Two-body problem : $H = 15$

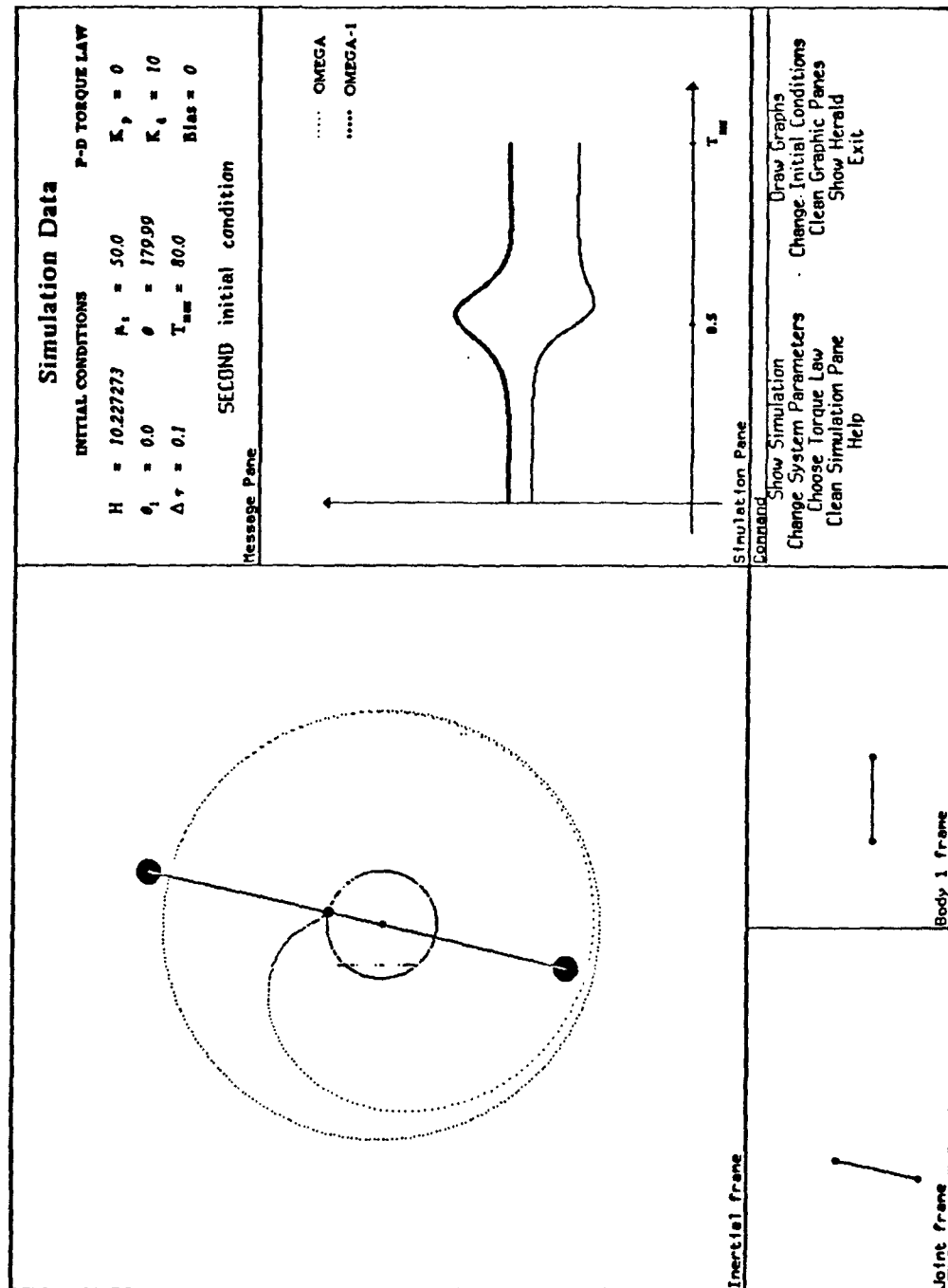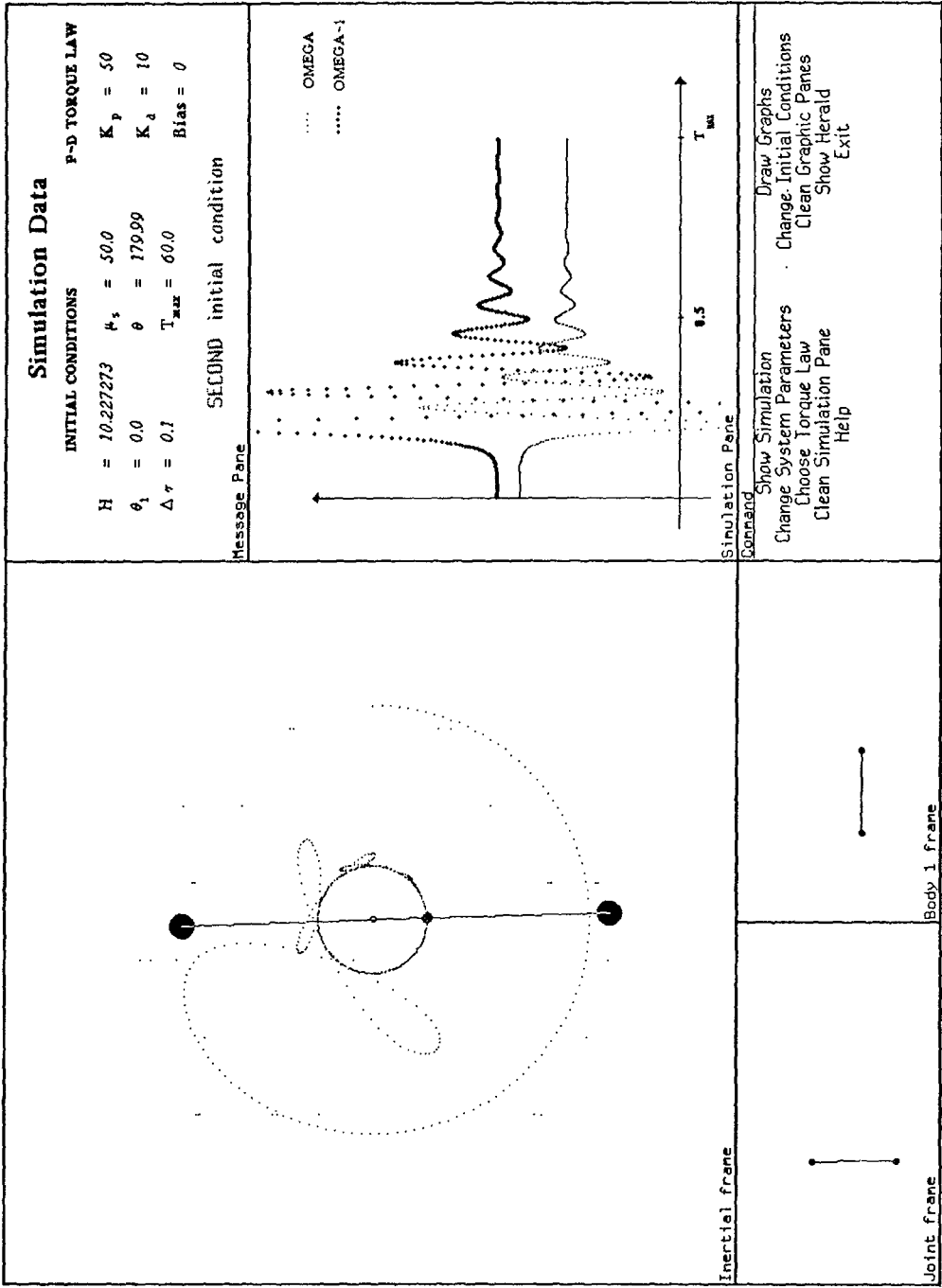Figure 7.8: Two-body problem: $K_d = 10$

Figure 7.9: Two-body problem : $K_p = 50 \; K_d = 10$

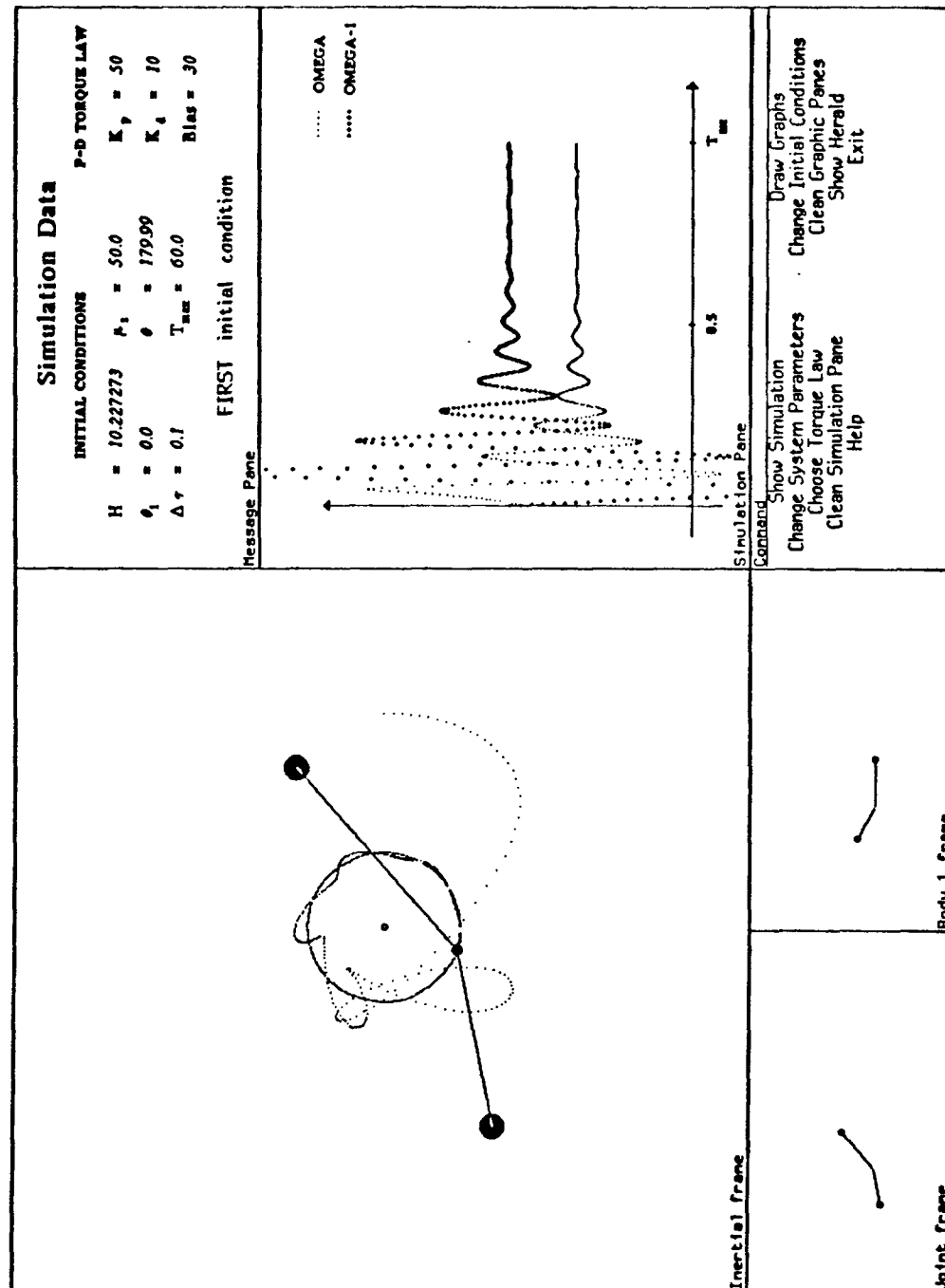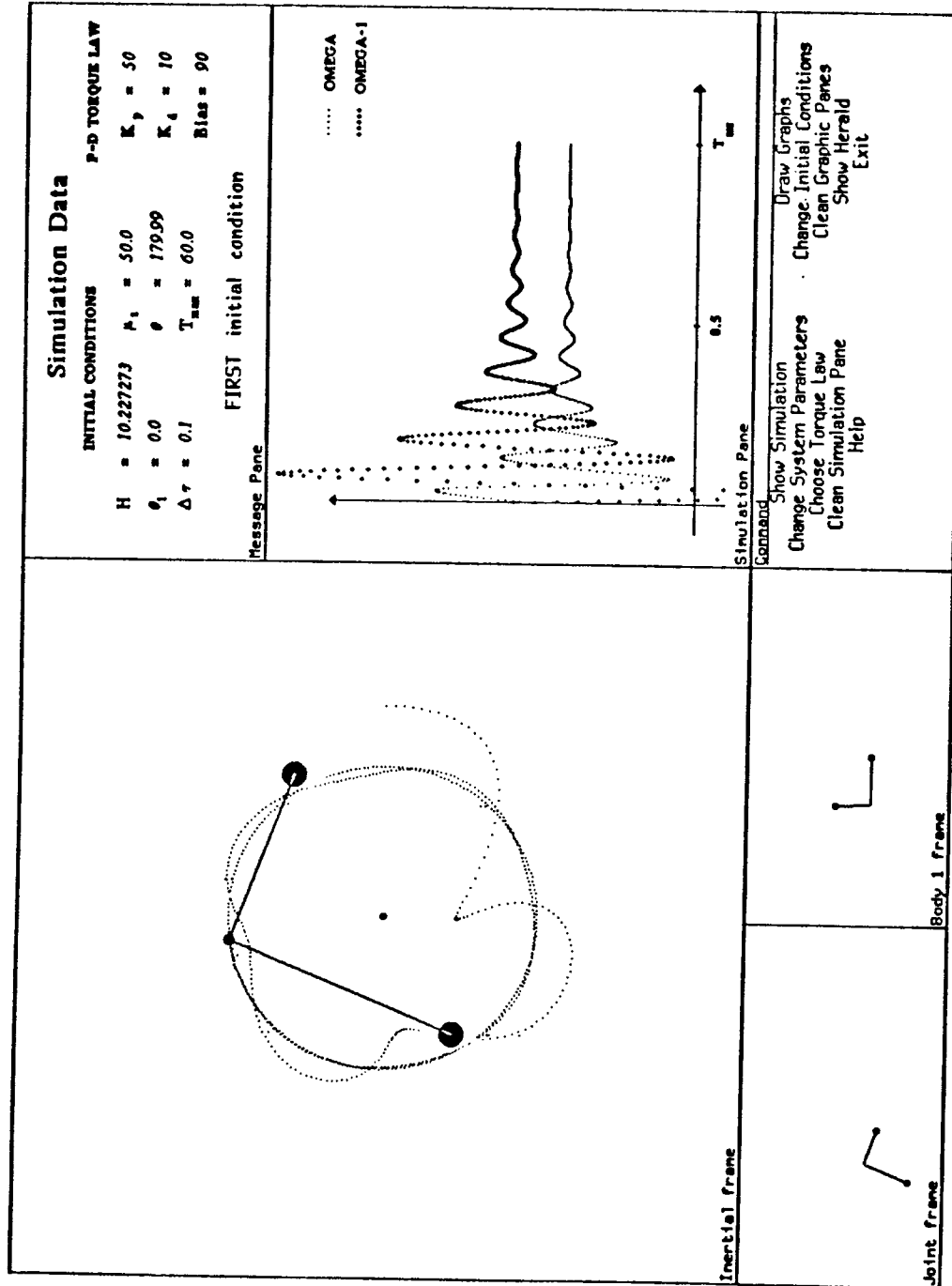Figure 7.10: Two-body problem : $K_p = 50$, $K_p = 50$, bias=30

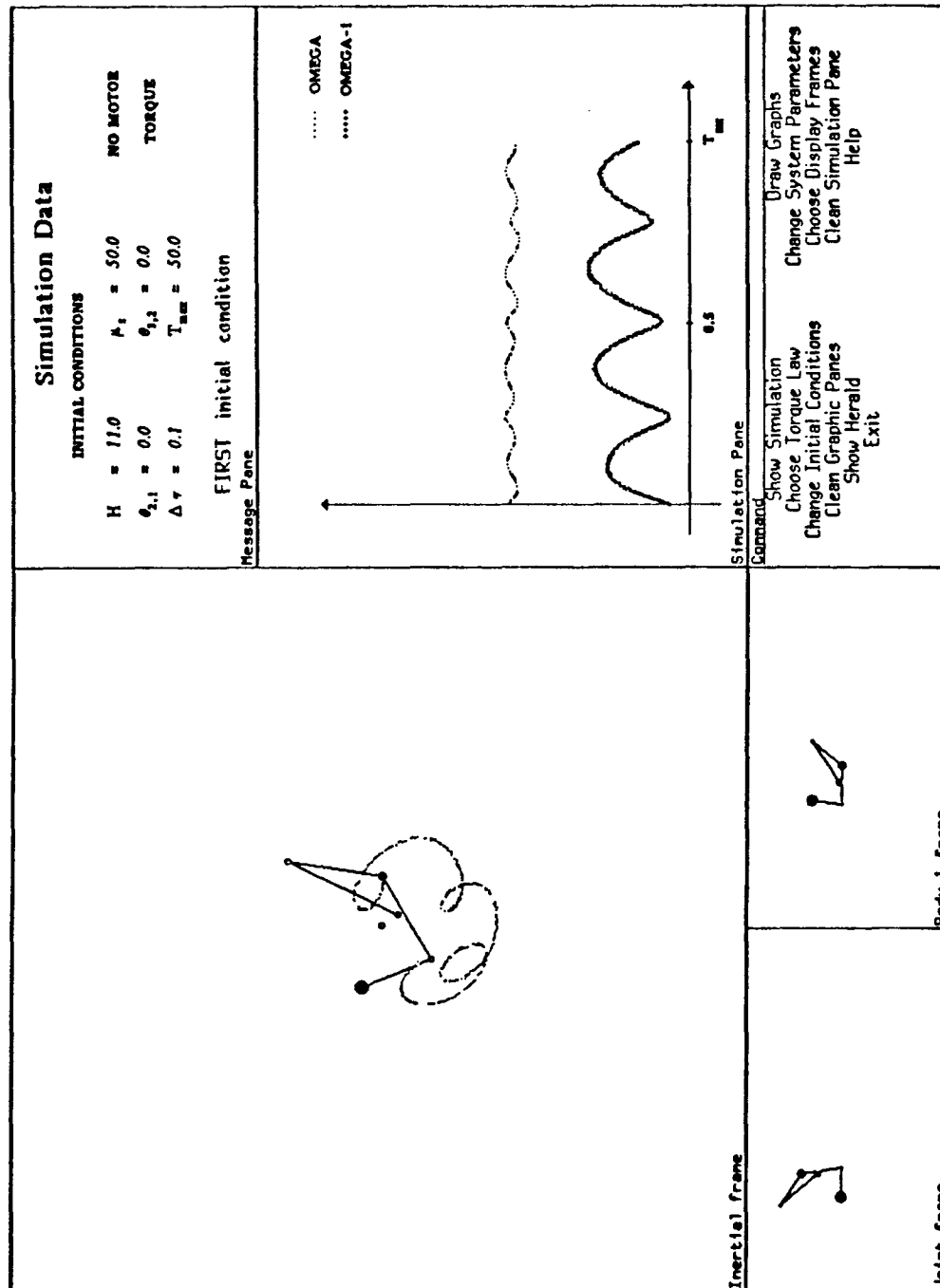Figure 7.11: Two-body problem : $K_p = 50, K_p = 50$, bias=90
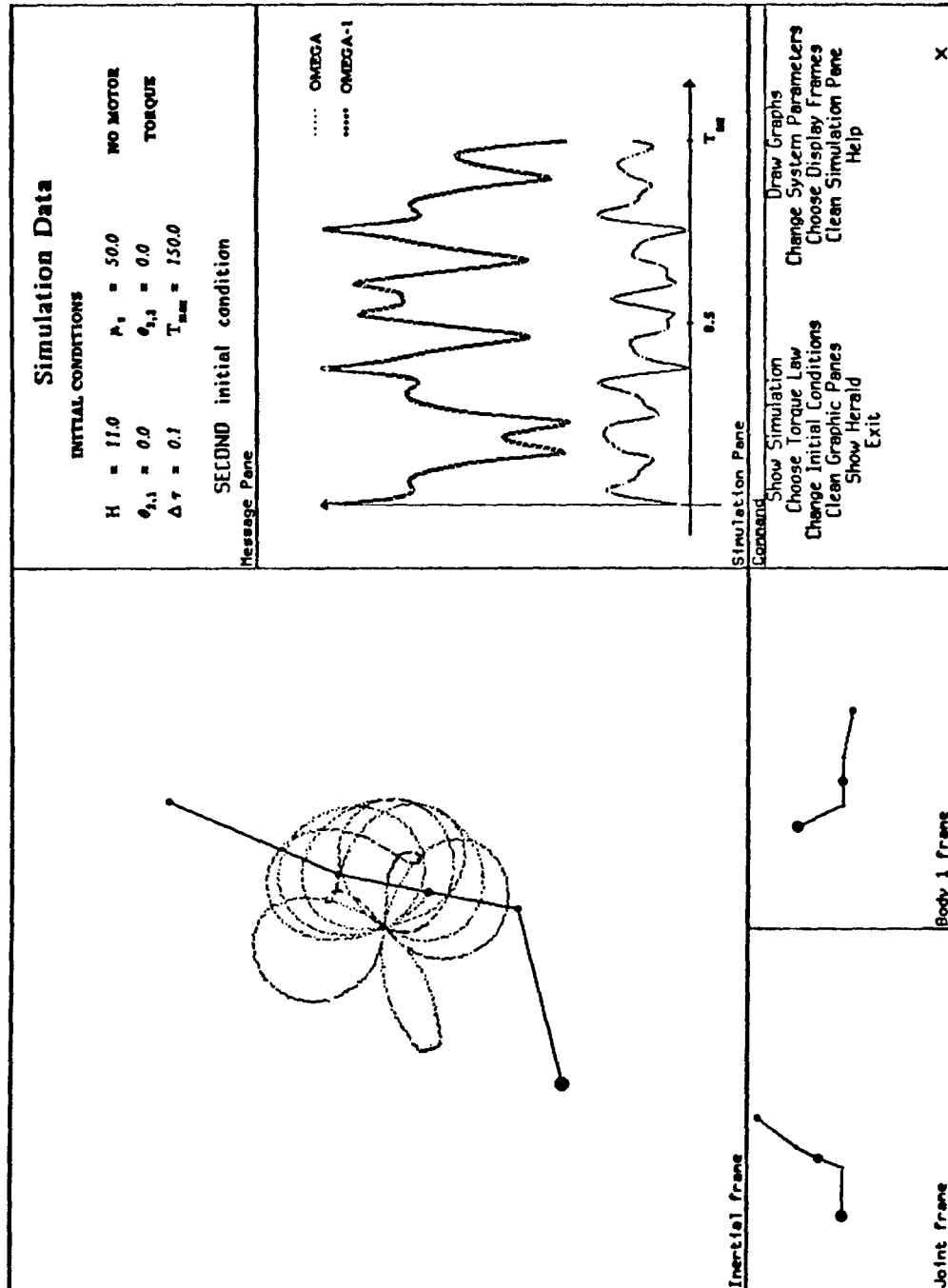
Figure 7.12: General three-body problem

127

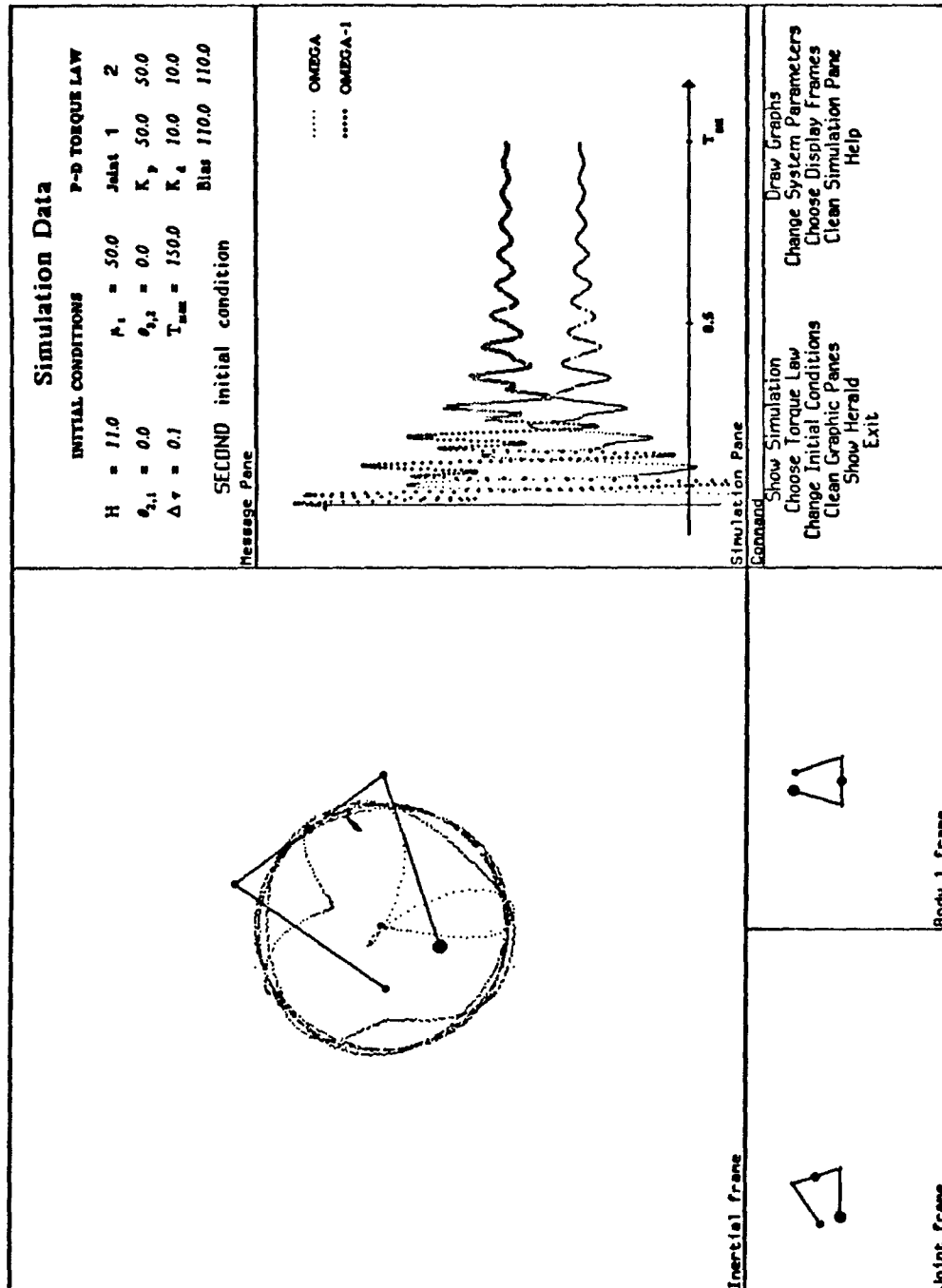Figure 7.13: Three-body problem : special kinematic case

Figure 7.14: Three-body problem : special kinematic case with joint torques

form on the basis of alpha-numeric data. Efforts in this area have lead to a variety of simulation tools. We mention here a few such tools. This list is by no means exhaustive.

(1) **NBOD** : A program written exclusively in FORTRAN [13], to simulate the dynamics of a multi - rigid body system, connected in the form of a tree structure [14], gyrostats and spring loaded point masses could also be taken into account.

(2) **TOAD** (Tele Operator Arm Design) : This program is written in PL1/FORMAC for a multi-link robot manipulator with revolute and prismatic (translational) joints [51].

(3) **OSSAM** (OHIO State Symbolic and Algebraic Manipulator) : It is written in LISP and was designed to reduce the use of memory. It can be implemented on a small computer such as PDP-11 [10].

(4) **EDYLMA** : (Equation Dynamiques Litterales d' un Manipulateur Artticule') Written for revolute joints only, in PL1/FORMAC [37].

(5) **EGAM** : (Equation Generation of Articulated Mechanisms) Written in PL1 / FORMAC for both revolute and prismatic joints. An evolution of EDYLMA [37].

(6) **DYMIR** : Written in REDUCE, it can take into account revolute, as well as, prismatic joints [5].

(7) **ARM** : Algebraic Robot Modeler, generates forward solution and Lagrangian dynamic robot model; implemented in 'C' and 'LISP' [42].

(8) **MESA-VERDE** : (MEchanism, SAtellite, VEhicle, and Robot Dynamics Equations) Simulates nonlinear dynamics and kinematics of articulated multibody systems, uses augmented body method. Written in PASCAL (ANSI 1983 standard).

(9) **DYNAMAN** : (DYnamics and Analysis of MANipulators) Program to automatically generate the dynamical equations and the Jacobian of a multi-link robot manipulator. Written in MACSYMA it can also generate FORTRAN code to simulate the dynamical equations so generated [49].

Symbolic programs in general are more efficient in terms of running time in comparison with numerical programs due to the following reason. A symbolically generated expression for a specific multibody system, is composed of non-zero variables

with fixed addresses. Its numerical evaluation takes little time. In a numerical program, large number of summations and multiplications of terms which are zero for a specific multibody system can cause substantial loss of computation time. Furthermore, computation of addresses for a large number of array elements with variable indices can take significant amount of computation time. Complicated multibody system evaluation based on symbolic methods can be faster by a factor of ten and more as compared to numerical programs [59].

Symbolic programs have the ability to compute "sensitivity" of the model with respect to parameters such as mass, length or inertia. This would be useful for design purposes. A symbolic tool allows us to simulate some nonlinear control techniques which would be difficult to realize using numerical methods [5]. Many these programs are computationally transparent and so are easier to implement and to debug.

Increasing availability of LISP machines has lead to the popularization of LISP based symbolic tools. These machines support a variety of languages including MAC-SYMA, PROLOG, REDUCE, FORTRAN-77 and C. The *windowing, object oriented programming* and the *menu driven programming* capabilities make the programming environment attractive. Excellent debugging facilities facilitates faster turn-around time. Evaluation of slices of the program inside the editor is possible. Reasonable graphic capabilities and good resolution are characteristic of such machines. A variety of fonts help display of equations in a compact form [3].

Symbolic tools could be used to explore the phase space characteristics of dynamical equations – like the computation of equilibria and also to study their stability properties. They could also be used as advanced (symbolic) "calculators" to compute, simplify and resolve symbolic expressions. In short a symbolic tool can be used as a *discovery tool*.

A number of symbolic computation languages like MACSYMA, REDUCE, PRO-LOG, MAPLE, and SCRATCHPAD II are available. We chose to use MACSYMA to implement our symbolic computation. It has a nice interactive facility, it can be imple-

---

[3]Symbolics 3600 series, TI explorer, Xerox Dandelion are some examples of LISP machines available in the market.

mented in any computer system which runs LISP, is easily available and consequently widespread in its usage. We have used MACSYMA to compute the equilibrium equations of a planar two-body and planar three-body systems. The stability of some of these equilibria has been computed using energy-Casimir method (see Chapter 5).

7.2.1 Some Symbolic Manipulation Programs

A general purpose computer program for the automatic generation of multibody systems in space, was created using the symbolic manipulation language MACSYMA. The program uses the augmented body approach as given by Wittenburg [59] to symbolically generate the dynamical equations. Dynamical equations for a three dimensional multibody satellite connected in the form of a tree structure can be generated. Individual bodies are modeled as rigid bodies, and are connected to each other by revolute joints with as many as six degrees of freedom per joint. Input to the program consists of the physical parameters of the satellite bodies like - mass, inertia tensor, relative locations of the centers of mass and the joints; and the position of the body 1 center of mass in the inertial coordinate frame. The external torques and forces acting on the satellite bodies could be given either in the inertial or the body frame of coordinates. The output is a set of second order ordinary differential equations representing the dynamics of the system. The dynamical equations of a planar two-body example in Quartararo [46] were generated using this program, and the results were found to be in complete agreement.

Another symbolic manipulation program to generate the dynamical equations of multibody systems in space was also implemented. Here we use a Newton-Euler approach which is based on the method of nested bodies due to Velman [57]. Details of the method are available in Frisch [13]. This program was also run with the previous example and the results were found to be in total agreement with the augmented body approach.

132

EIGHT

Dynamics and control of multibody systems has been the focus of this thesis. It has been our contention that a good understanding of the dynamics of multibody systems is imperative for formulating control strategies and for the eventual goal of controlling such complex systems. We have dealt with a subclass of multibody systems namely *planar multibody systems connected in the form of an open kinematic chain.* This assumption is not restrictive in the sense that lot of applications could be found.

A Hamiltonian formulation of the dynamics of a general tree connected multibody system was found. Existing *translational* and *rotational symmetries* in the problem reduce the space on which the dynamics evolve. A *Poisson structure (bracket)* on the reduced space was found and the dynamics represented in a elegant way using these brackets. Any external and internal torque acting on the system could be taken into account in the modeling. All this was presented in Chapter three.

Some interesting examples of few-body systems – two, three and N-body (chain), were worked out in Chapter four. Equilibria of the multibody system dynamics on the reduced space were studied in Chapter five. Non-degenerate equilibria (rotation of all the bodies in the system with a constant angular velocities) were of interest. Stability of such equilibria was examined using energy-Casimir method. A formulation of the energy-Casimir method for a general case of an N-body system was given. It was shown that for the planar two-body example there were two equilibria – a stretched

out one (stable one) and a folded one (unstable one). A graphic computer simulation study of the problem was also presented. We have also proved that there can be as many as six equilibria for the special kinematic case of planar three-body system where the system center of mass of the second body is along the line joining the two joints. The equilibria of an N-body system where all the bodies were symmetrical was studied and it was proved that the stretched out configuration is defintely an equilibrium. A numerical experiment conducted to find the stability of equilibria using the energy-Casimir method for specific cases of number of bodies ranging from $N = 2$ to $N = 10$ indicated that the stretched out configuration is stable.

Some important control problems were tackled in Chapter six. Global controllability of planar multibody systems was proved, given all joint torques plus an external torque (say a gas jet) on one of the bodies. Also the multibody system could be also I/O linearized by a feedback of the form $u(\underline{x}) = \alpha(\underline{x}) + \beta(\underline{x})\underline{v}$ where u is the control input of only joint torques. A stability theorem was proved which states that the system converges to a maximal invariant subset consisting of all the system equilibria on the introduction of a feedback of the form $T_i = C - i\dot{\theta}_{i,J(i)}$ where $C_i > 0$.

Chapter seven was the concluding chapter of the thesis and presented our efforts in applying *symbolic and LISP based computation* as tools for analysis and simulation of planar multibody systems. **OOPSS** – an Object Oriented Planar System Simulator based on object oriented programming methodology, with a general purpose architecture for generation, simulation and animation of planar multibody systems was proposed. **OOPSS** has been implemented for two and three-body systems in Zeta-lisp on a Symbolics 3600 series machine [4]. Forcing inputs like the joint torques could be introduced and equilibria could be displayed. A stabilizing input illustrates our stabilization theorem.

Future Work

We plan to extend the above formalism to three-dimensional systems i.e., for systems with one or more degrees of rotational freedom between two bodies. Some

---

[4]manufactured by Symbolics Inc, Cambridge, Mass.

134

work has been done in this regard by Grossman, Krishnaprasad and Marsden [16], where they consider two rigid bodies connected by a ball-in socket (three degrees of freedom) joint. Equilibria of complex multibody systems needs to be identified and stability issues studied. Extension of this modeling methodology to flexible systems are interesting to consider. One also would like to see a "controllability" theorem on the symplectic leaf given the joint torques only. Implementation of **OOPSS** for complex multibody systems is being considered.

Appendix 1

We give the results of a numerical experiment conducted to study the stability of the stretched out equilibrium ($\theta_{i+1,i} = 0$, $i = 1, N - 1$) for the symmetrical N-body (chain) example using energy-Casimir method. The experiment was conducted with the number of bodies varying from 2 to 10.

Finding the definiteness of the Hessian $d^2(H + C)$ at the above equilibrium is equivalent to finding whether the matrix given by equation (6.6) Chapter 5, is definite or not (since the psuedo inertia matrix $\mathbf{J}$ is always positive definite). Call this matrix M. Recall that the matrix M is a $(N - 1 \times N - 1)$ matrix. The numerical results are given below. Note that $\rho = d^2 m \omega_o^2$, where d is the distance between two adjacent joints, m is the mass of each body and ω_o is the angular velocity with which all the bodies in the system rotate at equilibrium.

N = 2

First principal minor of M $\qquad$ = 0.125.

So matrix M and thus $d^2(H + C)$ is positive definite.

N = 3

First principal minor of M $\qquad$ = 0.333ρ.

Second principal minor of M $\qquad$ = 0.10416ρ^2.

So matrix M and thus $d^2(H + C)$ is positive definite.

N = 4

First principal minor of M $\qquad$ = 0.5625ρ.

Second principal minor of M $\qquad$ = 0.5ρ^2.

Third principal minor of M $\qquad$ = 0.25ρ^3.

So matrix M and thus $d^2(H + C)$ is positive definite.

N = 5

First principal minor of M $\quad = 0.8\rho$.

Second principal minor of M $\quad = 0.12375\rho^2$.

Third principal minor of M $\quad = 0.17875\rho^3$.

Fourth principal minor of M $\quad = 0.12289\rho^4$.

So matrix M and thus $d^2(H + C)$ is positive definite.

N = 6

First principal minor of M $\quad = 1.041\rho$.

Second principal minor of M $\quad = 2.33\rho^2$.

Third principal minor of M $\quad = 5.906\rho^3$.

Fourth principal minor of M $\quad = 11.813\rho^4$.

Fifth principal minor of M $\quad = 10.336\rho^5$.

So matrix M and thus $d^2(H + C)$ is positive definite.

N = 7

First principal minor of M $\quad = 1.286\rho$.

Second principal minor of M $\quad = 3.795\rho^2$.

Third principal minor of M $\quad = 13.964\rho^3$.

Fourth principal minor of M $\quad = 49.093\rho^4$.

Fifth principal minor of M $\quad = 125.46\rho^5$.

137

Sixth principal minor of M $= 133.3\rho^6$.

So matrix M and thus $d^2(H + C)$ is positive definite.

N = 8

First principal minor of M $= 1.531\rho$.

Second principal minor of M $= 5.625\rho^2$.

Third principal minor of M $= 27.34\rho^3$.

Fourth principal minor of M $= 140.0\rho^4$.

Fifth principal minor of M $= 630.0\rho^5$.

Sixth principal minor of M $= 1960.0\rho^6$.

Seventh principal minor of M $= 2450.0\rho^7$.

So matrix M and thus $d^2(H + C)$ is positive definite.

N = 9

First principal minor of M $= 1.777\rho$.

Second principal minor of M $= 7.826\rho^2$.

Third principal minor of M $= 47.44\rho^3$.

Fourth principal minor of M $= 321.19\rho^4$.

Fifth principal minor of M $= 2107\rho^5$.

Sixth principal minor of M $= 11555\rho^6$.

Seventh principal minor of M $= 42370\rho^7$.

Eighth principal minor of M $= 60908\rho^8$.

So matrix M and thus $d^2(H + C)$ is positive definite.

N $= 10$

First principal minor of M $= 2.025\rho$.

Second principal minor of M $= 10.4\rho^2$.

Third principal minor of M $= 75.64\rho^3$.

Fourth principal minor of M $= 639.11\rho^4$.

Fifth principal minor of M $= 5548\rho^5$.

Sixth principal minor of M $= 44382\rho^6$.

Seventh principal minor of M $= 287101\rho^7$.

Eighth principal minor of M $= 1212205\rho^8$.

Ninth principal minor of M $= 1969834\rho^9$.

So matrix M and thus $d^2(H + C)$ is positive definite.

Appendix 2

DYNAMICS OF PLANAR MULTIBODY SYSTEMS

The multibody system data is in file :

DATA FILE : :>sreenath>planar>data3.macsyma.3

The path from center of mass of body 1 to body 2 is [1, 2]

The path from center of mass of body 1 to body 3 is [1, 2, 3]

Hamiltonian of the system is

$$
\begin{bmatrix} \dfrac{MU_1}{2} & \dfrac{MU_2}{2} & \dfrac{MU_3}{2} \end{bmatrix} \cdot J\_INV \cdot \begin{bmatrix} MU_1 \\ MU_2 \\ MU_3 \end{bmatrix}
$$

Note: J_inv is the matrix J ^-1

The **J** matrix is given below

$$
Col\ 1 =
$$

$$
\begin{bmatrix}
\dfrac{(M_1 M_3 + M_1 M_2)\, C\_1^2}{M_3 + M_2 + M_1} + IN_1 \\[2ex]
\dfrac{M_1 M_3 \sin(THETA_{2,1})\, C\_1\, E\_2}{M_3 + M_2 + M_1} + \dfrac{\cos(THETA_{2,1})\,(M_1 M_3\, C\_1\, E\_1 + (M_1 M_3 + M_1 M_2)\, B\_1\, C\_1)}{M_3 + M_2 + M_1} \\[2ex]
\dfrac{M_1 M_3 \cos(THETA_{3,2} + THETA_{2,1})\, C\_1\, D\_1}{M_3 + M_2 + M_1}
\end{bmatrix}
$$

$$
Col\ 2 =
$$

$$
\begin{bmatrix}
\dfrac{M_1 M_3 \sin(THETA_{2,1})\, C\_1\, E\_2}{M_3 + M_2 + M_1} + \dfrac{\cos(THETA_{2,1})\,(M_1 M_3\, C\_1\, E\_1 + (M_1 M_3 + M_1 M_2)\, B\_1\, C\_1)}{M_3 + M_2 + M_1} \\[2ex]
\dfrac{(M_2 + M_1)\, M_3\, E\_2^2 + (M_2 + M_1)\, M_3\, E\_1^2 + 2 M_1 M_3\, B\_1\, E\_1 + (M_1 M_3 + M_1 M_2)\, B\_1^2}{M_3 + M_2 + M_1} + IN_2 \\[2ex]
\dfrac{\cos(THETA_{3,2})\,((M_2 + M_1)\, M_3\, D\_1\, E\_1 + M_1 M_3\, B\_1\, D\_1)}{M_3 + M_2 + M_1} - \dfrac{(M_2 + M_1)\, M_3\, \sin(THETA_{3,2})\, D\_1\, E\_2}{M_3 + M_2 + M_1}
\end{bmatrix}
$$

$$
\text{Col 3} = \begin{bmatrix}
\dfrac{M_1 M_3 \cos(\theta_{3,2} + \theta_{2,1}) C\_1 D\_1}{M_3 + M_2 + M_1} \\[4ex]
\dfrac{\cos(\theta_{3,2})((M_2 + M_1) M_3 D\_1 E\_1 + M_1 M_3 B\_1 D\_1)}{M_3 + M_2 + M_1} - \dfrac{(M_2 + M_1) M_3 \sin(\theta_{3,2}) D\_1 E\_2}{M_3 + M_2 + M_1} \\[4ex]
\dfrac{(M_2 + M_1) M_3 D\_1^2}{M_3 + M_2 + M_1} + IN_3
\end{bmatrix}
$$

The HAMILTONIAN DYNAMICS are

Conjugate Momentum (i.e., mu's) Rates

$$
\frac{d}{dT}(MU_1) = \begin{bmatrix} MU_1 & MU_2 & MU_3 \end{bmatrix} \cdot \frac{dJ\_INV}{dTHETA_{2,1}} \cdot \begin{bmatrix} MU_1 \\ MU_2 \\ MU_3 \end{bmatrix}
$$

$$
\frac{d}{dT}(MU_2) = \begin{bmatrix} MU_1 & MU_2 & MU_3 \end{bmatrix} \cdot \frac{dJ\_INV}{dTHETA_{3,2}} \cdot \begin{bmatrix} MU_1 \\ MU_2 \\ MU_3 \end{bmatrix} - \begin{bmatrix} MU_1 & MU_2 & MU_3 \end{bmatrix} \cdot \frac{dJ\_INV}{dTHETA_{2,1}} \cdot \begin{bmatrix} MU_1 \\ MU_2 \\ MU_3 \end{bmatrix}
$$

$$
\frac{d}{dT}(MU_3) = - \begin{bmatrix} MU_1 & MU_2 & MU_3 \end{bmatrix} \cdot \frac{dJ\_INV}{dTHETA_{3,2}} \cdot \begin{bmatrix} MU_1 \\ MU_2 \\ MU_3 \end{bmatrix}
$$

Relative Angles (i.e, theta's) Rates

$$
\frac{d}{dT}(\theta_{2,1}) = \begin{bmatrix} 0 & 1 & 0 \end{bmatrix} \cdot J\_INV \cdot \begin{bmatrix} MU_1 \\ MU_2 \\ MU_3 \end{bmatrix} - \begin{bmatrix} 1 & 0 & 0 \end{bmatrix} \cdot J\_INV \cdot \begin{bmatrix} MU_1 \\ MU_2 \\ MU_3 \end{bmatrix}
$$

$$
\frac{d}{dT}(\theta_{3,2}) = \begin{bmatrix} 0 & 0 & 1 \end{bmatrix} \cdot J\_INV \cdot \begin{bmatrix} MU_1 \\ MU_2 \\ MU_3 \end{bmatrix} - \begin{bmatrix} 0 & 1 & 0 \end{bmatrix} \cdot J\_INV \cdot \begin{bmatrix} MU_1 \\ MU_2 \\ MU_3 \end{bmatrix}
$$

Bibliography

[1] Arnold, V. I., *Mathematical Methods of Classical Mechanics*, Springer Verlag, New York, 1978.

[2] Abraham, R., and Marsden, J. E., *Foundations of Mechanics*, Benjamin /Cummings, Reading, Mass., 1978.

[3] Abraham, R., Marsden, J. E., and Ratiu, T., *Manifolds, Tensor Analysis and Applications*, Addison-Wesley Publishing Inc., 1983.

[4] Brockett, R. W., "Feedback invariants of nonlinear systems", *IFAC Congress*, Helsinki, pp. 1115, 1978.

[5] Ceasreo, G. , and Nicolo, F., "DYMIR: A code for generating dynamic models of robots", *in preprint*, 1984.

[6] Clarke, M. M., et. al. "Requirements development for a Free-Flying Robot - The 'ROBIN"',*IEEE Intl. Conf. on Robotics and Automation*, San Fransisco, Calif., Vol 2 , p667-672, April 7-11, 1986.

[7] Covalt, C., "Orbiter Crew Restores Solar Max",*Aviation Week & Space Technology*, pp. 18-20, April 16, 1984.

[8] Courant, R., and Hilbert, D., " Methods of Mathematical Physics (I, II)", *Wiley*, New York, 1962.

[9] Denavit, J., and Hartenberg, R. S., " A kinematic notation for lower-pair mechanism based on matrices" *Trans. ASME Journal of Applied Mechanics*

Vol. 77, pp. 215-221, June, 1955.

[10] Dillon, S., R., " Computer assisted equation generation in linkage dynamics", *Thesis*, Ohio State University, 1973.

[11] Dwyer, T. A. W., "Exact nonlinear control of spacecraft slewing maneuvers with internal momentum transfer", *Journal of Guidance, Control, and Dynamics*, Vol 9, No.2, pp. 240-247, 1985.

[12] Fletcher, H. J., Rongved, L., and Yu, E. Y., "Dynamics analysis of a two-body gravitationally oriented satellite", *Bell Systems Tech. J.*, Vol 42, pp. 2239-2266, 1963.

[13] Frisch, H. P., "A vector-dyadic development of the equations of motion for N-coupled rigid bodies and point masses", *NASA TND-7767*, Oct., 1977.

[14] Frisch, H. P. "The NBOD2 User's and Programmer's Manual" in *NASA TP 1145* , Feb., 1978.

[15] Freund, "Fast nonlinear control with arbitrary pole placement for industrial robots and manipulators", pp. 147-168, *Robot Motion: Planning and Control*, Eds. Brady., M., Hollerbach, J., M., Jhonson, T., Lorenzo-Perez, Mason, M., T., MIT Press,Cambridge, Mass., 1982.

[16] Grossman, R., Krishnaprasad, P.S., and Marsden, J.E., "Dynamics of two coupled three dimensional rigid bodies", *Dynamical Systems approaches to Nonlinear Problems in Systems and Circuits*, eds., F.M.A. Salam and M. Levi, SIAM Publ., 1987 (in press).

[17] Guckenheimer, and Holmes, P. J., *Nonlinear Oscillations, Dynamical Systems, and Bifurcations of Vector Fields*, Springer-Verlag, New York, 1983.

[18] Holm, D., Marsden, J., Ratiu, T., and Weinstien, A., "Stability of rigid body motion using the Energy-Casimir method", *Contemporary Mathematics*, Vol 28, 1984.

[19] Holmes, P. J., and Marsden, J. E.,"Horseshoes and Arnold diffusion for Hamiltonian systems on Lie groups", *Indiana Univ. Math. J.*, 32, pp. 273-309, 1982.

[20] Holmes, P. J., and Marsden, J. E., "Melnikov's method and Arnold diffusion for perturbations of integrable Hamiltonian systems", *J. Math. Phys.*, vol 23, no.4, pp. 669-675, 1983.

[21] Horn, B. K. P., " Kinematics, statics and dynamics of two-dimensional manipulators", Eds. Winston, P., and Brown, R., *Artificial Intelligence : An MIT Perspective*, pp. 273-310, MIT Press, Cambridge, Mass. 1979.

[22] Hooker, W. W., and Margulies, G., "The dynamical attitude equations for a n-Body Satellite",*J. Astronaut. Sci.*, Vol. 12, pp. 123-128, 1965.

[23] Hunt L. R., Su, R., and Meyer, G., "Global transfer of nonlinear systems".*IEEE Transactions on Automatic Control,* Vol. AC-29, pp. 24-31, Jan. 1983.

[24] Hunt L. R., Su, R., and Meyer, G., "Design of multi-input nonlinear systems", *Differential Geometric Control Theory*, Ed. R. Brockett, R. Millman, H. Sussman, Stuttgart: Birkhauser, pp. 268-298, 1983.

[25] Isidori, A., "Non-Linear Control Systems : An Introduction", *Lecture Notes in Control and Information Science*, Vol 72, Springer-Verlag, New York, 1985.

[26] Isidori, A., and Krener, A. J., "On feedback equivalence of nonlinear systems", *System & Control Letters*, Vol 2, No. 2, August 1982.

[27] Jakubczyk, V. J., and Respondek, W., "On linearization of control systems", *Bull. Acad, Pol, Sci, Ser. Sci. Math*, 28, pp. 517-522, 1980.

[28] Jenkins, L. M., "Telerobotic work system-space robotics application", *IEEE Intl. Conf. on Robotics and Automation*, San Fransisco, Calif., Vol 2 , p804-06, April 7-11, 1986.

[29] Junkins, J. L., and Turner, J.D., "Optimal Spacecraft Rotational Maneuvers", *Elsevier Science Publishers*, Amsterdam, The Netherlands, 1986.

[30] Kailath, T., "Linear Systems", *Prentice Hall*, Englewood Cliffs, N.J., 1980.

[31] Khalil, W., " Modelization et commande par calculeteurs du manipulateurs ", *Thesis*, Universite' des Sciences et Technique du Languedoc, 1976.

[32] Krishnaprasad, P. S., "Lie-Poisson structures, dual-spin spacecraft and asymptotic stability", *Nonlinear Analysis, Theory, Methods and Applications*, Vol 9, NO. 10, pp. 1011-1035, 1985.

[33] Krishnaprasad, P. S., and Berenstein, C. A., "On the equilibria of rigid spacecraft with rotors",*Sys. and Contr, Lett.*, Vol 4, pp. 147-163, 1984.

[34] Krishnaprasad, P. S., and Marsden, J. E., "Hamiltonian structures and stability of rigid bodies with flexible attachments ", *Arch. Rat. Mech. Anal.*, 98, 71-93, 1986.

[35] Kirillov, A. A., "Elements of the Theory of Representations", *Springer*, New York, 1974.

[36] Kummer, M., "On the construction of the reduced phase space of a Hamiltonian system with symmetry ",*Indiana U. Math J.*, vol 30, 281-292, 1981.

[37] Liegeois, A., Khalil, W., Dumas, J. M., and Renauld, M. "Mathematical and computer models of interconnected mechanical systems ", *2nd International symposium on theory and practice of robots and manipulators*, pp. 5-17, Sept. 1976.

[38] Likins, P. W., "Analytical Dynamics and Nonrigid Spacecraft Simulation", *NASA Tech. Rept. 32-1593*, July 15, 1974.

[39] Longman, R. W., Lindberg, R., and Zed, M. F., *Satellite mounted robot manipulators - new kinematics and reaction moment compensation* (preprint).

145

[40] Marino, R., " Stabilization and feedback equivalence to linear coupled oscillators", *Int. J. Control* 39, 487-496, 1984.

[41] Marsden, J. E., and Weinstein, A., "Reduction of symplectic manifolds with symmetry", *Rep. Mathematical Physics*, 5, pp. 121-130, 1974.

[42] Murray, J. J., and Neuman, C. P., " ARM: An algebraic robot dynamic modeling program", IEEE 1984.

[43] Omohundro, S., "Geometric Hamiltonian structures and perturbation theory", *Local and Global Methods of Nonlinear Dynamics*, pp. 91-120, Springer-Verlag 1983.

[44] Pringle, R., Jr., "On the Stability of a body with connected moving parts", *AIAA J.*, Vol 4, pp. 1395-1404, 1966.

[45] Pringle, R., Jr., "Force-free motions of a dual-spin spacecraft", *AIAA J.*, Vol 7, pp. 1055-1063, 1969.

[46] Quartararo, R., "Two-body control for rapid attitude maneuvers", *Advances in Astronautical Sciences*, L.A. Morine ed., Vol 42, pp. 397-422, American Astronautical Society, San Diego (AAS 80-203), 1980.

[47] Roberson, R. E., and Wittenburg, J., "A dynamical formalism for an arbitrary number of interconnected rigid bodies with reference to the problem of satellite attitude control", *Proc. of the 3rd Intl. Congress of Automatic Control, London,1966*, pp. 46D.1-46D.8. Butterworth and Co., Ltd, London, England, 1967.

[48] Seshu, S., and Reed, M. B., "Linear Graphs and Electrical Networks", *Addison-Wesley Publishing Company, Inc.*, Reading, Mass., 1961.

[49] Sreenath, N., and Krishnaprasad, P. S. "DYNAMAN: A Tool for manipulator design and analysis", *IEEE Intl. Conf. on Robotics and Automation*, San Fransisco, Calif., Vol 2 , p836-842, April 7-11, 1986.

[50] Stefik, M., and Bobrow, D. G., "Object-Oriented Programming : themes and variations", *The AI magazine*, pp. 40-62, 1986.

[51] Sturges, R., " Teleoperators arm design program", *Report 3.2746* MIT Draper Lab. Cambridge Mass., 1973.

[52] Su, R., "On the linear equivalents of nonlinear systems", *Syst. & Cont. Lett.*, Vol 2, pp. 48-52, 1982.

[53] Tsai, L. -W., and Morgan, A. P., "Solving the kinematics of the most general six and five-degree-of-freedom manipulators by continuation methods", *J. of Mechanisms, Transmission, and Automation in Design*, Vol 107, pp. 189-200 June 1985.

[54] Tsinias, J., and Kaloupsidis, N., " On stabilizability of nonlinear systems" *Proc 21st IEEE Conf. on Decision and Control*, pp. 712-716, 1982.

[55] Vadali, S.R., and Junkins, J. L., "Optimal open loop and stable feedback control of rigid spacecraft attitude maneuvers", *J. of Astronautical Sciences*, Vol. 32, Jan-March pp. 105-122, 1984.

[56] van der Schaft, "Stabilization of Hamiltonian systems", *Nonlinear Analysis, Theory, Methods & Applications*, Vol 10, No. 10, pp. 1021-1035, 1986.

[57] Velman, J. R., "Simulation results for a dual-spin spacecraft",*Proc. of the symposium on Attitude Stabilization and Control of Dual-Spin Spacecraft, El Segundo, Calif., 1967,* , Rept. SAMSO-TR-68-191, 1967.

[58] Wertz, J., *Spacecraft Attitude Determination and Control*, Dordrecht, D. Reidel, 1978.

[59] Wittenburg , J. M., "Dynamics of Systems of Rigid Bodies", *B.G. Tuebner and Co.*, Stuttgart, West Germany, 1977.

[60] Wittenburg, J. M., "MESA-VERDE: A symbolic program for nonlinear articulated-rigid-body dynamics",*ASME Design Engg. Division Conf.*, 10-13, Cincinatti, Ohio, Sept., 1985.

[61] "Analysis of remote Operating Systems for Space-Based Servicing operations, Final Report", *NAS9-17066,Report SA-ROS-RP-111-1*,Grumman Corp.,Mar 1985 .

[62] "Space Station Needs, Attributes, and Architectural Options " Vol II - mission requirements, *SA-SSP-Rp008*, April, 20, 1983.

[63] "Space Station Flight Telerobotic Servicer Requirements document for definition and preliminary design", *SS-GSFC-0028*, April 1987.